ANNUAL REPORT
FOR
TECHNICAL, ANALYTICAL,
AND
COMPUTER SUPPORT

RESALAB

ANNUAL REPORT
FOR
TECHNICAL, ANALYTICAL,
AND
COMPUTER SUPPORT

Contract No. 952808
18 February 1970 - 17 February 1971

This work was performed for the Jet Propulsion Laboratory, California Institute of Technology, sponsored by the National Aeronautics and Space Administration under Contract NAS7-100.

Prepared For
Jet Propulsion Laboratory
Pasadena, California

By
Resalab Scientific
Menlo Park, California

TABLE OF CONTENTS

I. INTRODUCTION

This report covers work performed by Resalab Scientific for the Jet Propulsion Laboratory during the period 18 February 1970 to 17 February 1971. The bulk of the work effort during this time period was divided into three specific tasks. These were RTG Design Study, Material Study, and Special Studies. Shortly before the close of the first year's effort, an additional task, the Sublimation of Silicon-Germanium alloys was initiated.

The RTG Design Study involves the development of a rigorous mathematical model for the design and performance analysis of cylindrical silicon-germanium Thermoelectric Generators (RTG's) and consists of two parts, a steady-state (static) part and a transient (dynamic) part. The Material Study involves the definition and implementation of a material study that aims to experimentally characterize the long-term behavior of the thermoelectric properties of silicon-germanium alloys as a function of temperature. The sublimation of Silicon-Germanium alloys consists of analytical and experimental efforts aimed at the determination of the sublimation characteristics of these alloys and the study of sublimation effects on RTG performance. The Special Studies involve studies performed at JPL's request on a variety of specific topics on thermoelectric energy conversion.

II. RTG DESIGN STUDY

A. INTRODUCTION

The objectives of this task are the development of improved analytical techniques for the design and performance of RTG's, the programming of the resultant mathematical model for solution on a high speed computer and the application of the computer program to the performance evaluation of representative and/or specific RTG's in typical and/or specific deep space missions. The mathematical model is oriented towards silicon-germanium RTG's because existing models in this area are inadequate and because it is anticipated that it is RTG's of this type that will be used in most future deep space probes.

Most existing RTG design and performance analysis techniques are either highly approximate or else are complicated and unwieldy combinations of independent generation component design subroutines, many of which are frequently of questionable rigor. A comprehensive and accurate analytical technique therefore offers a presently unavailable tool for conveniently investigating the role of RTG's in either general or specific space applications. This technique is of obvious necessity to overall spececraft designers as well as to workers associated with components that directly interface with the RTG.

B. MATHEMATICAL MODEL

The mathematical model for the design and performance analysis of the RTG includes a number of unique features, such as the consideration of all RTG components in a single calculational sequence, the accurate accounting of the temperature dependence of the properties of the thermoelectric materials, the effective accounting of three-dimensional heat flow in all key components of the RTG, and the inclusion of the detailed effects of all passive components in the thermal and electrical circuits of the RTG. Although the overall geometry of the RTG is thus specified, the dimensions and materials of its components can be varied and changed at will in order to investigate RTG performance for any desired application. RTG fuel loading, the external sink temperature, and external load conditions have been made

input variables in the model such that RTG performance may be studied in terms of these variables. Accurate convergence routines for fixed heat input operation of a RTG are included as a part of the mathematical model.

The geometric model used for mathematical analysis is shown in Figures 1 and 2. The RTG is divided into two primary regions of interest, the active portion and the ends. The ends consist of the fuel capsule support, the end insulation and the end radiator area.

The active portion is divided into axial rings. The number of such rings is equal to the number of couples aligned axially in the converter. Thus the rings represent lateral slices of the converter within which all thermocouples are considered to have identical temperature distributions and power output. As the generator is assumed to be symmetrical end-to-end, the analysis is performed using one half of the generator.

The overall analysis of the RTG has been broken into two parts; that of the steady-state or static and that of the transient or dynamic performance. The static part of the analysis has received the bulk of the effort to date.

C. STATIC PERFORMANCE ANALYSIS

The logic diagram for the portion of the program dealing with the static performance is shown in Figure 3. The program starts with the input of the RTG geometry and other pertinent items such as fuel capsule thermal power and ratio of load to internal electrical resistance. The geometric input consists of various items describing the RTG, including the number of couples, number of strings of couples electrically in parallel, size of couples, etc. The input parameters are initially printed for verification and certain geometrical parameters including ring dimensions are calculated.

An initial iteration loop is entered in which the temperature distribution of all rings is held identical, i.e. the assumption is made that there is no axial heat flow in the RTG. This loop is exited when a heat balance calculation shows that the sum of calculated heats in various RTG components is in agreement with the specified heat input. The temperatures calculated for the various components in

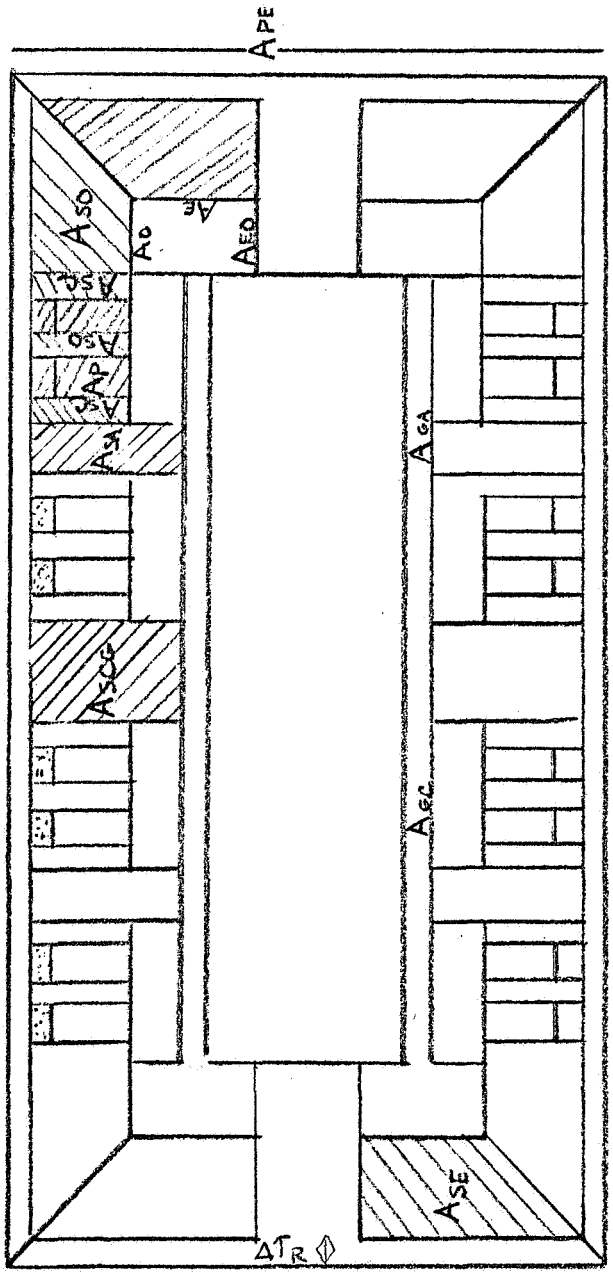

Figure 1 - OVERALL LATERAL VIEW OF RTG

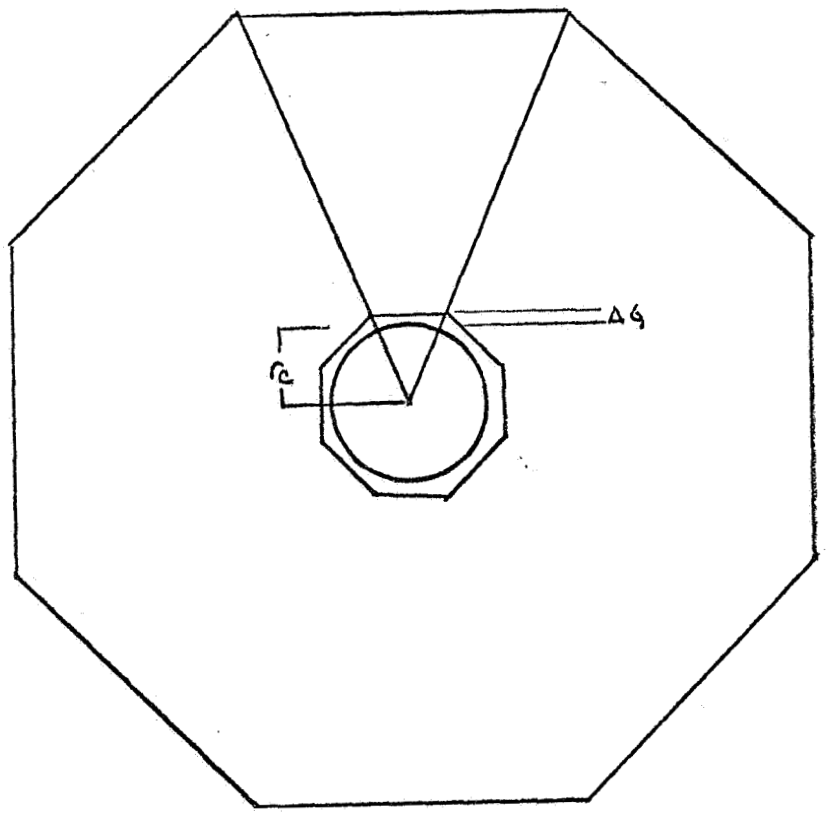

Figure 2 - OVERALL AXIAL VIEW OF RTG

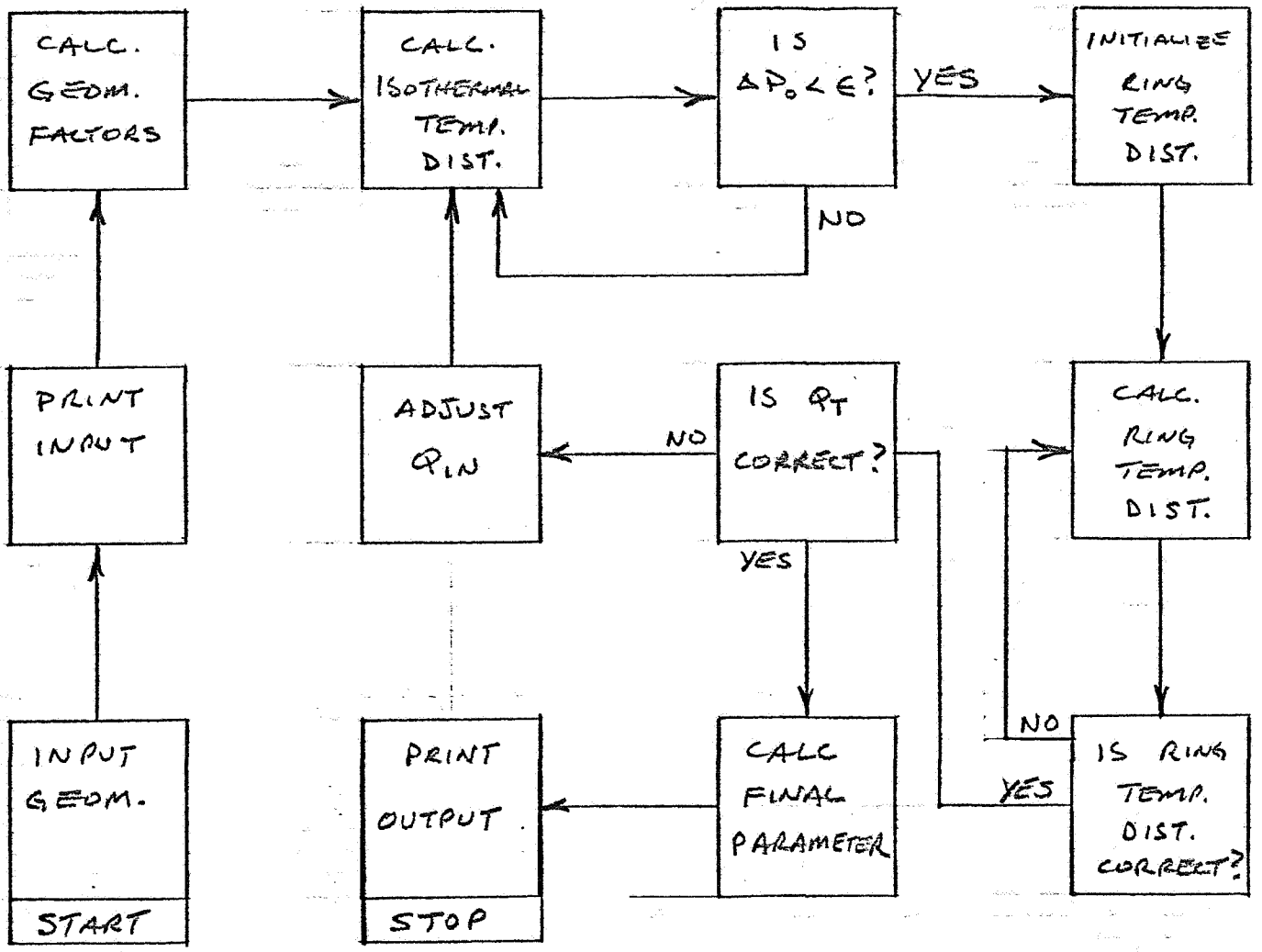

FIG. 3 STATIC PROGRAM LOGIC DIAGRAM

each ring in this iteration loop become the initial estimates for the corresponding temperatures for input to the next iteration loop.

The second iteration loop takes into account the axial heat flow between the individual rings of the generator. One by one, starting with the ring nearest the generator end, the axial heat flow between rings is then calculated. New component temperatures are calculated for each ring and this process is repeated until the temperature distribution yields a heat flow pattern which satisfies the specified total heat input.

A third iteration loop is imbedded in the second loop to calculate the heat transfer occurring relative to the end of the generator. Thus during each pass through the second iteration loop, the end heat transfer and temperature distribution is updated.

Once the convergence criterion for the second iteration loop has been satisfied, the program terminates by printing output information, including the temperature distribution and the electrical performance characteristics of the RTG.

D. DYNAMIC PERFORMANCE ANALYSIS

In addition to the work carried out on the static performance analysis, considerable progress has been made in the area of the dynamic performance analysis of a RTG.

Whereas the solution of the static performance is based upon a heat balance of the generator,the dynamic analysis includes the transient effect in an additive manner as expressed by

$$Q_{in} = Q_{out} + MC \frac{\partial T}{\partial \tau}$$

where Q_{in} = heat input to system,

Q_{out} = heat output from system, and

$MC \frac{\partial T}{\partial \tau}$ = heat absorbed or liberated by system.

The final term in the above equation accounts for the time rate of change of the temperature of the system and vanishes when the system is in thermal equilibrium.

Figure 4 shows the logic diagram of the program for dynamic RTG performance analyses. After input of the geometrical parameters which describe the generator, the heat input and the load voltage, the initial temperature distribution of the entire generator is supplied.

Certain geometric calculations are then performed including the mass of each component and the mass-specific heat product of each component.

Using the temperature distribution, the heat input and heat output of each component in the generator are evaluated. From this the heat absorbed or liberated within each component is computed according to the equation above. Using the mass specific heat calculations made earlier, the rate of change of temperature for each component is calculated and from this the new temperatures of the component are obtained. The above process is repeated for each of the time periods specified unitl the transient has been investigated for the total time of interest.

The programming of the equations necessary to carry out the steps described above is now in progress. Because of the similarities between the logic structure of the dynamic and static programs it is anticipated that the two programs will be combined into a single computer code capable of handling either static or dynamic RTG performance analysis.

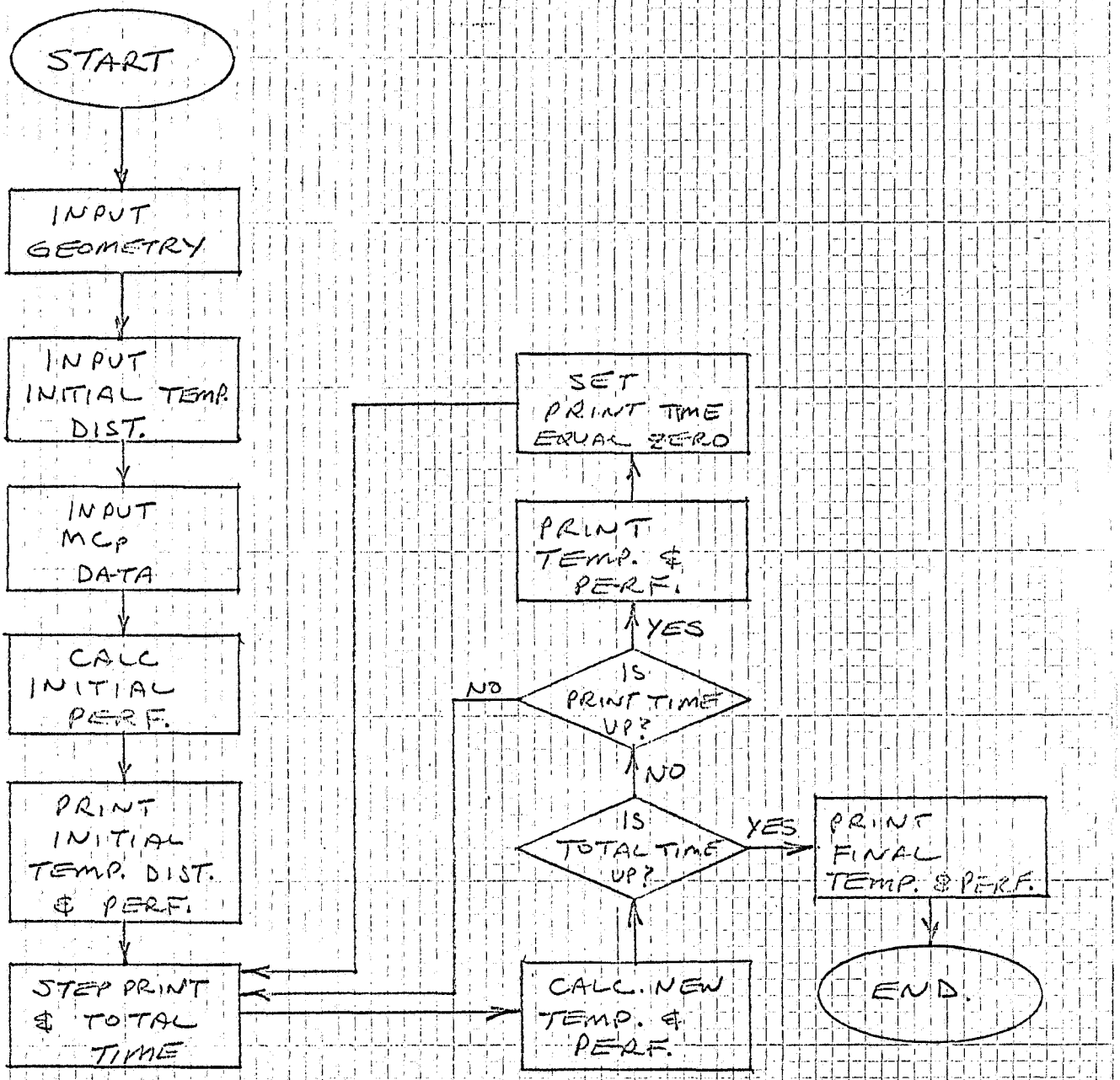
START
INPUT GEOMETRY
INPUT INITIAL TEMP. DIST.
INPUT MCp DATA
CALC INITIAL PERF.
PRINT INITIAL TEMP. DIST. & PERF.
STEP PRINT & TOTAL TIME
SET PRINT TIME EQUAL ZERO
PRINT TEMP. & PERF.
IS PRINT TIME UP?
YES
NO
IS TOTAL TIME UP?
NO
YES
CALC. NEW TEMP. & PERF.
PRINT FINAL TEMP. & PERF.
END.

Figure 4

III. MATERIAL STUDY

A. INTRODUCTION

This part of the overall program is aimed at characterizing the long-term behavior of the thermoelectric properties of silicon-germanium alloys, developing a solid-state dopant precipitation model, and investigating the effects of factors such as raw material purity and material preparation techniques on the thermoelectric properties of silicon-germanium alloys.

A detailed study plan was prepared for this task early in the overall program. This plan was submitted to the Jet Propulsion Laboratory for approval and upon receipt of approval, the implementation of the study outlined in the plan was initiated. The implementation of the study has involved essentially two independent preliminary courses of action. The first involved the design and construction of test equipment suitable for conducting the experimental phases of the study and the second consisted of defining the silicon-germanium alloy test sample requirements of the study and ordering these test samples from the RCA Corporation. Whereas work on the design and construction of the test equipment needed to perform the material study proceeded according to plan and was completed before the end of the time period covered by this report, the receipt of test samples from the RCA Corporation was extremely slow and the first few samples were received at the very end of the period. No test data on the time/temperature behavior of silicon-germanium alloys were thus obtained during the report period. Analytical work on the precipitation of phosphorus in n-type 63 a/o Si - 37 a/o Ge alloy and 80 a/o Si - 20 a/o Ge alloy was however carried out as a special study during this period. The results of this work are summarized elsewhere in this report.

The present discussion of the material study task will primarily concern itself with the background of the task and the work done on the design and construction of the test equipment needed to conduct the experimental study. The status of required test samples procurement will also be reviewed.

B. BACKGROUND DISCUSSION

A fairly good qualitative understanding exists of the time and temperature dependence of the thermoelectric properties of silicon-germanium alloys. Inasmuch

as much of this subject has already been covered in fair detail elsewhere[1], there exists little reason for the repetition of a detailed discussion here. Nevertheless, in view of its applicability to the topic at hand and for purposes of completeness, a brief summary of the factors underlying the time dependence of the thermoelectric properties of silicon-germanium alloys is appropriate.

The worth of a material for thermoelectric energy conversion is approximately indicated by the so-called figure-of-merit which combines the three thermoelectric properties, the Seebeck coefficient S, the electrical resistivity ρ and the thermal conductivity k in the well known relationship

$$Z = \frac{S^2}{\rho k} \quad .$$

It has generally been established that extrinsic semiconductors with carrier concentration values in the range 10^{19} to 10^{21} carrier per cubic centimeter possesses values of figure-of-merit higher than those of any other grouping of materials; silicon-germanium alloys are semiconductors for which the figure-of-merit maximizes in the extrinsic range for carrier concentration values of the order of 2×10^{20} carriers per cubic centimeter. As with extrinsic semiconductors in general, the bulk of the indicated carrier concentration in silicon-germanium alloys is obtained through the addition of impurities during crystal growth. Each impurity atom, or dopant atom, as they frequently are called, in solid solution in the crystal donates one or more carriers to the lattice. Because of the high carrier concentration required for maximizing the figure-of-merit it is usually found that only a relatively few dopants exist for any given semiconductor that have solid solubilities sufficiently great for yielding the desired impurity carrier concentration. In silicon-germanium alloys only certain of the Group III and Group V elements satisfy this requirement.

The addition of Group III elements to silicon-germanium alloys yields material with p-type characteristics because Group III elements possess three valence electrons, one less than is required to form complete bonds with the four nearest

neighbor silicon and germanium atoms. The deficiency of an electron manifests itself exactly as if an electron were neutralized by a positive carrier; hence, the p-type behavior of the crystal. Of all Group III elements, it is boron that has the highest solid solubility in silicon-germanium alloys. In fact, the solid solubility of boron in silicon-germanium alloys is sufficient to enable doping of the alloys to carrier concentration values of the order of 10^{21} carriers per cubic centimeter, far in excess of those required for maximizing the figure-of-merit. Silicon-germanium alloys doped with boron for maximum figure-of-merit are therefore doped considerable below the solid solubility limit of boron in these alloys. The result is that the system of dopant and lattice is in equilibrium and the properties of boron doped p-type silicon-germanium alloys are stable with time and temperature. Although other Group III elements could also be used as dopants, it is boron that because of its high solid solubility is usually used as the p-type dopant for silicon-germanium alloys. The solid solubilities of other Group III elements in silicon-germanium alloys, although relatively great, are smaller than that of boron, and, in fact, in most cases are marginal for the attainment of maximum figure-of-merit values.

The addition of Group V elements to silicon-germanium alloys yields material with n-type characteristics. Group V elements possess five valence electroncs, one more than is needed to form complete bonds with the four nearest neighbor silicon and germanium atoms. The excess electron is consequently very weakly bound to its parent atom and thermal energy, even at room temperature, is sufficient to unbind it and make it a free carrier. Each Group V dopant atom therefore contributes one n-type carrier to silicon-germanium alloys. In order to obtain a carrier concentration of the order of 2×10^{20} carriers per cubic centimeter required for maximizing the figure-of-merit of silicon-germanium alloys, it is consequently necessary to dope the alloys to impurity concentrations of the same order. Unfortunately, none of the Group V elements possesses a solid solubility in silicon-germanium alloys sufficient at all temperatures for accomplishing this. Because it comes closest, however, to satisfying the solid solubility requirement, it is phosphorus that is commonly used as the n-type dopant in silicon-germanium alloys.

Phosphorus exhibits a so-called retrograde solid solubility in silicon-germanium alloys. The solid solubility attains a maximum at temperatures of the order of 900 to 1100°C and decreases at both higher and lower temperatures. In order to maximize the figure-of-merit of phosphorus doped silicon-germanium alloys, it is therefore necessary to dope the alloys to impurity concentration values consistent with the maximum solid solubility of dopant at temperatures in the range of 900 to 1100°C. When this is done, however, there exists an excess of dopant at both higher and lower temperatures; silicon-germanium alloys doped in this manner are super-saturated with dopant. Because of the resultant instability, the system of dopant and lattice tends to equilibrium by precipitating any dopant in excess of its solid solubility at any given temperature. This effect of a decreasing dopant, and hence carrier concentration, manifests itself in changed electrical properties as a function of time; both the electrical resistivity and Seebeck coefficient increase with time in such a manner that the quantity S^2/ρ slightly decreases. Inasmuch as the thermal conductivity remains nearly unchanged, the figure-of-merit of n-type silicon-germanium alloys slightly decreases with time.

The rate and extent to which the thermoelectric properties of n-type silicon-germanium alloys change with time is obviously temperature dependent. At the temperatures of maximum solid solubility of phosphorus, the material is in equilibrium and thus little change takes place. At temperatures exceeding those of maximum dopant solid solubility, the precipitation process goes to completion extremely fast because of the high temperatures in question. It is at temperatures below those of maximum dopant solid solubility that observable long-term changes in the electrical properties of n-type silicon-germanium alloys occur. Because the solid solubility of phosphorus decreases with temperature at temperatures below the solid solubility maximum, the "driving force" for precipitation increases with decreasing temperatures. The net result of the opposing temperature dependences of these two mechanisms is that it is at intermediate temperatures in the range of 300 to 700°C that the biggest changes occur in the electrical properties of n-type silicon-germanium alloys as a result of dopant precipitation. At very low temperatures, such as room temperature, precipitation proceeds so slowly as to be practically unobservable.

Inasmuch as dopant precipitation in n-type silicon-germanium alloys is a diffusion limited process, the carrier concentration, and hence the thermoelectric properties of electrical resistivity and Seebeck coefficient have exponential-like time dependences. Initially the values of these properties change fairly rapidly. As time proceeds, however, the rate of change decreases until it vanishes as dopant solid solubility equilibrium is approached asymptotically. The process has an extremely long time constant; at the intermediate temperatures at which the biggest changes typically occur in thermoelectric properties of n-type silicon-germanium alloys, it is projected that the process has not gone to completion even after several years of operation.

Because the electrical resistivity and Seebeck coefficient both depend on the carrier concentration, in principle it is possible to predict the behavior of either property on the basis of the known behavior of the other property. This interrelationship of electrical resistivity and Seebeck coefficient has been experimentally well documented for n-type silicon-germanium alloys over a wide range of temperatures and carrier concentration values and is illustrated in Figure 5. It has been established that the data of Figure 5 are applicable for all silicon-germanium alloys with silicon contents in the range of 60 a/o silicon to 80 a/o silicon and higher. By means of Figure 5 it is possible to predict the values of either the electrical resistivity or Seebeck coefficient of n-type silicon-germanium alloys on the basis of known values of the other property for any temperature in the range of 300 to 1100°K. Extrapolation of data in Figure 5 enables the approximate extension of the known interrelationship of properties to even higher temperatures. From Figure 5 it is seen that increased electrical resistivity values are accompanied by increased Seebeck coefficient values in n-type silicon-germanium alloys; the electrical resistivity is an inverse function of carrier concentration and generally increases as a result of dopant precipitation. It is thus possible to monitor only one of these electrical properties of n-type silicon-germanium alloys in order to completely characterize the electrical behavior of the alloys as a function of time. Relationships between electrical resistivity and Seebeck coefficient, similar to those of Figure 5 , are also known for the p-type silicon-germanium alloys.

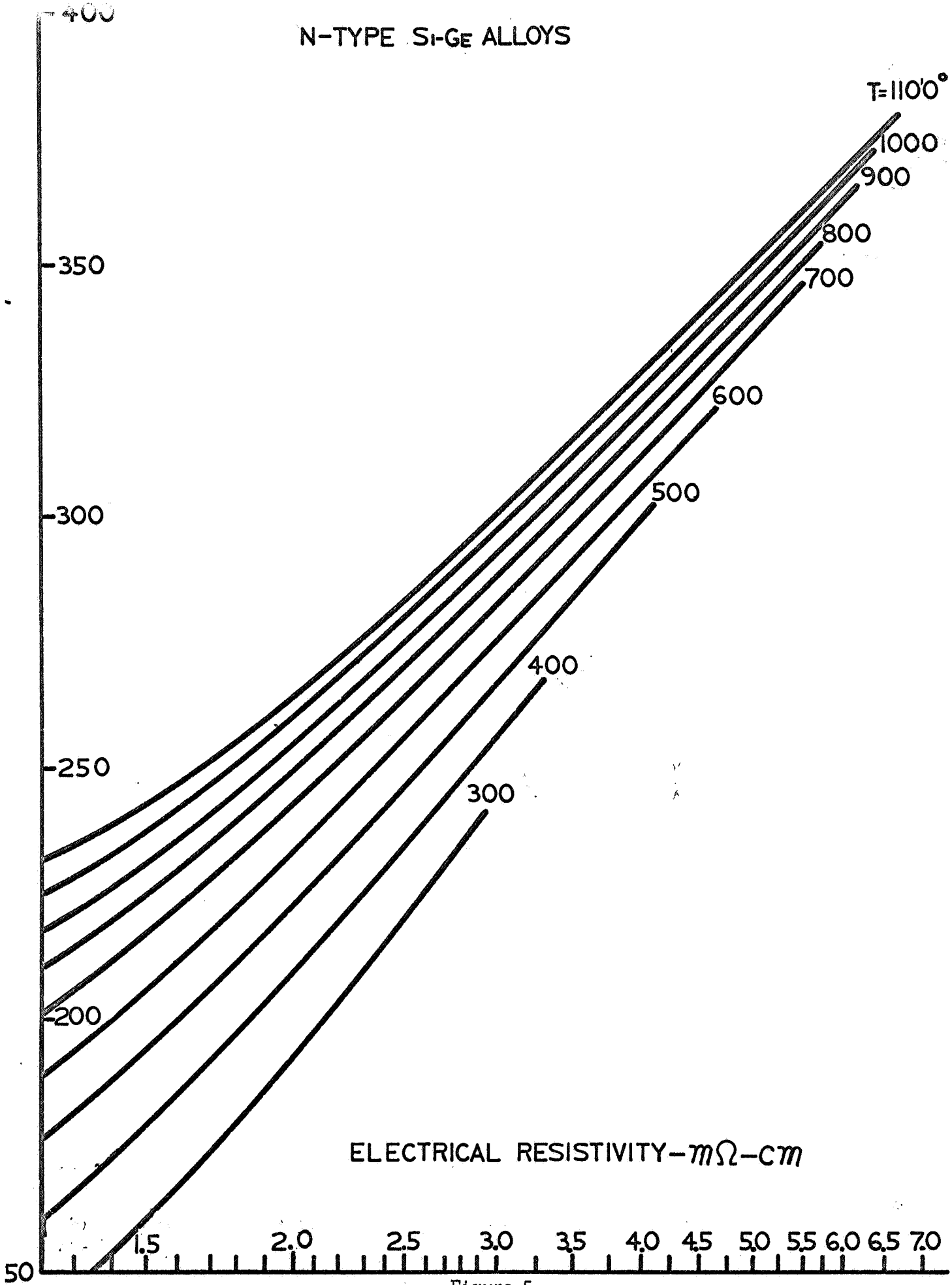
N-TYPE Si-Ge ALLOYS
T=1100°K
1000
900
800
700
600
500
400
300
400
350
300
250
200
50
ELECTRICAL RESISTIVITY-mΩ-cm
1.5
2.0
2.5
3.0
3.5
4.0
4.5
5.0
5.5
6.0
6.5
7.0

Figure 5

As concerns the remaining thermoelectric property, the thermal conductivity, it has been established for n-type silicon-germanium alloys that relatively small changes in carrier concentration are nearly self-compensating such that the effect on thermal conductivity is practically negligible. It is probable, however, that large changes in carrier concentration, such as anticipated for the alloys at the intermediate temperatures in very long-term operation, have a measurable effect on thermal conductivity. In general, it may be expected that dopant precipitation will lead to somewhat reduced values of thermal conductivity, a condition that tends to off-set some of the reduction in performance associated with increased values of electrical resistivity and Seebeck coefficient. Therefore, although the behavior of electrical resistivity and Seebeck coefficient as a function of time probably control the overall performance characteristics of n-type silicon-germanium alloys in long-term operation, for completeness it is also necessary to consider the behavior of the thermal conductivity.

C. EXPERIMENTAL PROCEDURE

The basic experimental method to be used in the determination of long-term behavior of the thermoelectric properties of silicon-germanium alloys is one that determines the electrical resistivity of selected samples as a function of time at a variety of different operating temperatures. The use of known relationships between electrical resistivity and Seebeck coefficient, such as illustrated in Figure 5, enables the determination of corresponding Seebeck coefficient behavior from measured values of electrical resistivity. For simplicity, and because there is no evidence, either theoretical or experimental, that microscopic in-gradient dopant diffusion either occurs to any significant extent or contributes to changes in the thermoelectric properties of silicon-germanium alloys, the bulk of the experimental effort will involve the isothermal annealing of test samples. For completeness, a few samples will be subjected to in-gradient annealing. In the latter case attempts will not only be made to monitor electrical resistivity but also the Seebeck coefficient as a function of temperature.

Although expected to be relatively minor, some change in the thermal conductivity of n-type silicon-germanium alloys, as discussed in the preceding section,

may be anticipated after extended operating times. It is planned therefore to investigate this phenomenon by performing thermal conductivity measurements on selected samples prior to and after long-term anneal. Inasmuch as all precipitation related thermal conductivity changes are expected to be most pronounced at the intermediate operating temperatures, the effort in this area will be restricted to samples that are annealed at temperatures in the range of 400 to 600°C. The choice of these temperatures coincides with the upper useful range of measurement of direct thermal conductivity by means of a comparative method that will be used on the program. Changes in thermal conductivity at higher and lower temperatures, if any, are expected to be quite small and thus easily estimated from the measured behavior of the electrical properties of the test samples.

The primary purpose of the planned study is to establish the long-term behavior of the thermoelectric properties of the 80 a/o silicon - 20 a/o germanium alloy at different temperatures. Although the bulk of the experimental effort will thus concern itself with the 80 a/o silicon content alloy, the study will also consider other alloy compositions for purposes of enabling a more complete understanding of the precipitation process in silicon-germanium alloys. It is thus planned to also include alloys with other silicon contents in the study. All alloys will not receive equal emphasis in the study. Next to the 80 a/o silicon - 20 a/o germanium alloy, it is planned to most thoroughly investigate the alloy with a silicon content of 63 a/o.

The bulk of the experimental effort will concern itself with phosphorus doped n-type silicon-germanium alloys, because it is these alloys that exhibit the most pronounced changes in thermoelectric properties with operating time. For completeness and because small changes have on occasion been observed in the thermoelectric properties of p-type silicon-germanium alloys with operating time at temperatures in the range of 500 to 800°C, it is planned to include some p-type samples in the overall study. The number of such samples, however, will be kept small. Moreover, because of recent interest in the practical large-scale use of silicon-germanium alloys prepared by means of hot pressing, it is alloys prepared by this technique that will receive the greatest attention in the planned study. Most of the material evaluated in the study will be purchased from the RCA Corporation because

it is this material that is planned for use in aerospace devices, such as the Multi-Hundred Watt RTG. Additional material will be prepared by Resalab Scientific if on the basis of preliminary findings in the planned study it becomes advisable to also investigate specially prepared materials in regards to purity of raw materials and variation in preparation technique.

Most of the silicon-germanium alloy samples in the planned study will be in the shape of parallelepipeds of dimensions 0.25 x 0.25 x 1.5 inches. The samples that will be used to evaluate the effects of dopant precipitation on thermal conductivity will be right cylindrical with about 5/8 inch diameter and 1.5 inch length. The samples used for in-gradient tests will be of the latter configuration and dimensions.

For completeness of results, the planned study of long-term behavior of the thermoelectric properties of silicon-germanium alloys will primarily consist of two experimental parts. The first part will establish the beginning-of-life behavior of silicon-germanium alloy properties at a number of temperatures for operating times up to one year. The second part will empirically establish the end-of-life properties through dopant variations introduced during material preparation. The rationale of the approach in question is best explained with reference to Figure 6. The electrical resistivity of n-type silicon-germanium alloys has the characteristic exponential-behavior illustrated by the lower curves in Figure 6; the electrical resistivity starts at relatively low values and in time asymptotically approaches the value at any given temperature that corresponds to the equilibrium solid solubility of dopant at that temperature, illustrated by the dashed line in Figure 6. If the initial dopant concentration is reduced, the system of dopant and lattice is more nearly in equilibrium and the degree of supersaturation decreases. The corresponding electrical resistivity behavior as a function of time can now be represented by the top solid curve below the dashed line; the total change in electrical resistivity as a function of time decreases as the initial dopant concentration in the alloy approaches its equilibrium solid solubility. If the initial dopant concentration is reduced to levels below those of the equilibrium solid solubility, it is expected that the electrical resistivity will remain constant with time because the condition of dopant supersaturation no longer exists; this condition is illustrated by the upper-most solid curves in Figure 6.

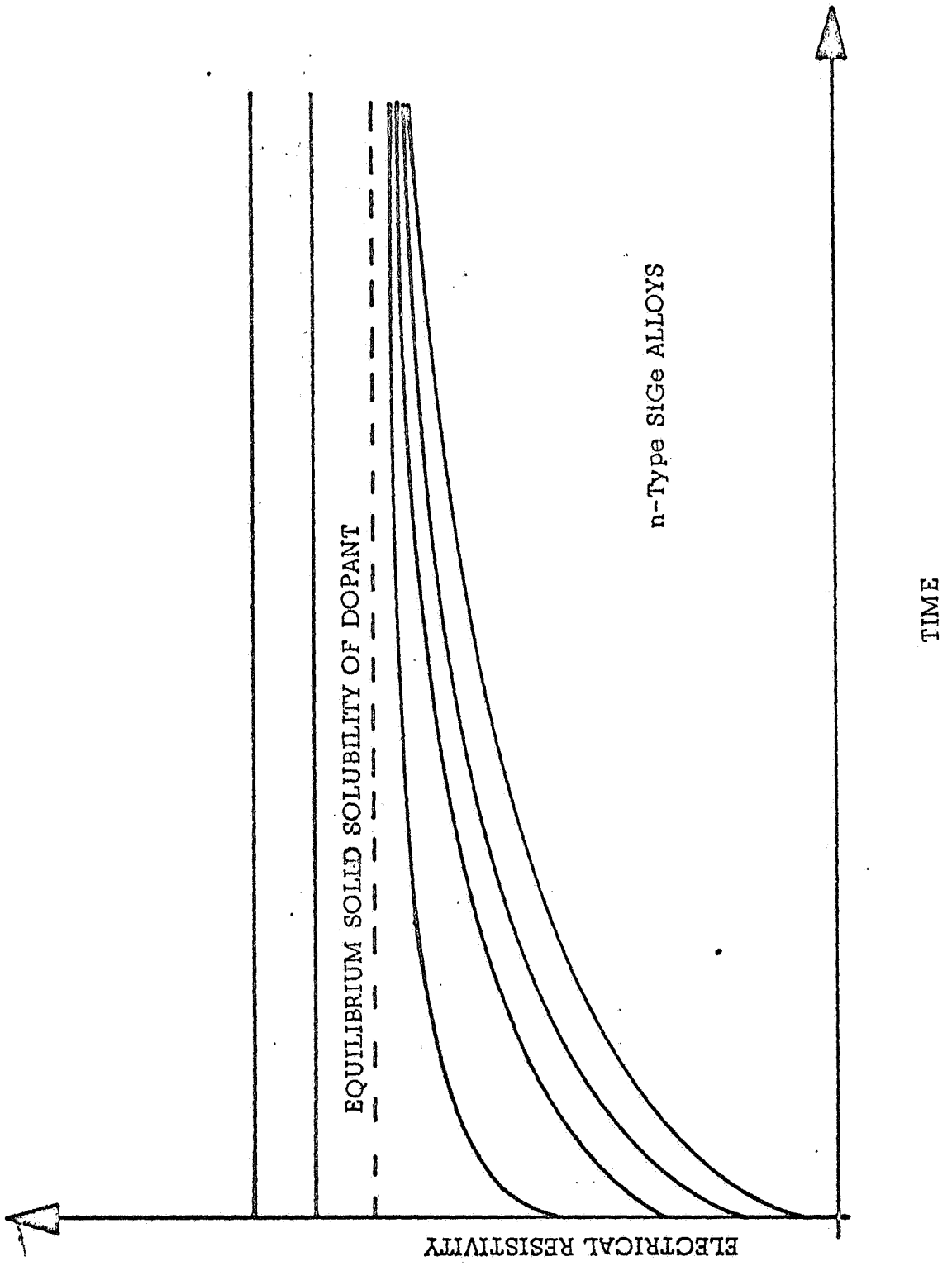
n-Type SiGe ALLOYS
EQUILIBRIUM SOLID SOLUBILITY OF DOPANT
ELECTRICAL RESISTIVITY
TIME

Figure 6

In principle, it is possible to determine the life behavior of the electrical properties of standard highly doped silicon-germanium alloys by measuring these properties as a function of time until the attainment of solid solubility equilibrium. Inasmuch as the time constants involved pertain to times measurable in years, it is impractical to determine the long-term behavior of the thermoelectric properties of silicon-germanium alloys solely by the anneal and measurement of highly doped samples. Although this will be done in the planned program to establish initial behavior of properties up to operating times of the order of one year, the solid solubility equilibrium levels will be empirically determined by testing at any given temperature a number of samples with a range of doping levels. The experimental part of the planned program will thus consist of two parts, the first of which will determine the beginning-of-life characteristics of silicon-germanium alloys with compositions already discussed and the second of which determines the equilibrium dopant solid solubilities for alloys having silicon contents of 63 and 80 a/o. The results of the two experimental parts of the program will be evaluated and combined by analyses, the third part of the program, that attempt to arrive at a self-consistent precipitation model for the system of silicon-germanium and dopant. This model will then permit the prediction of silicon-germanium alloy properties for any operating time. It is thus possible to characterize the behavior of silicon-germanium alloy thermoelectric properties in long-term operation through the pursuit of an experimental program of relatively short duration.

On the basis of past investigations of the time dependence of silicon-germanium alloy thermoelectric properties, it is known that the biggest changes in these properties occur at temperatures in the range of 300 to 700°C. As already explained, there is little change in these properties at higher and lower temperatures. The emphasis of the planned material study program will therefore be placed on the experimental investigation of the time dependence of silicon-germanium alloy thermoelectric properties in this range of temperatures. It is planned to conduct the long-term annealing studies specifically at 300, 400, 500, 600 and 700°C, with shorter term tests planned also at somewhat higher temperatures.

Although silicon-germanium alloys are capable of air as well as vacuum operation, it is planned to conduct all tests of the planned program in vacuum at ambient pressures of the order of 10^{-5} to 10^{-6} Torr. The reason for testing in vacuum is two-fold. First, the vacuum conditions will stimulate those presently envisioned for silicon-germanium alloy devices that will actually be used in long-term operation and second, the vacuum test conditions will enable the use of refractory metal thermocouples, lead-wires and probes for the instrumentation of test samples.

D. ISOTHERMAL ANNEAL

In performing the isothermal annealing tests a large number of test samples and a wide range of operating temperatures are being considered. The samples are to be tested in the temperature range of 300 - 700°C with temperature increments of 100°C. The majority of samples will be tested at the intermediate temperature levels where the most significant changes in thermoelectric properties are expected to occur. Tests at higher temperatures, 800 and 900°C, will be conducted for a time interval of sufficient duration to confirm the expected minimal changes in thermoelectric properties of silicon-germanium alloys.

A multi-tube furnace has been designed and fabricated to meet the requirements of the experimental program. The entire furnace consists of 42 independently heated quartz tubes which are wrapped with Kanthal "A" heater wire. The tubes are linearly tapered with the heater wire wrapping density increasing toward the outer edges to account for end-losses. This procedure permits flattening of the axial temperature profiles along the tubes. The furnace tubes are inserted into the "honeycomb" furnace rack which is constructed of 316 stainless steel and Marimet-45* thermal insulation. Whereas the stainless steel furnace rack is used only as a structural member, the insulating board forms the individual compartments for the quartz furnace tubes. Insulation is used to minimize thermal coupling between adjacent furnace units.

An isometric view of the stainless steel rack structure is shown in Figure 7. The rack is designed to accept sheets of insulating board to form an enclosed

---

* Johns-Manville tradename

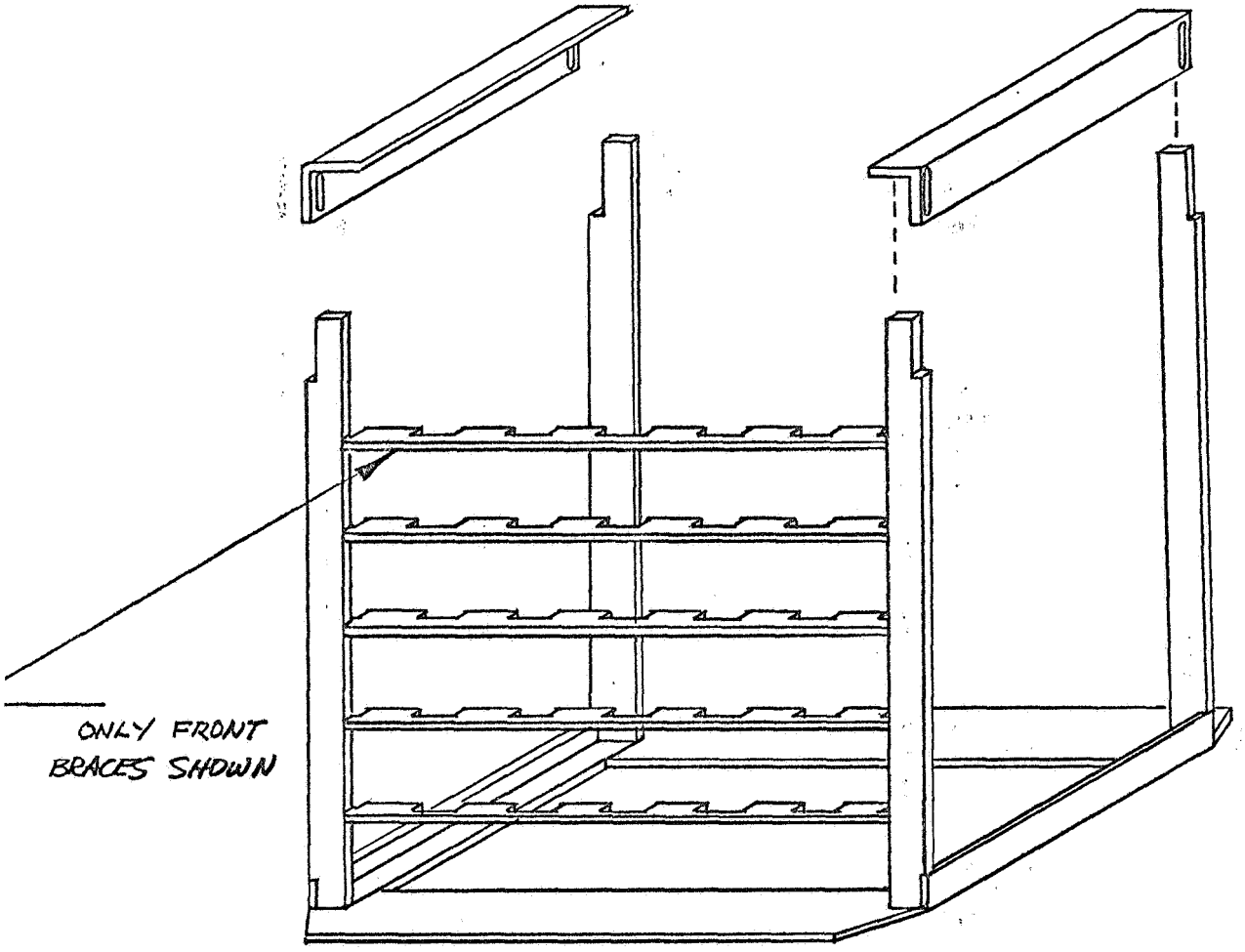

Figure 7 - ISOTHERMAL ANNEALING FURNACE RACK
OVERALL VIEW

structure with 42 individual compartments. A partial full-scale front view of the complete furnace structure is shown in Figure 8. The insulated compartments are somewhat larger than the furnace tubes in order to allow the insertion of thermally conductive metal tubes, should additional flattening of the axial temperature profile be required. Elementary heat transfer considerations indicate this additional temperature flattening will not be required when samples of 1.5 inch length are being heated. The addition of metal tubes is almost certainly required, however, in the case of longer test samples.

A simple variac arrangement that uses well regulated input power is utilized to heat the furnace tubes. The input power is obtained from a 3KVA regulator which is mounted within the heater power rack. The regulator is capable of maintaining an output accuracy of ± two percent while the input line may vary from 90 to 140 volts. A schematic diagram of a typical two ampere heater power panel is shown in Figure 9. It has been determined that the two ampere heater capacity will provide sufficient power for temperature levels of 300, 400 and 500°C; while, three and four ampere heater capacity will be required for the higher temperatures. Heater current and voltage measurements will be recorded by panel meters located near the heater adjustment variac. Figure 10 is a schematic diagram of the meter panel to be used in these measurements.

Since it is desired to determine the long-term thermoelectric property changes that occur in a vacuum environment, a vacuum system suitable for the tests had to be provided. Of primary importance is the capability of the system to handle the gas load at temperature as well as provide adequate interlock protection should some anomaly occur. A high capacity oil diffusion system employing a stainless steel bell jar is being used with interlocking provision as shown in Figure 11. The vacuum system is protected from the loss of chamber cooling, over pressure, and loss of diffusion pump cooling.

An automatic data system will be used exclusively to monitor sample temperatures and resistance. Temperature readings will be made hourly and the resistance measurements will in general be performed on a weekly schedule unless rapid

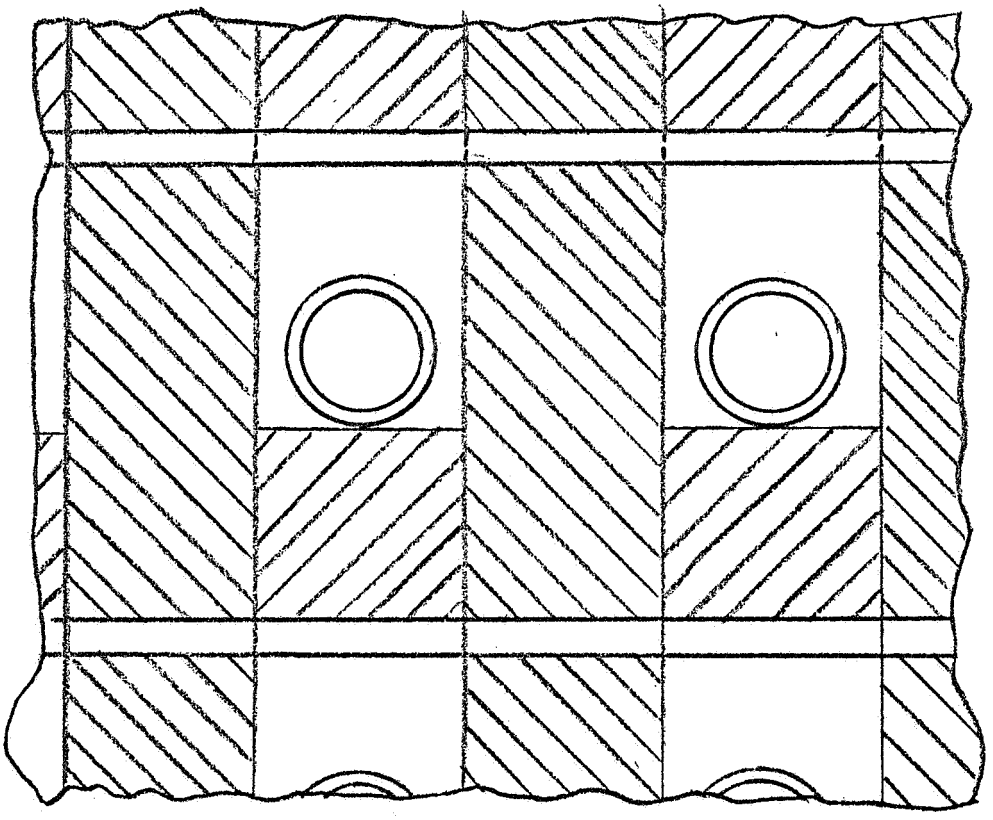

Figure 8 - ISOTHERMAL ANNEALING FURNACE RACK
CLOSE-UP VIEW OF END

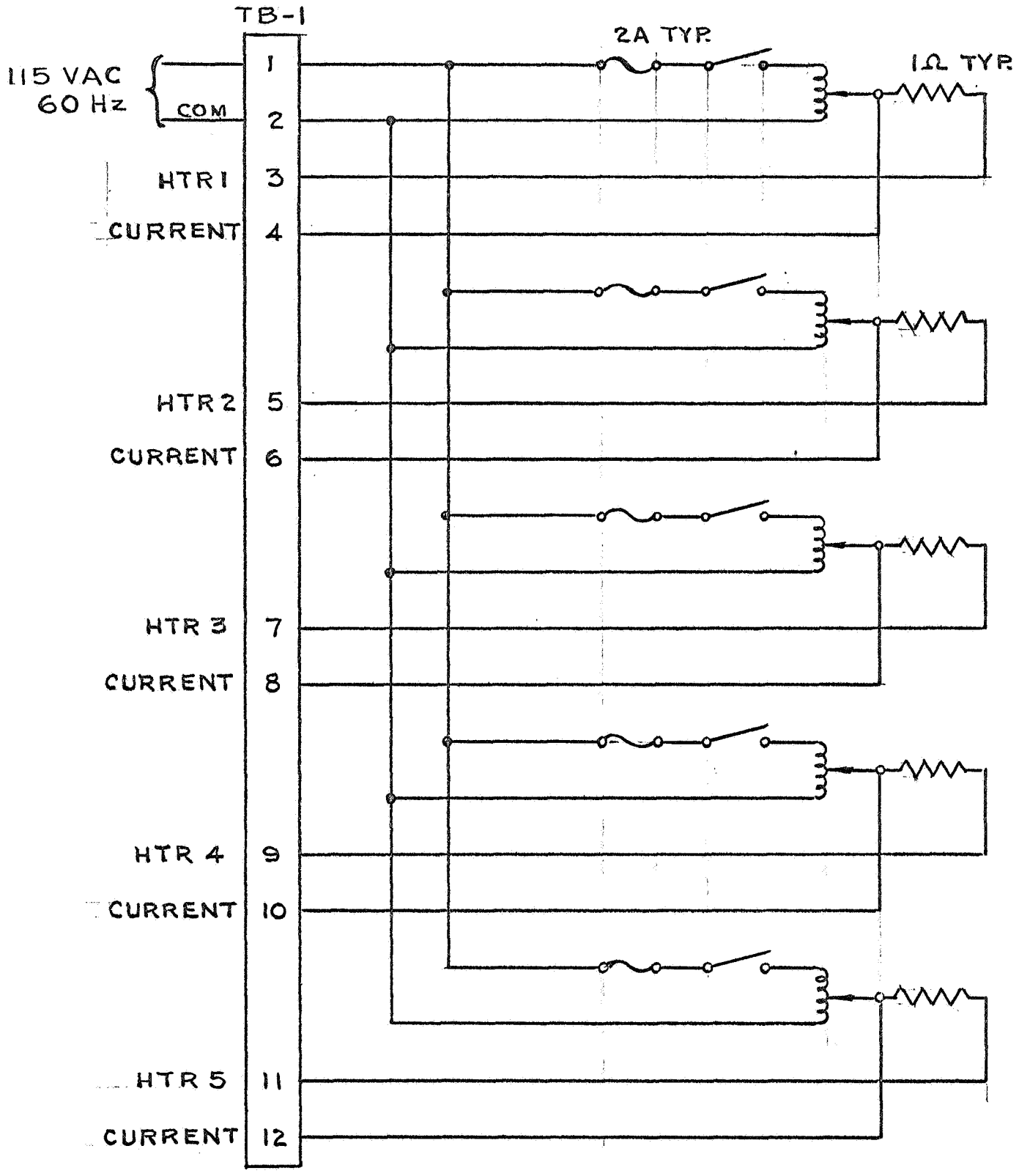

Figure 9 - SCHEMATIC FOR ELECTRICAL HEATER POWER

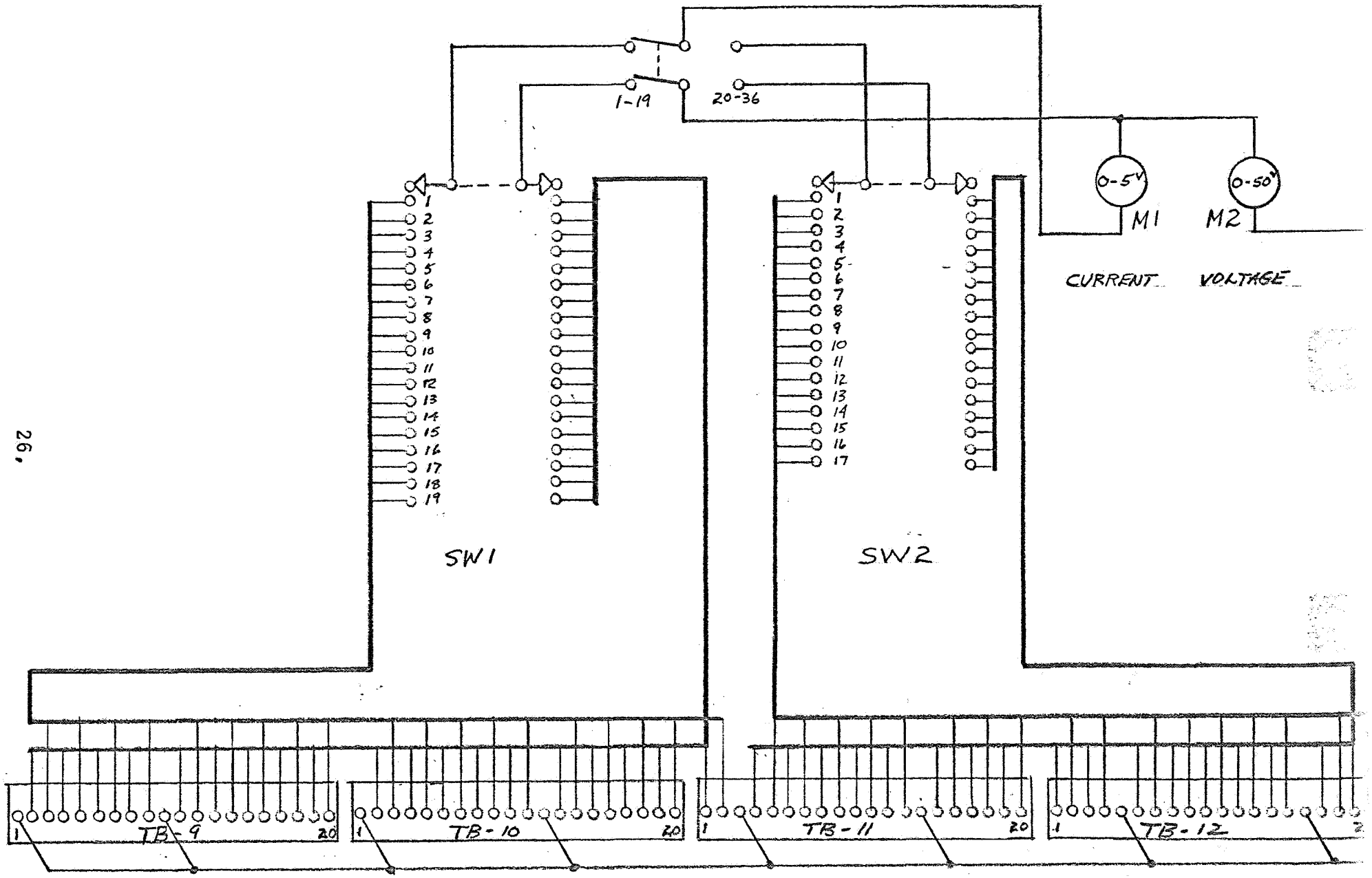

METER PANEL

FIG. 10

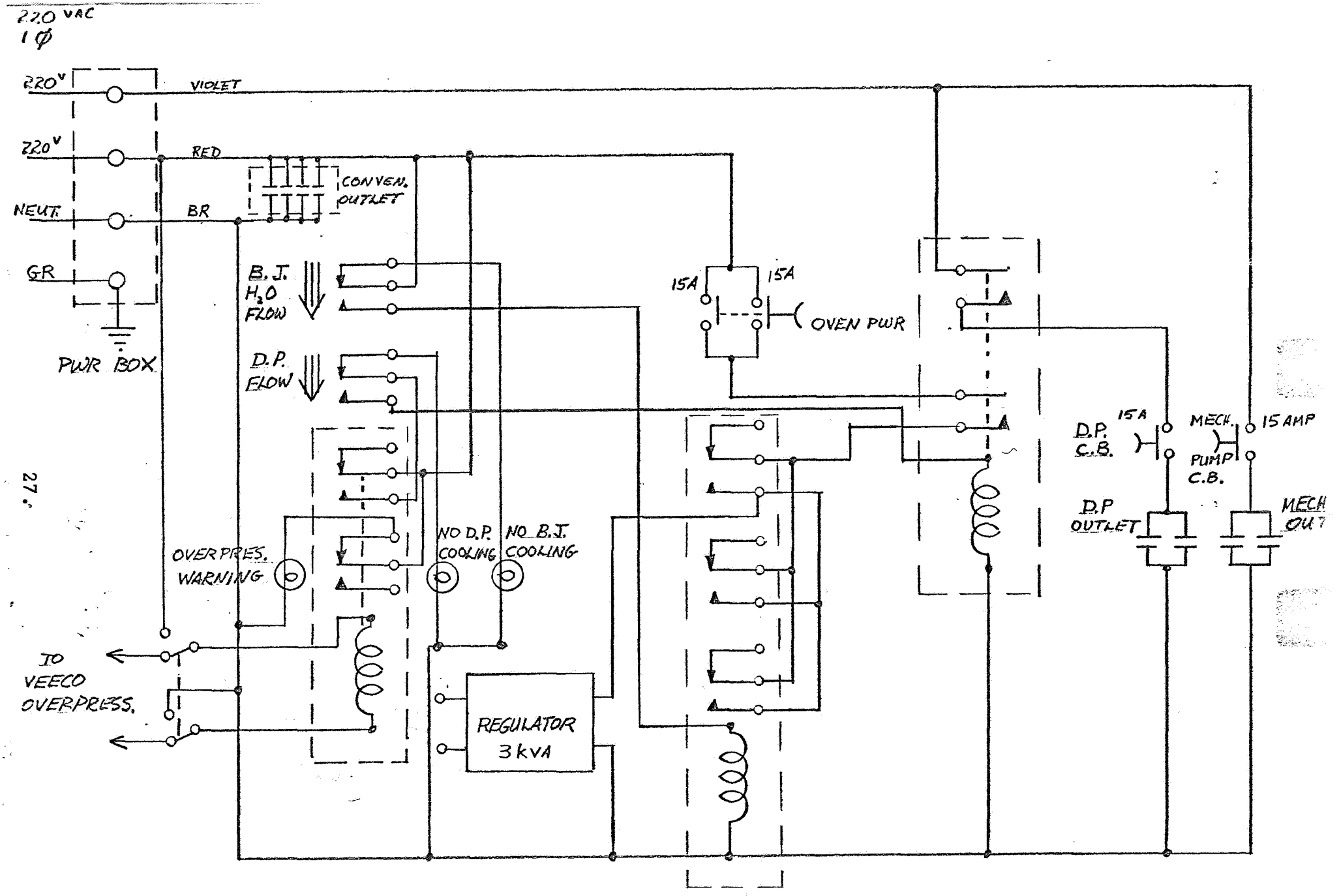

INTERLOCK & PWR. DIST.

FIG. 11

changes are occurring. The frequency of resistance measurements is extended to a weekly interval because of the semi-automatic method to be used in data collection. In addition, the measurements will require rather lengthly data reduction even though processing will be accomplished on a time-sharing computer.

E. IN-GRADIENT TEST

Four cylindrical silicon-germanium alloy samples of 5/8 inch diameter by 1.5 inch length will be subjected to in-gradient annealing between 50 and 1000°C. Although there is no evidence that in-gradient dopant diffusion occurs to any significant extent, these tests will be performed for completeness. The samples will be instrumented with a minimum of four uniformly spaced tungsten/niobium thermocouples for the purpose of temperature, electrical resistivity and Seebeck coefficient measurement as a function of time. The four test samples will be comprised of silicon-germanium alloys with silicon contents of 63 and 80 a/o. One sample of each polarity will be tested for both alloy compositions. Also, since some small changes in the thermal conductivity of the n-type samples are likely to occur, the conductivity of these samples will be measured both before and after in-gradient testing.

The in-gradient test fixture has been designed to operate between the temperature extremities of 50 to 1000°C. For the given sample length, an axial temperature gradient of the order of 250°C/cm will be realized. The fixture to be used in these tests is shown in Figure 12. The test fixture consists of a water cooled copper heat sink common to all four samples, and four molybdenum heater disks placed on the top of each individual sample and spring loaded into position. Heat is supplied to each sample by three spiral shaped Kanthal "A" heater wires. These heater wires are placed inside Al_2O_3 insulating tubes and then the tubes are inserted into the molybdenum heater disk as shown in Figure 13. Each Kanthal "A" heater element dissipates approximately 118 watts at 2.5 amperes which yields a total heat input nearly twice that calculated to be required.

Silica cylinders are placed around the test samples and the intervening space is filled with Sil-O-Cel insulating powder. Ceramic stand-offs are located around the parameter of the copper heat sink to provide an instrumentation "tie point" for modular assembly.

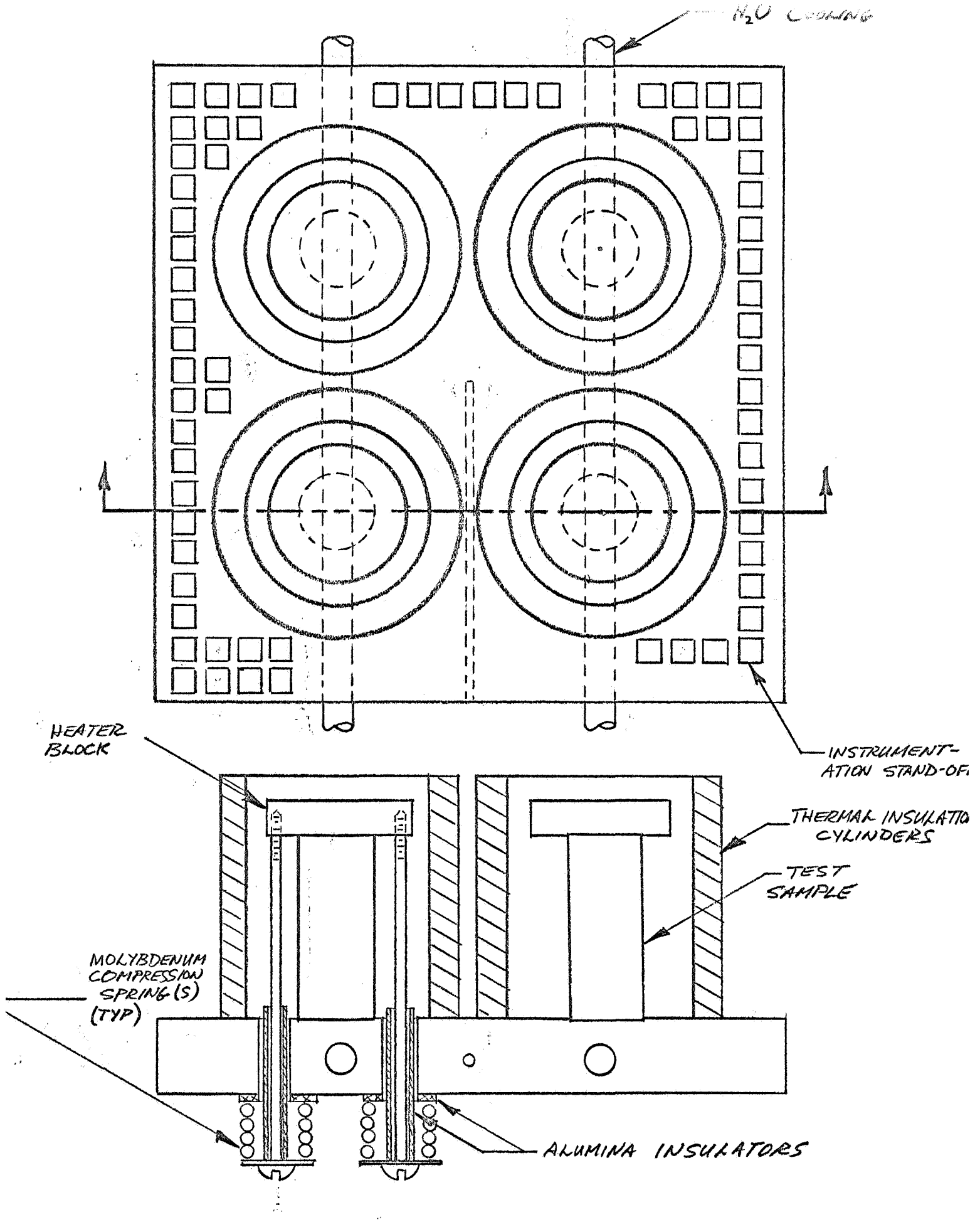

Figure 12 - IN-GRADIENT TEST FIXTURE

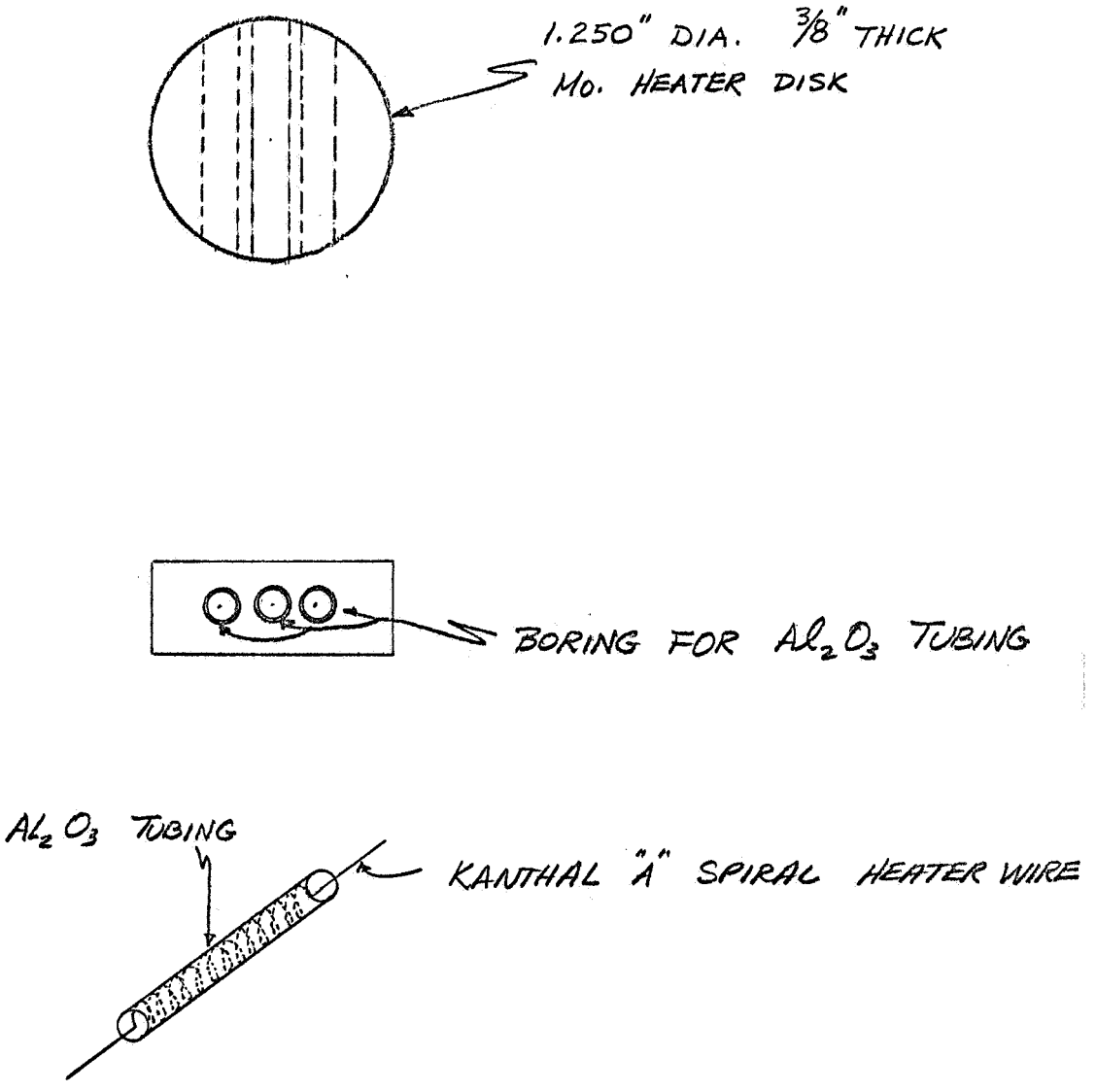

Figure 13 - HEATER DISK

A two inch diffusion system will be used to perform in-gradient testing. A panel designed to provide power to the four molybdenum heater disks, as well as to monitor different parameters, has replaced an obsolete two heater panel. In addition, a switching panel has been included to permit the semi-automatic recording of data. The switching panel, described in the Second Quarterly Report, contains provisions for continuously monitoring cold-junction temperature and switching to measure hot-junction temperature as well as Seebeck voltage, temperature and resistance. The schematic diagram of the in-gradient test station power supply is shown in Figure 14.

F. THERMAL CONDUCTIVITY MEASUREMENTS

It has been established for n-type silicon-germanium alloys that relatively small changes in carrier concentration are nearly self-compensating, such that the effect on thermal conductivity is practically negligible. It is probable, however, that large changes in carrier concentration, such as anticipated for the alloys at the intermediate temperatures in very long-term operation, have a measurable effect on thermal conductivity. In general, it may be expected that dopant precipitation will lead to somewhat reduced values of thermal conductivity, a condition that tends to off-set some of the reduction in performance associated with increased values of electrical resistivity and Seebeck coefficient. Therefore, although the behavior of electrical resistivity and Seebeck coefficient as a function of time probably control the overall performance characteristics of n-type silicon-germanium alloys in long-term operation, for completeness it is also necessary to consider the behavior of the thermal conductivity.

Thermal conductivity measurements will be performed utilizing the comparative technique. The fixture to be used in these tests is shown in Figure 15. The apparatus consists of two molybdenum blocks wrapped with tantalum sheathed heater wire. The "stack" is composed of two pyroceram heat meters with the unknown sample located in the center position. The stack is spring loaded ($\approx$170 PSI) against the heater blocks with gold-spacers at the interfaces to minimize surface irregularities. An additional 0.001 inch thick refractory diffusion barrier is placed on each end of the sample to avoid material contamination.

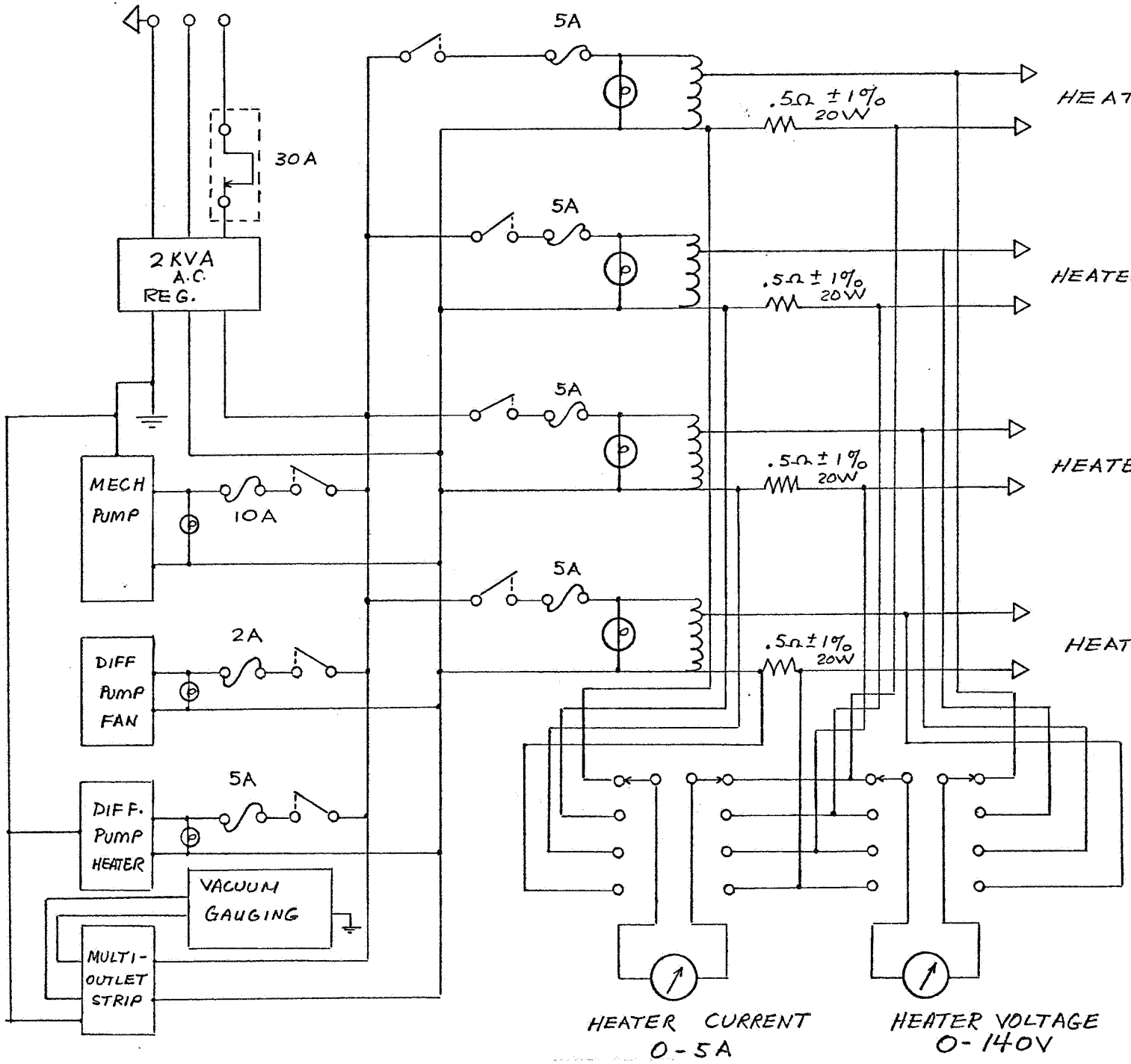

FIG. 14

IN GRADIENT
TEST STATION
POWER SUPPLY

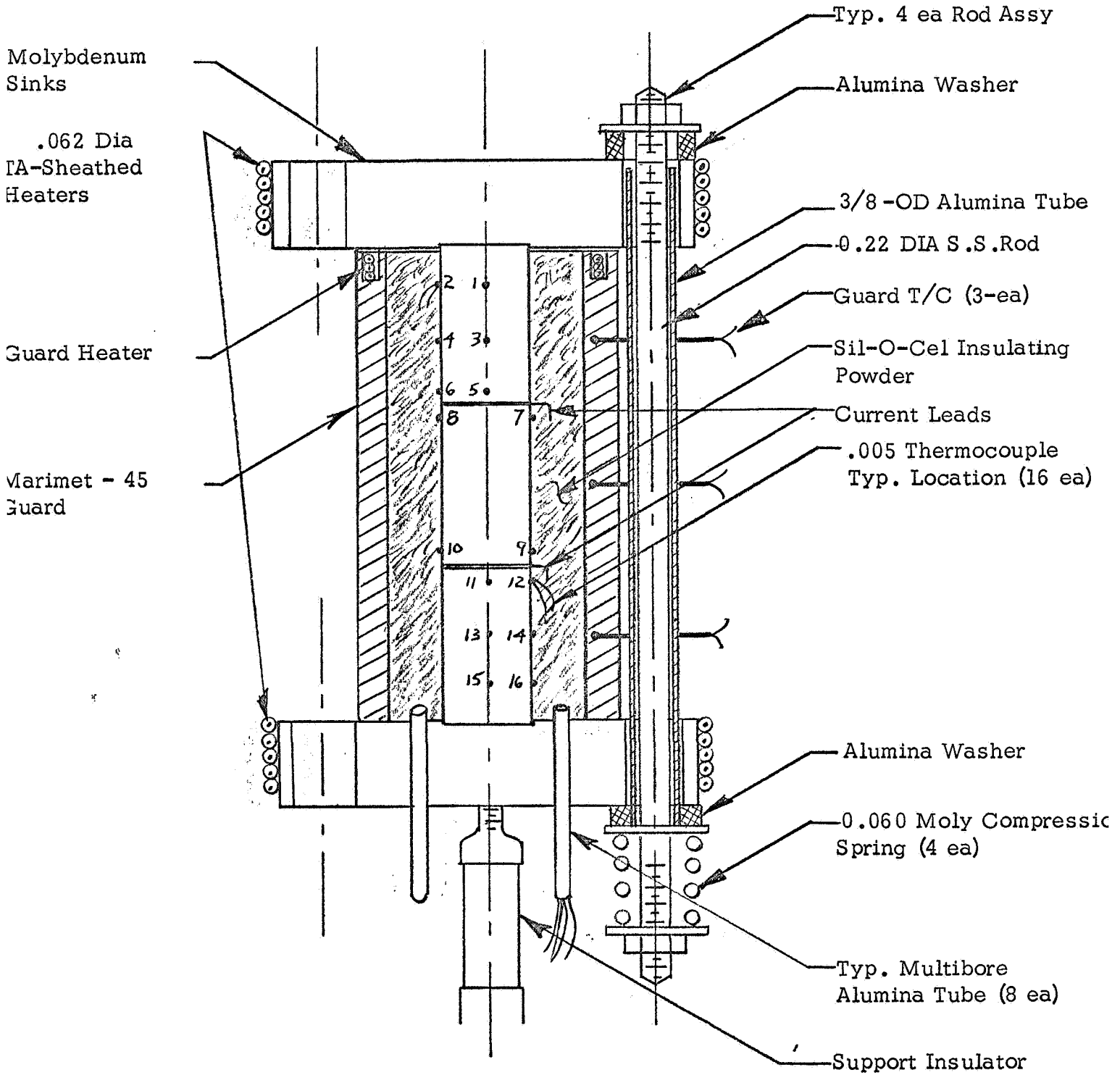

Figure 15 - APPARATUS FOR THE MEASUREMENT OF THERMOELECTRIC PROPERTIES

The "stack" is surrounded by a combination of Sil-O-Cel and a Marimet-45 insulation cylinder. The heater located in the top of the Marimet-45 guard-cylinder allows adjustment of its temperature so as to nearly match the profile of the stack and thereby minimize radial heat losses. Tungsten-niobium thermocouples are located at the numbered positions to allow monitoring of the required temperatures. Thermocouples enter the test fixture through eight multi-bore tubes located on the bottom heater block and are made of wires of 0.005 inch diameter to minimize conductive heat losses. Not shown in the figure is the external furnace which surrounds the test fixture during operation.

The comparative thermal conductivity apparatus can be used to measure the temperature dependence of both resistivity and Seebeck coefficient. For this purpose, the only additional instrumentation required, beyond that needed for thermal conductivity measurements, is the current lead attachment to the refractory diffusion barrier. The addition of the current leads permits "four-probe" resistance measurements with the sample thermocouples providing the voltage probes. In determining the Seebeck coefficient, common legs of the sample thermocouples are used as voltage probes.

What appears to be an excess of heat meter thermocouples actually provides information that allows graphical integration of the heat flow through each pyroceram section. The three thermocouple pairs in each heat meter, are used to establish heat flow as a function of position along the "stack" and thus by extrapolation the heat flow through the sample may be established. Surface and center-line couples are included in order to measure the radial temperature gradient and corresponding radial heat flow in the meter sections.

G. THERMOCOUPLE CALIBRATION

The planned extensive use of tungsten-niobium thermocouples in this program suggested that a special calibration sequence be performed on the particular spools of wire that will be used for instrumentation. Although calibration results have previously been reported for this type of a thermocouple[2], the use of tungsten-niobium thermocouples is rather unique. The calibration was performed because the voltage output characteristics of each wire lot may differ slightly due to different impurity levels.

The tungsten-niobium calibration thermocouples were made by spot welding the ends of two 0.005 inch diameter wires together. A chromel-alumel reference couple was spot-welded on top of the junction and the double thermocouple was installed in a vacuum furnace. The oven temperature was increased in small increments and the millivolt output from each thermocouple recorded after temperature equilibrium had been achieved. The chromel-alumel thermocouple was referenced to 0° C and the temperature was recorded on a millivolt bridge. The output voltage of the tungsten-niobium thermocouple was read directly on a H.P. 3405A integrating D.V.M. with no intervening reference junction. The results of these tests are shown in Figure 16. The present experimental results are compared to those of Raag and Kowger[2] in the figure and good agreement is noted. It is interesting to note that good agreement exists between the data even though a zero degree reference junction was used in the earlier experiment and the reference junction of the present experiment was made at ambient temperature. This phenomenon is a result of the fact that W-Nb thermocouples produce negligible output voltage in the temperature range of 0 to 50°C. A behavior of this type is not common to most conventional thermocouple materials.

H. VOLTAGE PROBE LOCATION

Since "four-point probe" resistance measurements are to be performed on all of the various tests associated with this task, a special test has been performed to assess the effects of non-uniformity in current flow near the current leads. This non-uniformity is to be expected since the current probes are formed by simply spot-welding a .010 inch diameter wire to the end of the sample. At distances far removed from the current probe, current flow will be uniform and a constant resistance is calculated. As the current probe is approached, lateral current is noted which in turn causes a lower voltage probe reading. Thus, a lower resistance value is recorded.

The results of these tests are shown in Figure 17. In the figure, the sample resistivity is plotted versus the average distance between the current/voltage probes. This distance is taken as the arithmetic mean of the two distances D1 and D2 shown in the figure. It is observed that a current/voltage probe distance of the order of 0.5 cm is required to obtain consistent resistivity values. In relation to the 1.5 inch

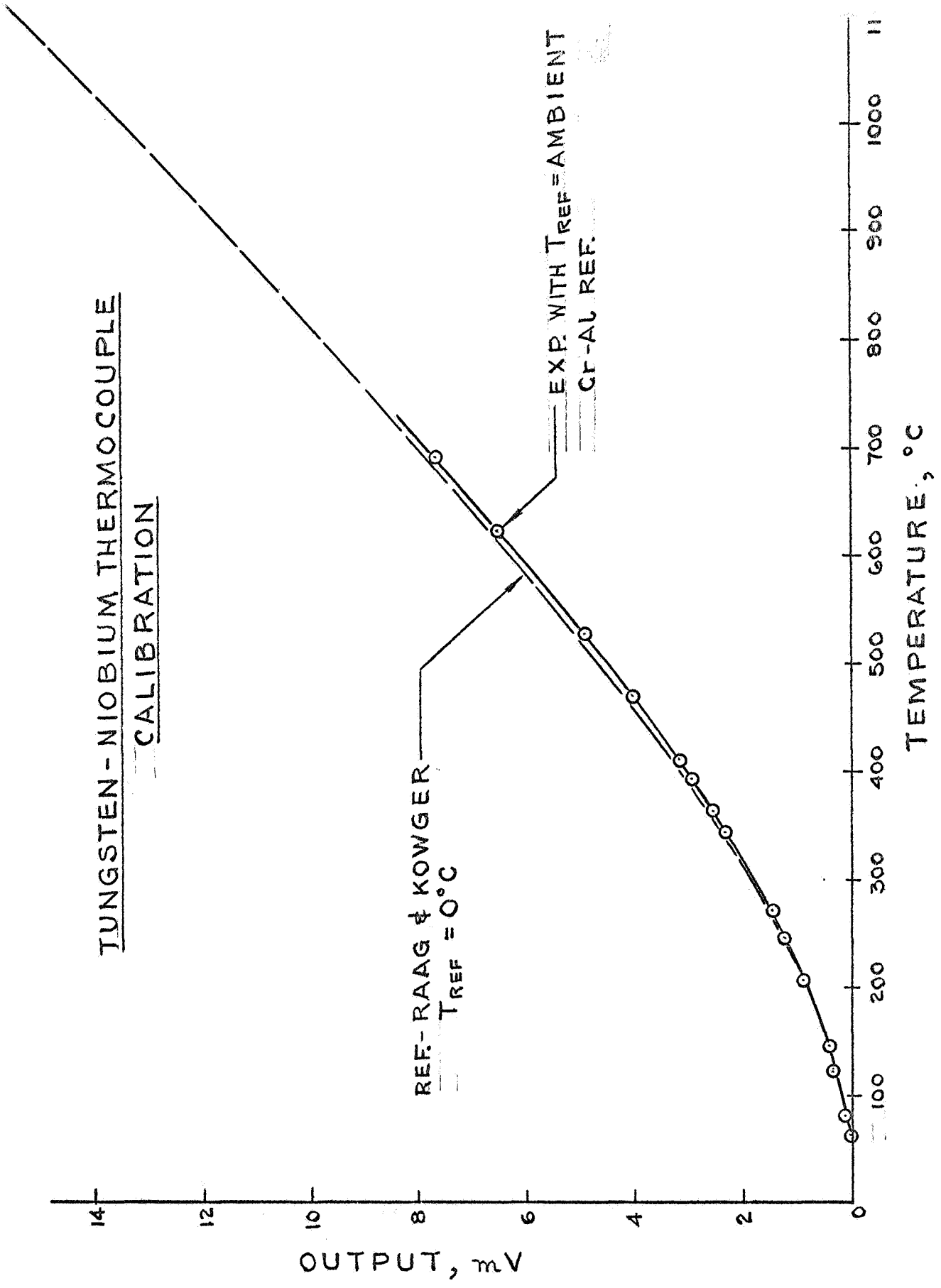

Figure 16 - CALIBRATION CURVE FOR THE TUNGSTEN-NIOBIUM THERMOCOUPLE

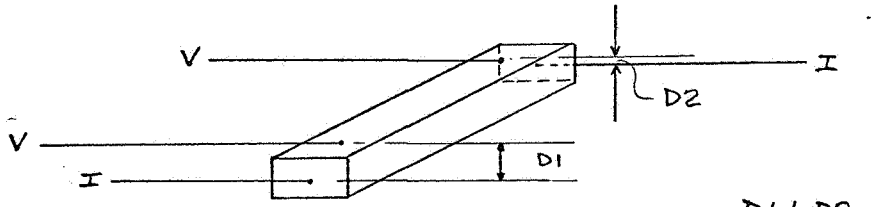

MATERIAL: Si Ge

MEASUREMENT DEVICE: KEITHLY "503" MILLIOHMMETER

$$\Delta L = \frac{D1 + D2}{2}$$

RESISTIVITY, 10^{-3} Ω - CM

2.0

1.0

0

.25

.5

.75

1.0

CM

DISTANCE OF VOLTAGE PROBES FROM CURRENT PROBES (ΔL)

FIG. 17 RESISTIVITY DEPENDENCE OF PROBE

length samples, this indicates that the voltage probes may be separated from each other by approximately one inch. Maximum separation is desired since distance measurement errors are thereby minimized.

1. Test Samples

Whereas the bulk of test facilities for material property tests described above were completed during the present reporting period, none of the tests could be started because of the unavailability of test samples. During the very end of the report period, a preliminary shipment of eight isothermal test samples of composition 80 a/o Si - 20 a/o Ge were received from the RCA Corporation. These eight test samples are parallelepipedal in configuration, with dimensions of 1.50 x 0.25 x 0.25 inch and include five hot-pressed n-type and three hot-pressed p-type samples. Although these samples are too few in number to justify the use of the isothermal test rack for their test, it is planned to nevertheless start isothermal testing with them because it appears that the delivery of additional test samples will further consume substantial time. The planned testing will be performed in a smaller four-tube furnace at temperatures of 300, 400, 500 and 600°C.

In the meantime, however, these samples have enabled the establishment of techniques for spot-welding refractory metal lead wires and thermocouples to the samples and have permitted the determination of the effect of voltage probe location on electrical resistance measurements, as already discussed. The use of these samples has also enabled the verification of direct-current electrical resistance measurement techniques that will be used in the isothermal annealing tests. Room temperature electrical resistance measurements on the eight test samples yielded ac and dc electrical resistivity values as follows:

Sample No.	Type	Electrical Resistivity-mΩ-cm	
		ac	dc
1	n	0.940	0.945
2	n	1.032	1.032
3	n	0.960	0.955
4	n	1.028	1.030

Sample No	Type	Electrical Resistivity-mΩ-cm	
		ac	dc
5	p	1.120	1.130
6	p	1.089	1.100
7	p	0.973	0.973
8	n	1.000	1.000

IV. SUBLIMATION STUDIES

A task dealing with the sublimation of silicon-germanium alloys and the effects of sublimation on RTG performance was initiated during the close of the present reporting period. This task consists essentially of analytical studies dealing with sublimation (e.g., see Section B under Special Studies), of the experimental determination of sublimation of silicon-germanium alloys and of the construction of special test modules for the evaluation of sublimation effects on device performance.

Whereas all of the analytical studies dealing with sublimation of silicon-germanium alloys are being performed at Resalab, some of the basic experimental work has been let to Gulf General Atomics because of their experience and facilities for performing sublimation studies. Although experimental work at Gulf was started prior to the end of the present reporting period, this work consisted primarily of equipment calibration and thus did not as yet yield any results on the sublimation of silicon-germanium alloys.

Five thermoelectric test modules were designed to provide test vehicles for sublimation studies at JPL. Three modules have already been fabricated, one of which has been completely assembled and delivered to JPL. The remaining modules are awaiting receipt of MHW type Air-Vac thermocouples for final assembly. The three fabricated modules contain dynaquartz thermal insulation and are intended for constant temperature operation to assess kinetic sublimation effects on thermoelectric device performance. The remaining two modules will employ a multifoil thermal insulation that consists of molybdenum foils separated by astroquartz cloth. The multifoil modules are intended for constant heat input tests in which thermal insulation stability is of paramount importance. The constant heat input operation of the two modules enables actual RTG operation to be closely simulated.

The test modules are constructed from 316-stainless steel and are modularized to allow thermocouple removal at any time during the test. The thermocouples are mounted on the four sides of a "box" 3.7 inches square and 2 inches thick. The hot shoes of the thermocouples form a one inch square center cavity within which a resistance heater is inserted. The heater is constructed from a 3/4 inch diameter

molybdenum cylinder containing a multi-turn tungsten filament. The outer surface of the cylinder is roughened to enhance radiation from its surface. The bottom of the cylinder is slightly polished to reduce radiation losses. Each thermocouple within the module is instrumented with a tungsten/niobium thermocouple at the hot and cold junctions. The hot junction thermocouple is contained in a double bore ceramic tube and is inserted in a pre-machined hole in the hot shoe. The cold-junction thermocouple is mechanically held under the element by a 6-40 NC attachment screw.

Analytical determinations of total heat input required as well as radiator temperature were made for the modules prior to module fabrication. The results of the calculations indicated that less than 100 watts thermal power is needed to achieve a thermocouple hot-junction temperature of 1200°C. At their hot-junction temperature, the heater filament may be expected to operate at less than 1600°C and the radiator may operate at as high a temperature as 450°C, depending on its emissivity and mounting assembly.

Because of the intended high temperature operation of the dynaquartz insulation system used in the fibrous-insulated test modules, special tests were undertaken to determine the dimensional stability of different thermal insulations operating at 1200°C. Ths insulations examined in this test include:

1. Dynaquartz
2. Astroquartz
3. Zircar
4. Microquartz
5. Min-K

Preliminary results indicate that all of the above insulations, with the exception of Min-K, may be satisfactorily used at 1200°C if proper allowance is given to Zircar and Microquartz for volume shrinkage. The Dynaquartz and Astroquartz have remained exceptionally stable after 130 hours of testing at 1200°C in vacuum. It should be noted that all of the materials examined undergo a phase change and stiffen slightly upon exposure to elevated temperatures.

V. SPECIAL STUDIES

A. THERMOELECTRIC PROPERTIES OF SILICON GERMANIUM ALLOYS

1. Introduction

Recent emphasis on the development of practical high performance thermoelectric power conversion systems capable of reliable long-term operation has brought silicon-germanium alloys and their associated technology into renewed focus. It is generally accepted that of all possible thermoelectric power conversion systems, it is those using silicon-germanium alloys that best combine the desirable qualities of high performance, good reliability and low weight when operated at hot side temperatures of the order of 1700 to 2000°F. Whereas limitations due to maximum heat source operating temperature capabilities have in the past restricted the operation of practical thermoelectric power conversion systems to somewhat lower temperatures, recent developments in high temperature heat source technology have alleviated this situation; as a result, active development work has started on high temperature silicon-germanium thermoelectric systems.

The accelerated emphasis on the practical utilization of silicon-germanium alloys in practical thermoelectric power conversion devices has necessitated a re-examination of the state of the technology. Most gaps still extant in the technology are being filled or probably will be filled in the foreseeable future. Even before this is accomplished, however, there exists a need for interim information required in analytical and design efforts in the definition of a variety of power conversion systems. One area in which the need for such interim information exists is the one of long-term time and temperature dependence of silicon-germanium alloy thermoelectric properties. It was the purpose of this study to fill this requirement by presenting analytically derived thermoelectric property data as a function of time and temperature for the phosphorus doped n-type SiGe alloy. The corresponding data for the p-type alloy are essentially independent of time and are available in the literature. Nevertheless, for completeness, a set of such data for the boron doped p-type alloy has been included.

2. Background Discussion

The design of thermoelectric power conversion systems are generally concerned with the performance at the end of life because there usually exists a minimum performance requirement that the system must satisfy at that time. In designing for the end of life performance, it is necessary to have available information on the time and temperature behavior of various system components in order that a meaningful design may be formulated. Of all the components making up a thermoelectric power conversion system, obviously it is the thermoelectric material and its behavior that usually has the most important bearing on system performance. For this reason, detailed information on the time and temperature behavior of the thermoelectric properties of the active material used in a thermoelectric device is a necessary prerequisite to the practical design of such a device.

Although extensive information exists on the operation of certain silicon-germanium alloys in various thermoelectric modules and devices for extended time periods, the information is such that, it does not yield detailed thermoelectric property data on the silicon-germanium alloys. Such data have traditionally been obtained from thermoelectric material studies. Several such studies have been conducted since 1961[3], the time when silicon-germanium alloys were first suggested in this country as promising thermoelectric materials. Unfortunately most studies concerned with the thermoelectric properties of silicon-germanium alloys have mainly involved the establishment of these properties in the "as-grown" state of the material as a function of alloy composition. Although initial thermoelectric properties are important in material optimization studies and the establishment of initial generator performance characteristics, they do not enable the end-of-life design of a thermoelectric generator because thermoelectric properties frequently change with time. Thus, because the thermoelectric properties of silicon-germanium alloys, especially those of the n-type alloys, are known to undergo changes with operating time as a result of dopant precipitation, this study of the time dependence of the thermoelectric properties of certain silicon-germanium alloys was undertaken.

Practically all projected long-term thermoelectric property data on silicon-germanium alloys has involved the alloy with a composition of 63 a/o Si - 37 a/o Ge. It is this alloy that up to the present has received the most extensive use in practical thermoelectric energy conversion devices because of the compatibility of its thermal expansion characteristics with those of tungsten as an electrode material for silicon-germanium alloys. However, alloys with a composition of about 80 a/o Si - 20 a/o Ge possess the most optimum performance characteristics (maximum figure-of-merit), and also posses some other advantages over the commonly used 63 a/o Si - 37 a/o Ge alloy. Some of the more important of these are an approximately 100°C higher solidus temperature, a closer match between the thermoelectric properties of the n- and p-type alloys and a slightly higher tensile strength. The higher solidus temperature means that the 80 a/o silicon content silicon-germanium alloy can be operated at temperatures higher than those considered maximum for the 63 a/o Si content alloy. The more closely matched thermoelectric properties of the 80 a/o silicon content n- and p-type silicon-germanium alloys result in nearly equal-sized thermoelements for optimum thermocouple performance. For reasons of symmetry, equal sized thermoelements generally enable the construction of fairly rugged thermocouples. The 63 a/o silicon content silicon-germanium alloy requires n- and p-type thermoelement cross-sectional areas in the ratio of about 1.5 to 2.0 for optimum thermocouple performance. Some ruggedness is lost in this configuration. Finally, indications exist that the thermoelectric properties of the 80 a/o silicon content silicon-germanium alloy generally change less as a function of operating time than those of the 63 a/o silicon content alloy. This means that the performance of devices using the former alloy is more stable than of those that use the latter alloy.

In view of the renewed interest in the utilization of high silicon content silicon-germanium alloys in practical thermoelectric energy conversion devices, the requirement has arisen for thermoelectric property data as a function of operating time for the 80 a/o silicon alloy as well as for the 63 a/o alloy.

It is recognized that analytically derived data are no better than the model on which they are based. Although a good qualitative understanding exists of the solid state model underlying the thermoelectric properties of silicon-germanium alloys and the dependence of these properties on time and temperature, considerable effort will still be necessary to formulate a complete quantitative understanding. The only way in which this is possible is through extensive experimental work. In the meantime, however, the analytically derived thermoelectric property data for silicon-germanium alloys will temporarily fill a much needed requirement.

3. Precipitation Kinetics

The worth of a material for thermoelectric energy conversion is approximately indicated by figure-of-merit which combines the three thermoelectric properties, the Seebeck coefficient, S ; the electrical resistivity, ρ; and the thermal conductivity, k, in the well known relationship

$$Z = \frac{S^2}{\rho k} .$$

It has generally been established that extrinsic semiconductors with carrier concentration values in the range 10^{19} to 10^{21} carriers per cubic centimeter possess values of figure-of-merit higher than those of any other group of materials; silicon-germanium alloys are semiconductors for which the figure-of-merit maximizes in the extrinsic range for carrier concentration values of the order of 2×10^{20} carriers per cubic centimeter. As with extrinsic semiconductors in general, the bulk of the indicated carrier concentration in silicon-germanium alloys is obtained through the addition of impurities during crystal growth. Each impurity atom in solid solution in the crystal donates one or more carriers to the lattice. Because of the high carrier concentration required for maximizing the figure-of-merit it is usually found that only a relatively few dopants exist for any given semiconductor that have solid solubilities sufficiently great for yielding the desired impurity carrier concentration. In silicon-germanium alloys only certain of the Group III and Group V elements satisfy this requirement.

Phosphorus exhibits a so-called retrograds solid solubility in silicon-germanium alloys. The solid solubility attains a maximum at temperatures of the order of 900 to 1100°C and decreases at both higher and lower temperatures. In

order to maximize the figure-of-merit of phosphorus doped silicon-germanium alloys, it is therefore necessary to dope the alloys to impurity concentration values consistent with the maximum solid solubility of dopant at temperatures in the range of 900 - 1100°C. When this is done, however, there exists an excess of dopant at both higher and lower temperatures; silicon-germanium alloys doped in this manner are super-saturated with dopant. Because of the resultant instability, the system of dopant and lattice tends to equilibrium by precipitating any dopant in excess of its solid solubility at any given temperature. This effect of a decreasing dopant, and hence carrier concentration, manifiests itself in changed electrical properties as a function of time. Both the elctrical resistivity and Seebeck coefficient increase with time in such a manner that the quantity S^2/ρ slightly decreases. Inasmuch as the thermal conductivity remains nearly unchanged, the figure-of-merit of n-type silicon-germanium alloys slightly decreases with time.

The rate and extent to which the thermoelectric properties of n-type silicon-germanium alloys change with time is obviously temperature dependent. At the temperatures of maximum solid solubility of phosphorus, the material is in equilibrium and thus little change takes place. At temperatures exceeding those of maximum dopant solid solubility, the precipitation process goes to completion extremely fast because of the high temperatures in question. It is at temperatures below those of maximum dopant solid solubility that observable long-term changes in the electrical properties of n-type silicon-germanium alloys occur. Because the solid solubility of phosphorus decreases with temperature at temperatures below the solid solubility maximum, the "driving force" for precipitation increases with decreasing temperatures. The diffusion rate of phosphorus in the silicon-germanium matrix, diffusion preceding precipitation at a nucleation site, however decreases with decreasing temperatures. The net result of the opposing temperature dependences of these two mechanisms is that it is at intermediate temperatures in the range of 300 - 700°C that the biggest changes occur in the electrical properties of n-type silicon-germanium alloys as a result of dopant precipitation. At very low temperatures, such as room temperature, precipitation proceeds so slowly as to be practically unobservable.

Although no all-encompassing model exists for quantitatively describing the precipitation of phosphorus in silicon-germanium alloys for all times, Ekstrom and Dismukes[4] have suggested that a model due to Slyozov and Lifshitz[5] reasonably accounts for at least a part of the process. In this model the precipitate phase consists of particles of nearly continuously varying radii. The surface energy of the particle-solution interface determines this critical radius. Particles having radii smaller than the critical value tend to redissolve in the matrix whereas particles with radii exceeding the critical radius tend to grow as the precipitation proceeds. The two competing processes initially decrease the precipitation rate to values less than expected from a diffusion limited precipitation process by itself. At long times, after complete dissolution of the small particles, the precipitation rate in silicon-germanium alloys approaches that solely due to a diffusion limited precipitation process. The initial distribution of precipitated particles with nearly continuously varying radii is introduced into the alloys during crystal growth and related high temperature treatments. It should be noted that in materials that exhibit a retrograde dopant solid solubility, nearly invariably there coexist a precipitate phase and a solute phase, even when the overall doping level is purposely kept below the maximum dopant solid solubility level.

According to the model of Slyozov and Lifshitz[5], a diffusion-limited precipitation process which accounts for the re-solution of small precipitate particles due to surface energy may be represented by

$$\left[\frac{C_i - C_e}{C_t - C_e}\right]^3 = \left[\frac{4}{9}\left(\frac{C_e}{C_p}\right)\left(\frac{C_i - C_e}{C_e}\right)^3 \frac{D}{\beta^2}\right] t + B,$$

where B is a constant and β is defined as

$$\beta = \frac{2M\sigma}{\delta RT}$$

In the above equations, C_i is the initial solute concentration, C_t is the solute concentration at time t, C_p is the concentration of solute in the precipitate phase and C_e is the equilibrium dopant solid solubility. D is the dopant diffusion coefficient at temperature T, M is the mean atomic weight of the matrix, σ is the

interphase surface energy, δ is the density of the matrix, and R is the gas constant. It may appear that the constant B should assume the value of unity. Ekstrom and Dismukes[4], however, point out that B=1 is not physically meaningful if the characteristic precipitate particle size distribution is not present at the start of the precipitation process. The model represented by the above equations reasonably accounts for the precipitation of phosphorus in silicon-germanium alloys after the first few hours of the precipitation process. The processes extant during the first few hours appear to be closely related to the previous thermal history of the alloys; it is not uncommon for the carrier concentration to remain constant or even increase initially. Although Ekstrom and Dismukes[4] obtained good agreement between theory and experiment for precipitation times exceeding a few hours, most of their work involved only the first 1000 hours of the precipitation process. It is therefore not precisely known how good the agreement between theory and experiment is at much longer precipitation times.

4. Thermoelectric Properties of Silicon-Germanium Alloys

Although most of the work on phosphorus precipitation in silicon-germanium alloys reported by Ekstrom and Dismukes[4] pertains to alloys with a silicon content of 70 a/o, they did extend it in a preliminary manner also to alloys with silicon contents of 80 a/o and 85 a/o. Most of this latter work, however, remains unreported. It has been necessary, therefore, to re-apply the theory to the 80 a/o Si - 20 a/o Ge and 63 a/o Si - 37 a/o Ge phosphorus doped alloys in an effort to determine the long-term behavior of their thermoelectric properties.

Underlying the present application of the precipitation model are experimental data on the time dependence of the electrical resistivity of phorporus doped silicon-germanium alloys in the temperature range 400 to 800°C for operating times up to 1500 hours. Some of these experimental data have been reported in Reference 3. The application of the model to the experimental data has enabled the evaluation of constants in the equation. Maintaining the constants at fixed values, it has been possible to calculate the time dependence of the carrier concentration in the phosphorus doped silicon-germanium alloys. The carrier concentration values thus derived have been converted to electrical resistivity through the inclusion of electronic

charge and carrier mobility, the dependence of the latter on carrier concentration being taken into account. Known relationships[3] between electrical resistivity and Seebeck coefficient for n-type silicon-germanium alloys have been used to determine the time dependence of the Seebeck coefficient from the electrical resistivity data. The thermal conductivities of the alloys have been assumed to remain constant with time; experimental findings[3] give validity to this assumption for carrier concentration changes of several tens of percent. The effect of much greater changes in carrier concentration may, however, be observable and must be experimentally determined.

Figure 18 shows plots of electrical resistivity of the phosphorus doped 63 a/o Si - 37 a/o Ge alloy as a function of temperature for a variety of operating times in the range of zero hours to 12 years. It is to be recognized that the zero-hour data, the so-called initial data, are dependent on the details of crystal growth and related thermal history of the material and thus are not completely unique. Samples with different thermal histories will have slightly different initial properties. Because slight changes in the electrical resistivity result in similar changes in the Seebeck coefficient, such that the quantity S^2 / ρ is nearly unchanged, the effect of small differences in thermoelectric properties has little effect on device performance. Figure 19 shows the corresponding plots of the Seebeck coefficient referenced to absolute. The thermal conductivity of the alloy is shown in Figure 20. Only one set of data is given for the thermal conductivity as it has been assumed that the thermal conductivity of silicon-germanium alloys is independent of time.

The thermoelectric property data for the phosphorus doped 80 a/o Si - 20 a/o Ge alloy are shown as a function of time and temperature in Figures 21 to 23. Figure 21 shows the electrical resistivity as a function of temperature for operating times in the range of zero hours to 12 years. Figure 22 shows plots of the Seebeck coefficient of the phosphorus doped 80 a/o Si - 20 a/o Ge alloy as a function of time and temperature. The thermal conductivity of the alloy is shown in Figure 23. Again as with the 63 a/o Si - 37 a/o Ge alloy, only one set of data is given for the thermal conductivity.

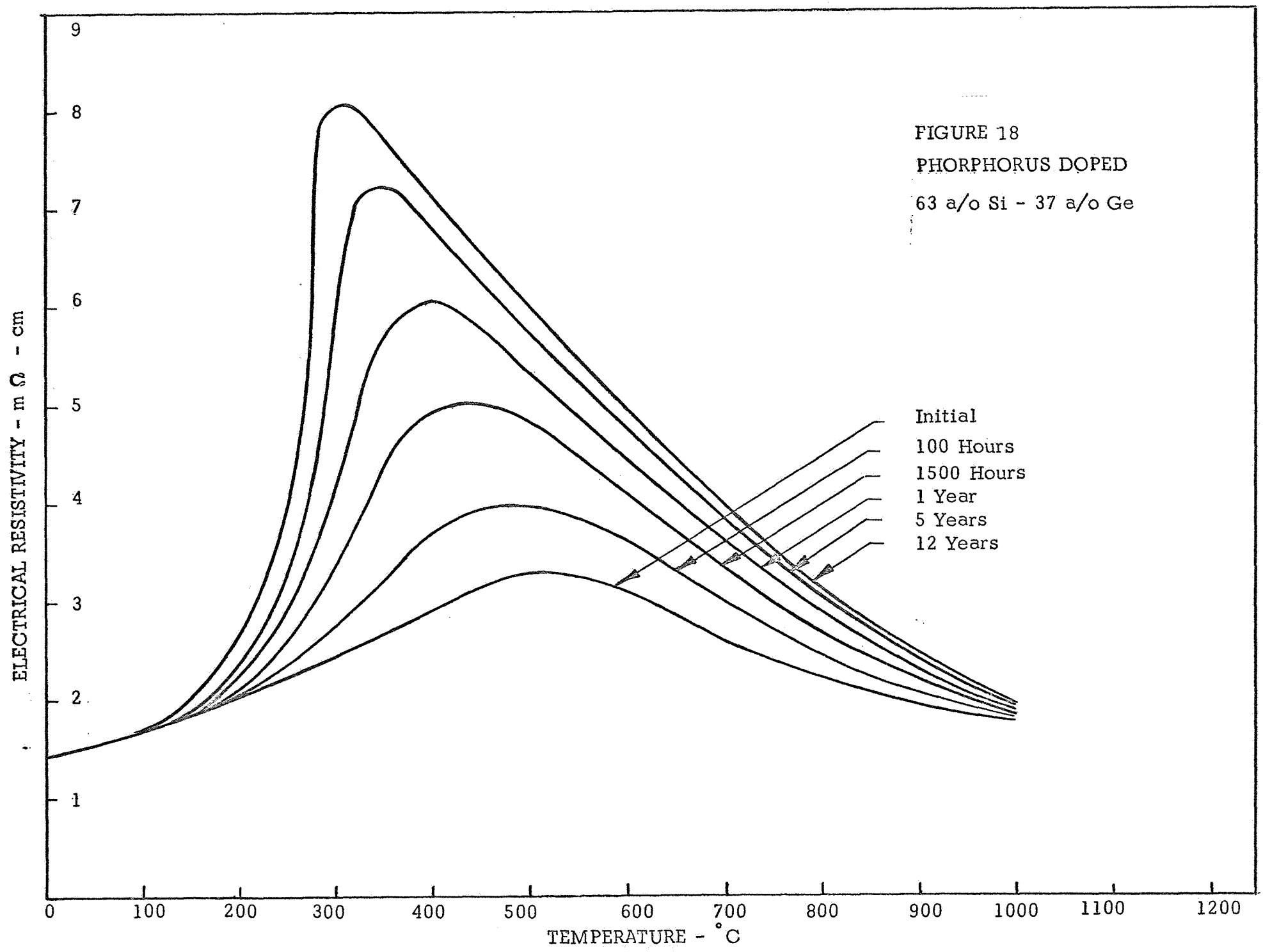
FIGURE 18
PHORPHORUS DOPED
63 a/o Si - 37 a/o Ge
Initial
100 Hours
1500 Hours
1 Year
5 Years
12 Years
ELECTRICAL RESISTIVITY - m Ω - cm
TEMPERATURE - °C
9
8
7
6
5
4
3
2
1
0
100
200
300
400
500
600
700
800
900
1000
1100
1200

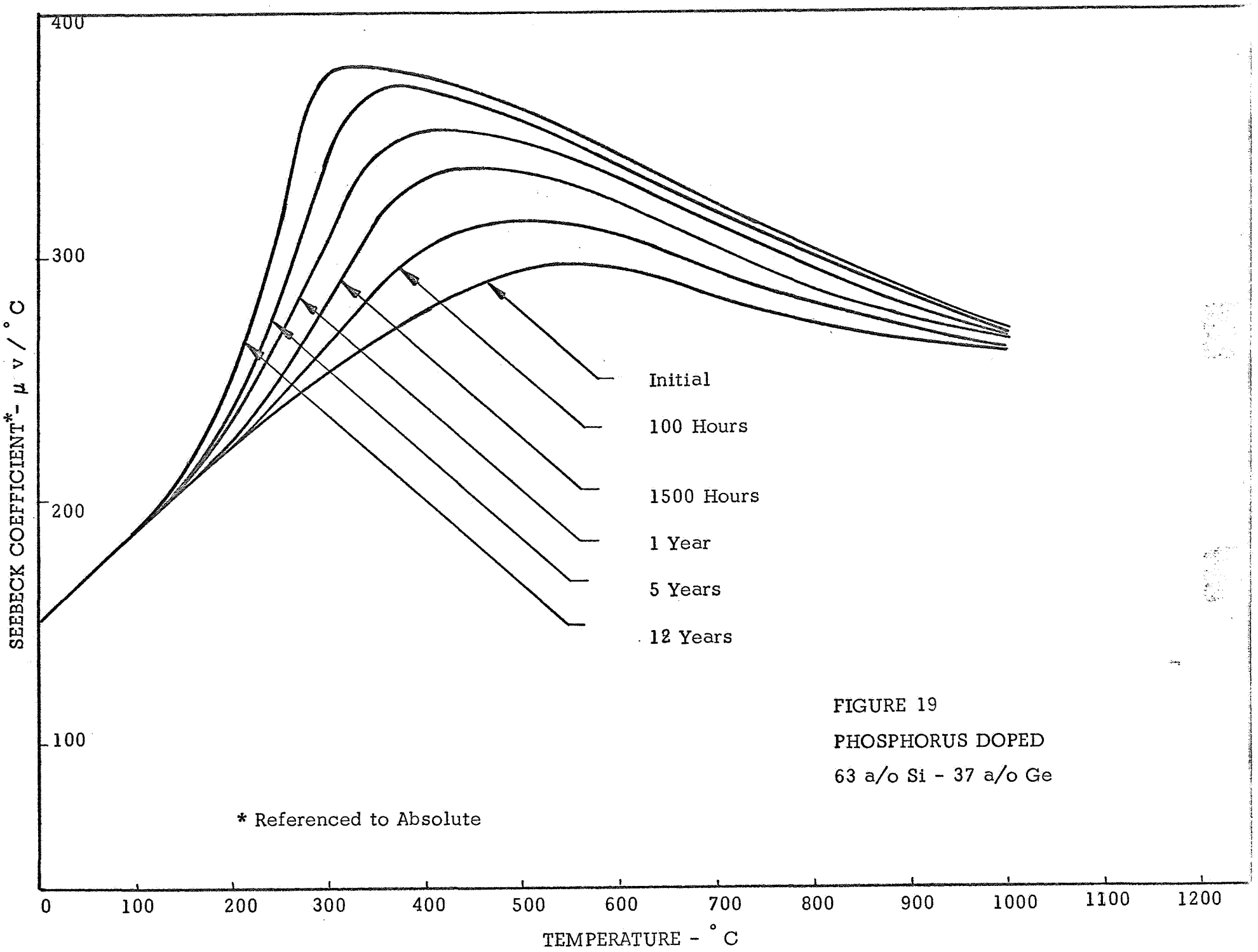

FIGURE 19
PHOSPHORUS DOPED
63 a/o Si - 37 a/o Ge

* Referenced to Absolute

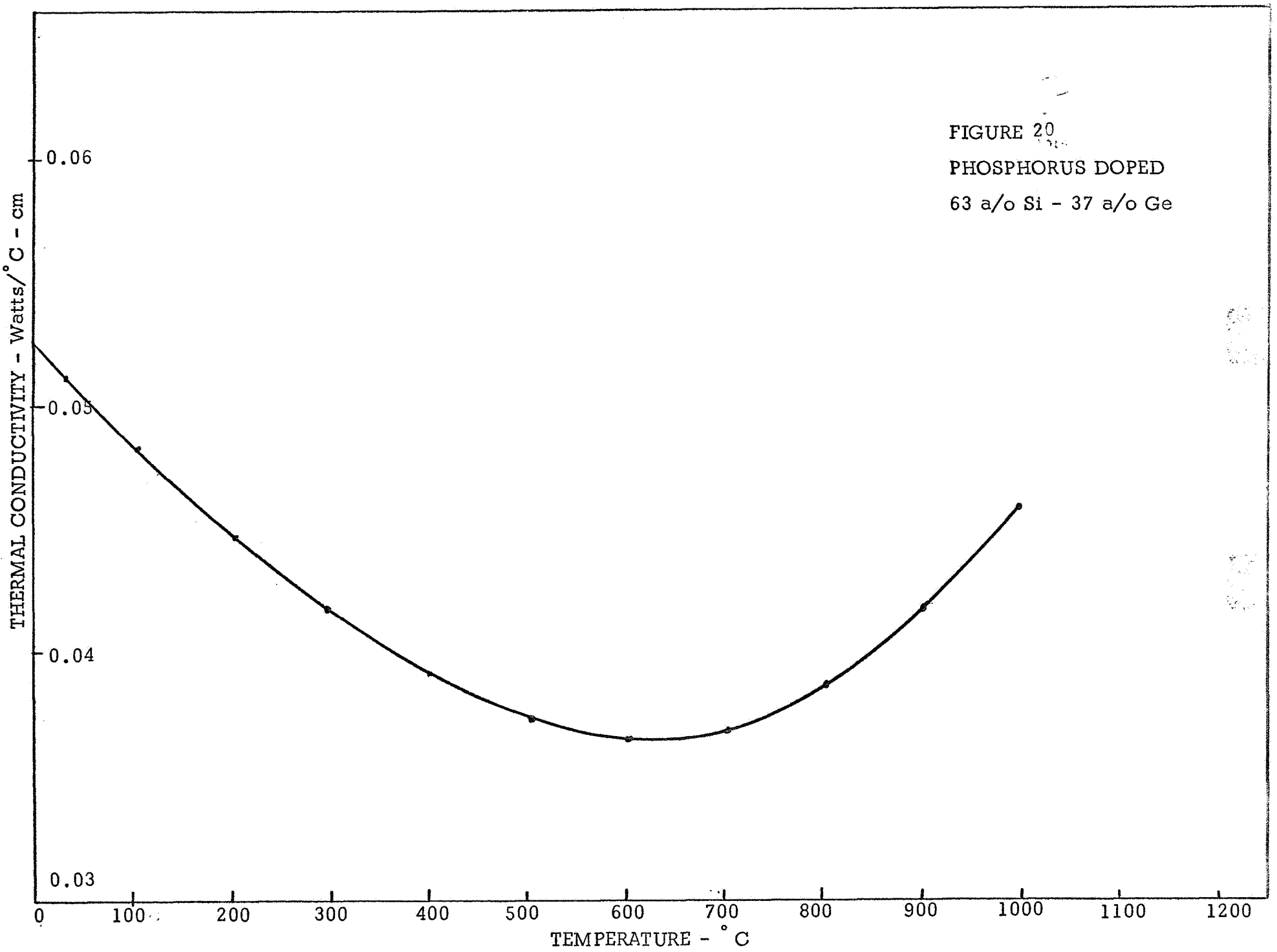
FIGURE 20
PHOSPHORUS DOPED
63 a/o Si - 37 a/o Ge
THERMAL CONDUCTIVITY - Watts/°C - cm
0.06
0.05
0.04
0.03
0
100
200
300
400
500
600
700
800
900
1000
1100
1200
TEMPERATURE - °C

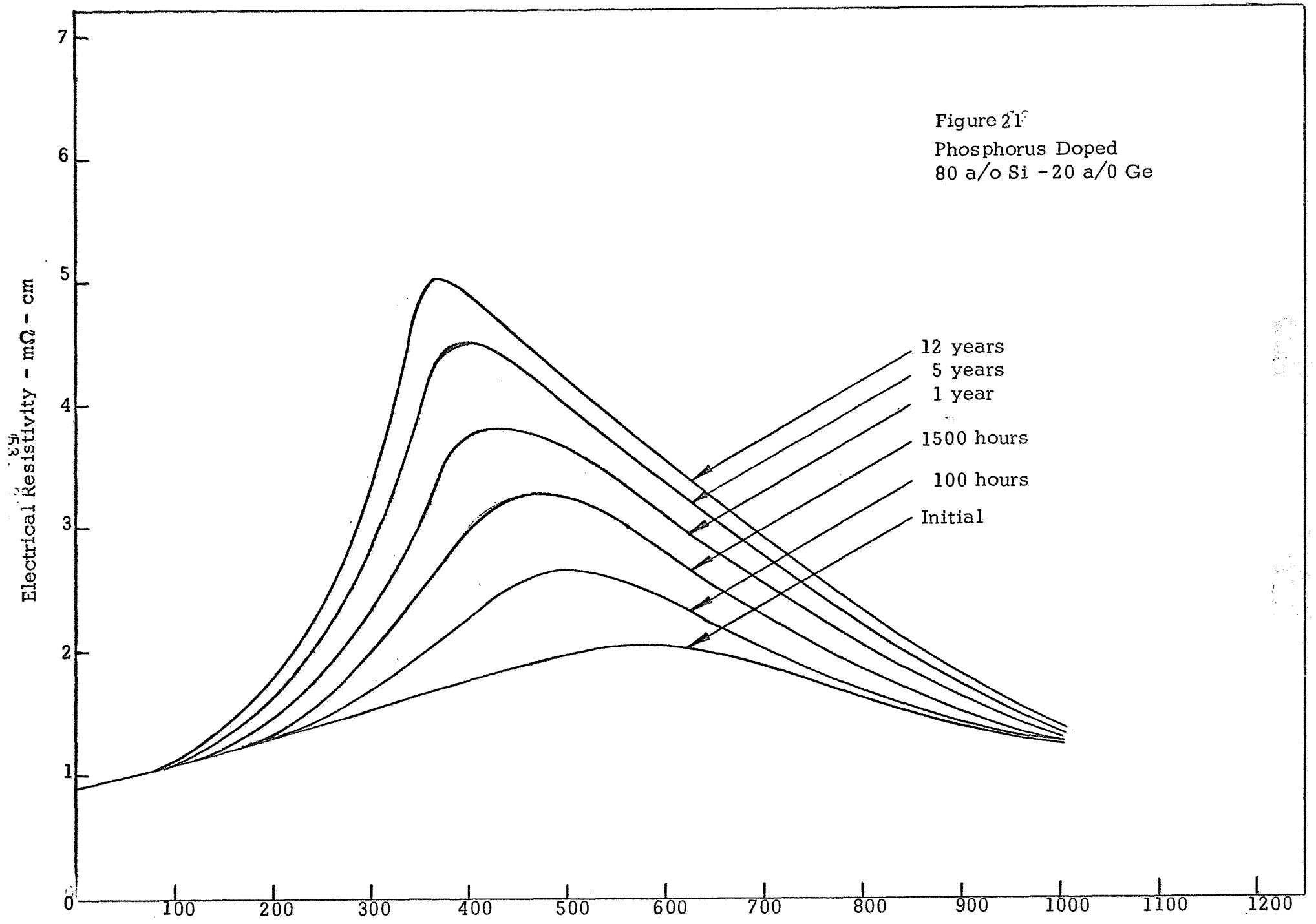
Figure 21
Phosphorus Doped
80 a/o Si - 20 a/0 Ge
Electrical Resistivity - mΩ - cm
0
1
2
3
4
5
6
7
100
200
300
400
500
600
700
800
900
1000
1100
1200
12 years
5 years
1 year
1500 hours
100 hours
Initial

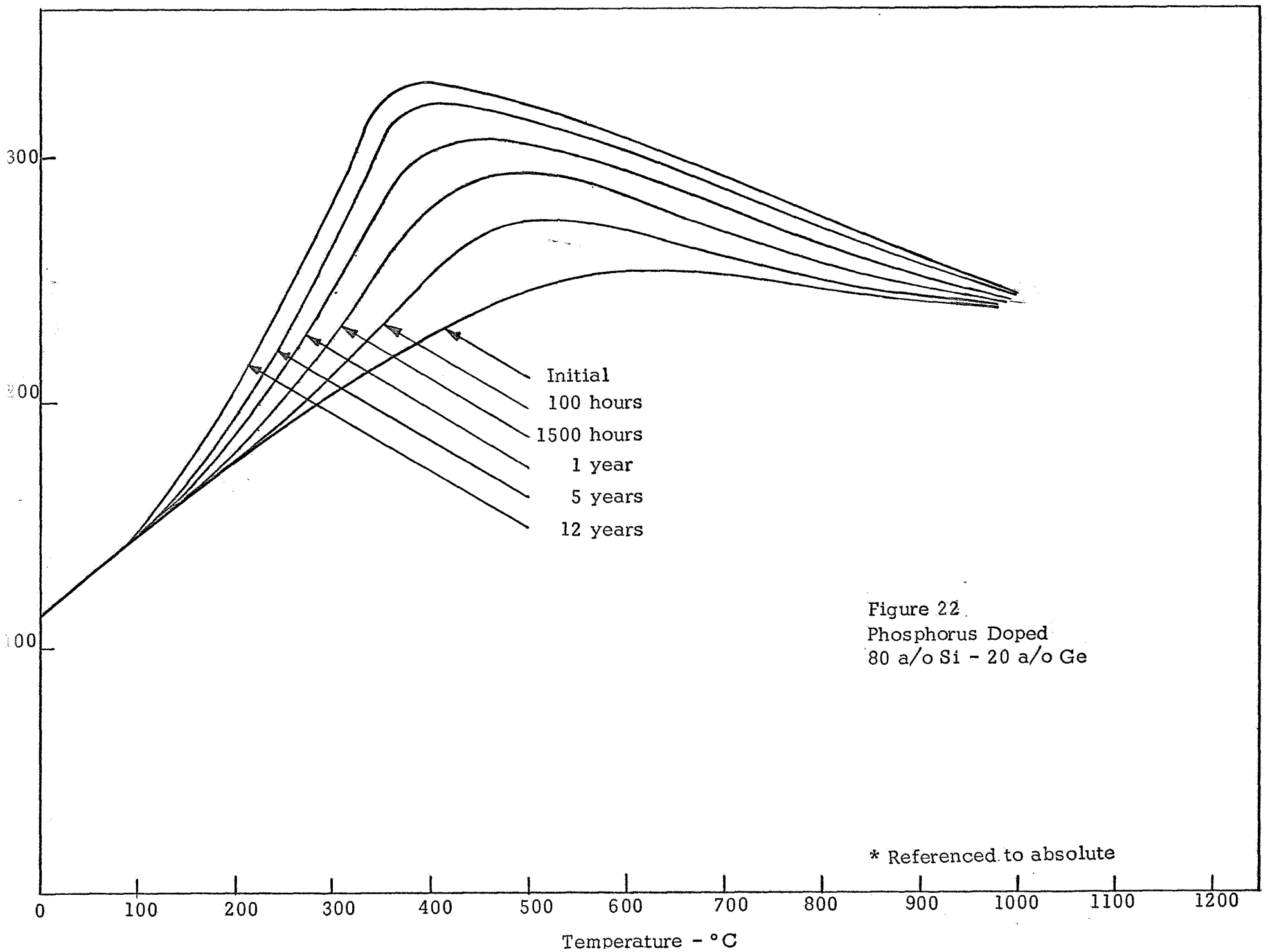

Figure 22
Phosphorus Doped
80 a/o Si - 20 a/o Ge

* Referenced to absolute

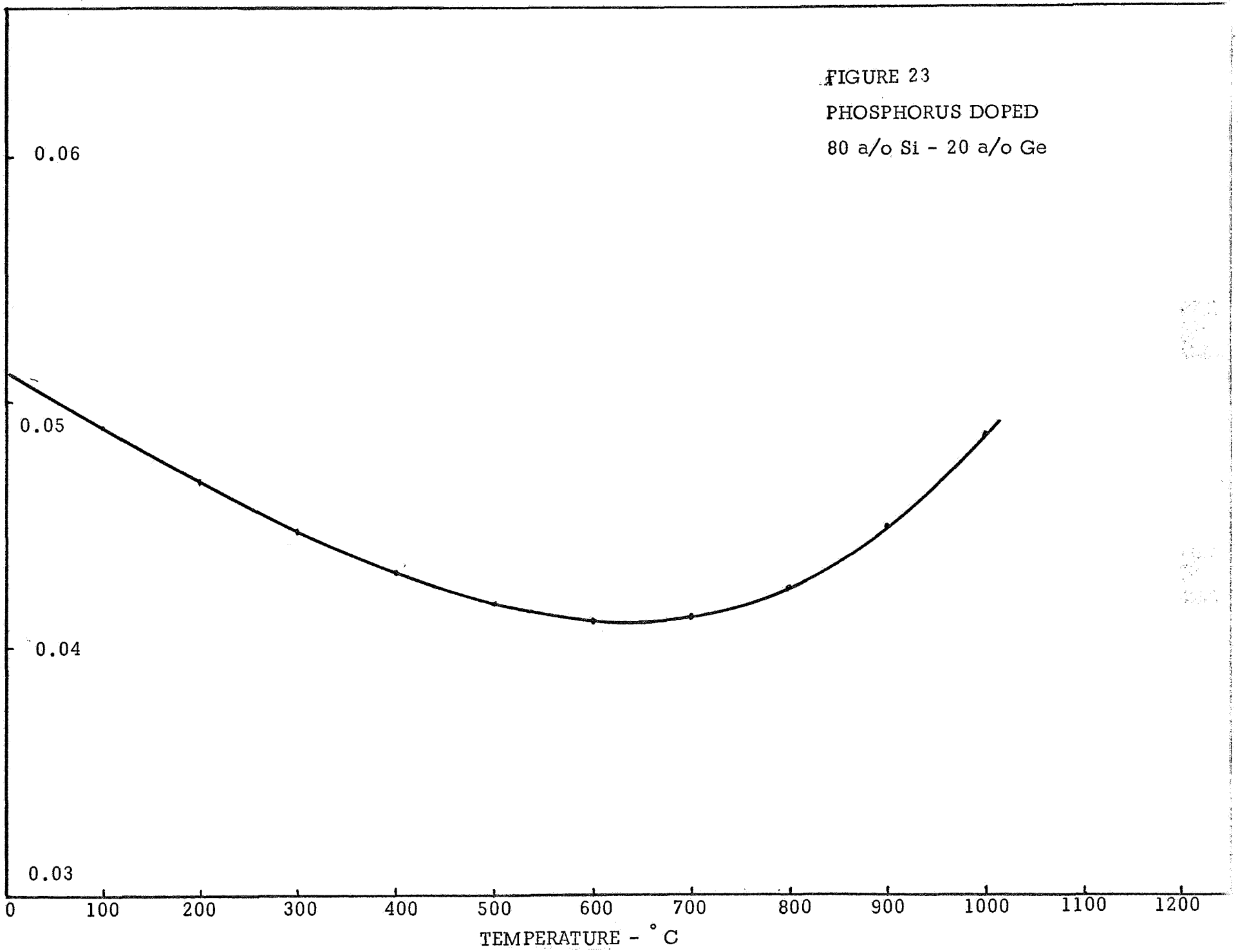
FIGURE 23
PHOSPHORUS DOPED
80 a/o Si - 20 a/o Ge
THERMAL CONDUCTIVITY - Watt/°C - cm
0.06
0.05
0.04
0.03
0
100
200
300
400
500
600
700
800
900
1000
1100
1200
TEMPERATURE - °C

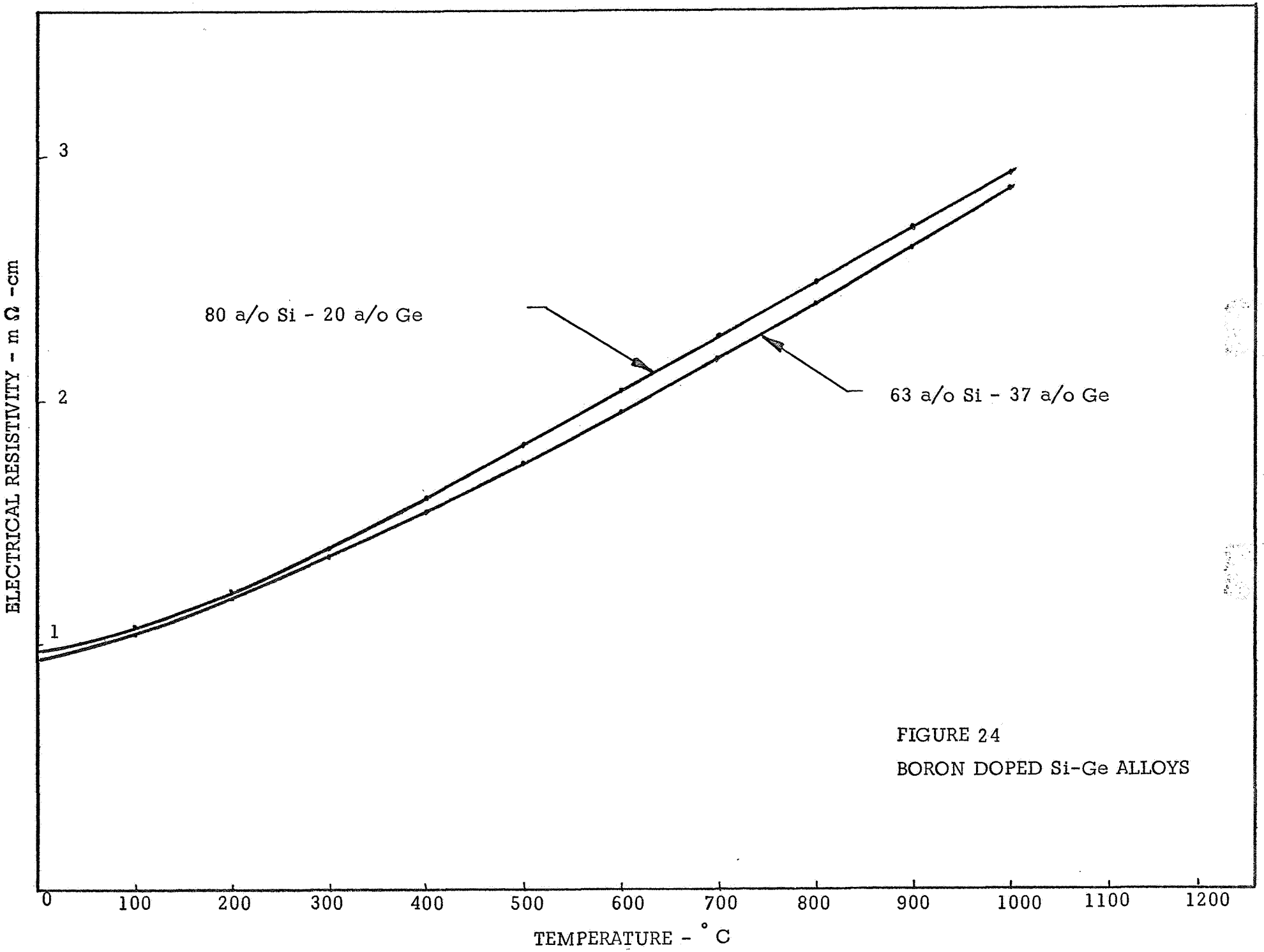

FIGURE 24

BORON DOPED Si-Ge ALLOYS

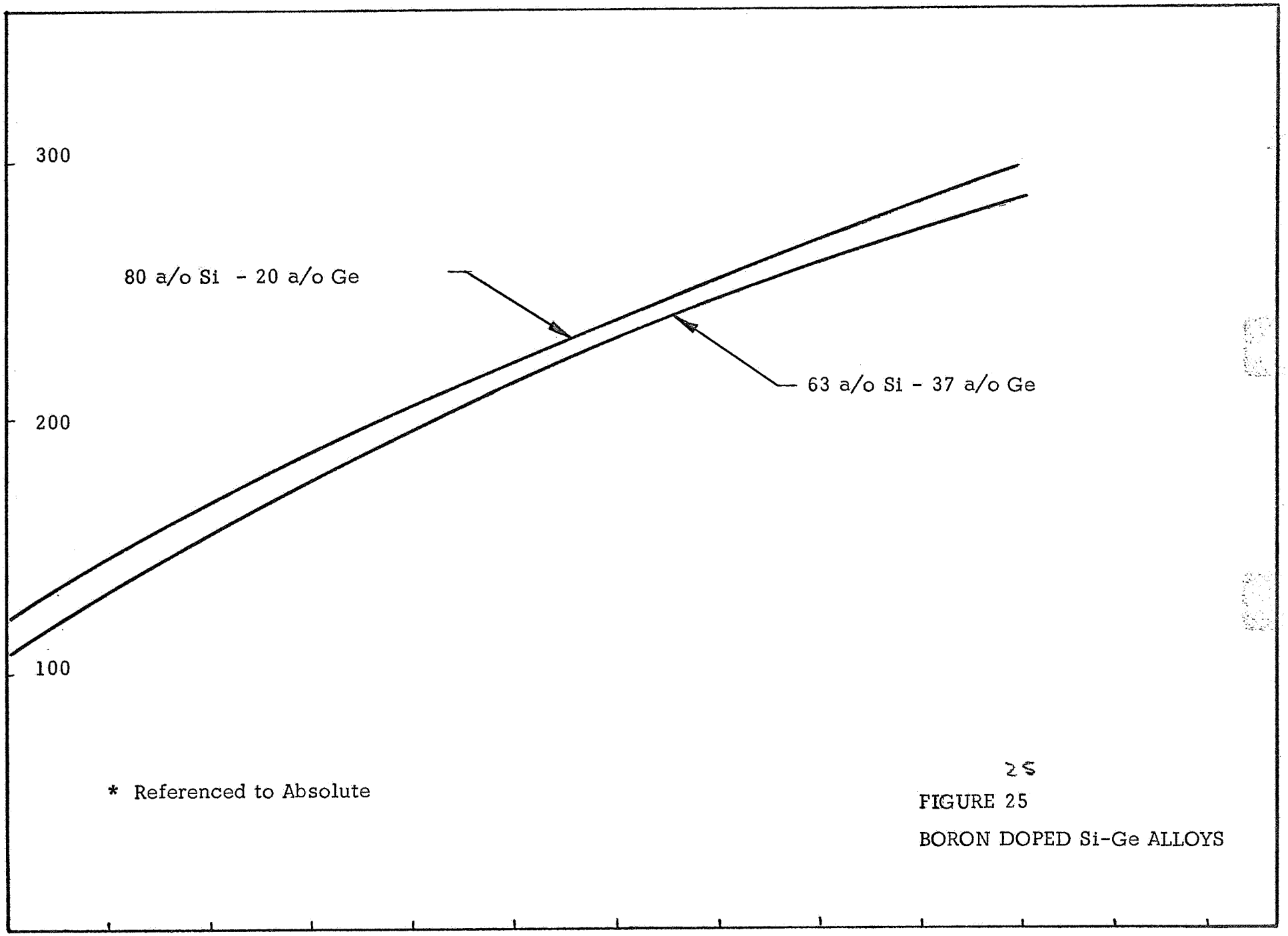

* Referenced to Absolute

FIGURE 25

BORON DOPED Si-Ge ALLOYS

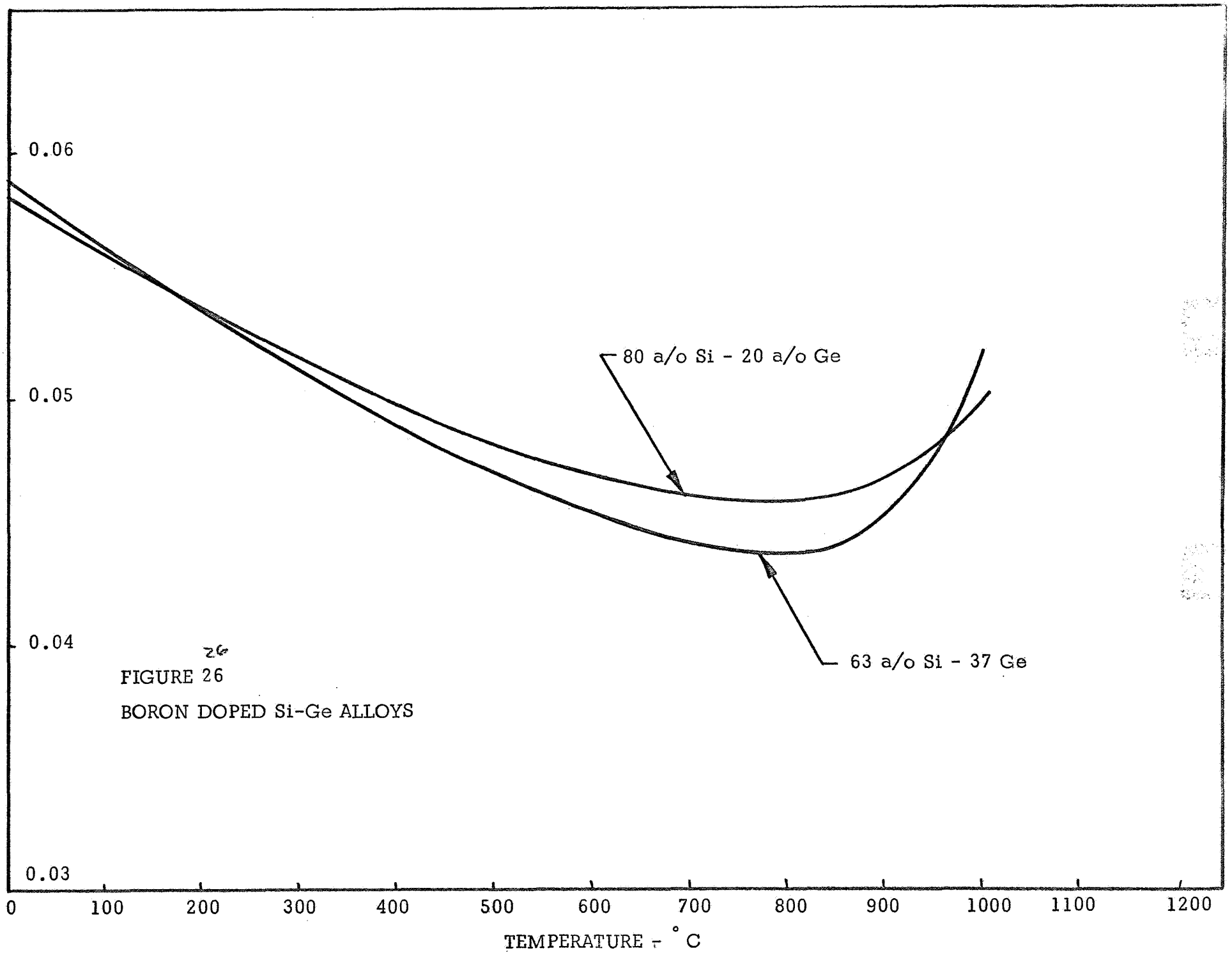

FIGURE 26

BORON DOPED Si-Ge ALLOYS

values also exists in the case of the 63 a/o Si - 37 a/o Ge alloy and, moreover, whether n- and p-type silicon-germanium alloys have measurably different values of specific heat. Although uncertainties thus exist in the calculated values of specific heat of silicon-germanium alloys, for lack of experimental data it was deemed advisable for the purposes of this study to retain the use of calculated values of specific heat for the 63 a/o Si - 37 a/o Ge alloy even though it is recognized that the calculated values may well be somewhat in error.

The thermal conductivity data of the n- and p-type 80 a/o Si - 20 a/o Ge alloy in Figures 23 and 26 are average data based on a fairly large number of samples independently measured at several laboratories. These data, although also derived from thermal diffusivity measurements, at least approximately account for uncertainties in calculated specific heat values and thus should be fairly accurate. It should be noted that the thermoelectric property data given here for the n- and p-type 80 a/o Si - 20 a/o Ge alloy are data mutually agreed upon by a number of groups interested in this alloy* and will be used by these groups until additional information warrants the updating of the data. The thermoelectric property data given in this study for the n- and p-type 63 a/o Si - 37 a/o Ge alloy are data based on less extensive experimentation and have not undergone as much evaluation as those of the higher silicon content alloy. Nevertheless, it is believed that these data are reasonably accurate. The area of greatest question, that of specific heat values, should however be experimentally further explored for the 63 a/o Si - 37 a/o Ge alloy. The available information on the specific heats of 63 a/o Si - 37 a/o Ge and 80 a/o Si - 20 a/o Ge alloys is summarized in Figure 27 in terms of plots as a function of temperature. Figure 27 shows the calculated specific heats of the two silicon-germanium alloys, along with the experimental values obtained at the Battelle Memorial Institute for the 80 a/o Si - 20 a/o Ge alloy. Although originally reported in terms of per unit mass, for sake of consistency, the latter values are here given in terms of specific heat per unit volume. Volume expansion with temperature has been taken into account.

---

* Meeting between representatives of JPL, Resalab, AEC, Sandia, GE and RCA, Harrison, New Jersey, on August 19, 1970.

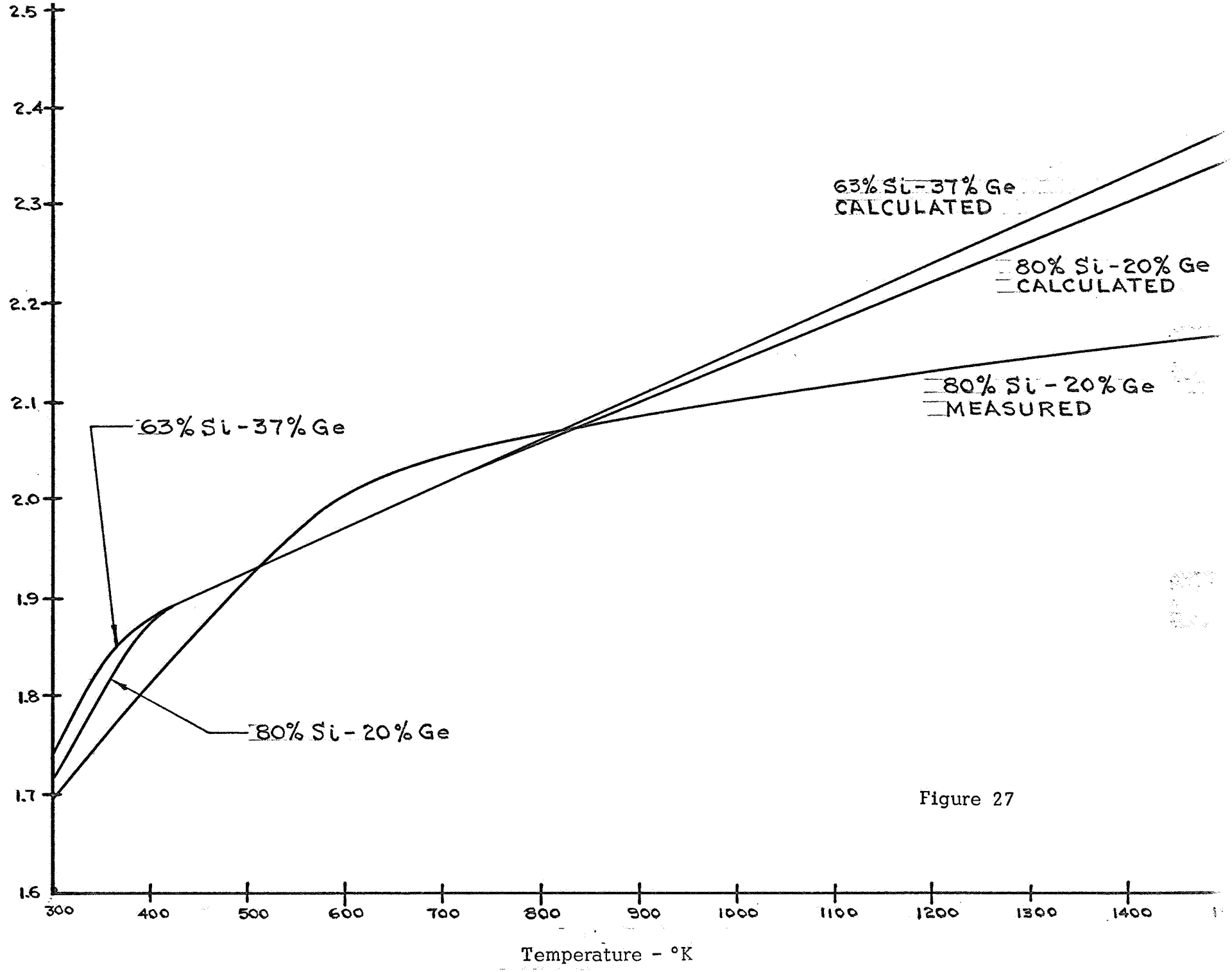
2.5
2.4
2.3
2.2
2.1
2.0
1.9
1.8
1.7
1.6
300
400
500
600
700
800
900
1000
1100
1200
1300
1400
63% Si - 37% Ge
CALCULATED
80% Si - 20% Ge
CALCULATED
80% Si - 20% Ge
MEASURED
63% Si - 37% Ge
80% Si - 20% Ge
Specific Heat - Joule/cm³ - °K
Temperature - °K

Figure 27

B. SiGe SUBLIMATION

Frequently overlooked in the operation of a RTG are such processes as vapor phase transport and compatibility of materials used in generator construction. An example of these processes is the sublimation commonly experienced in lead-telluride generators which operate at elevated temperatures. When operated at hot junction temperatures below 1000°C sublimation in silicon-germanium RTG's has proven of little consequence. However, with the design of the MHW-RTG with a 1100°C beginning-of-life hot junction temperature, as well as its proposed use over extended periods, it became necessary to investigate the question of silicon-germanium thermoelement sublimation in terms of its operating temperature and time, as well as other difficulties related to high beginning-of-life operating temperatures.

Whereas the free sublimation rates of silicon and germanium can be calculated from published data on vapor pressure of these materials, it is not possible to do so for silicon-germanium alloys. It was therefore decided to obtain sublimation rates by interpolation between data calculated for silicon and germanium. It was also assumed that the n- and p-type thermoelements of the couple both possess circular cross-sections, that the rates of both types of silicon-germanium are identical and that sublimation from each thermoelement is unimpeded by the proximity of the other leg. In actual fact, sublimation from the sides of the thermoelements facing each other is reduced because of a baffling effect.

A general result of sublimation is an overall reduction in effective thermoelement cross-sectional areas and a consequent increase in thermocouple hot junction temperature - an often disastrous combination that can exist in well insulated generators without any special effort at baffling.

The present study has focused on the MHW-RTG with its beginning-of-life thermocouple hot junction temperature of 1100°C and the required operating life of 12 years. The use of an effective thermoelement operating temperature enables the calculation of the net sublimation rate from each thermoelement at the beginning-of-life operating temperatures. This effective thermoelement operating temperature is given by:

$$T_{eff} = \frac{\int_{T_C}^{T_H} Tf(T)dT}{\int_{T_C}^{T_H} f(T)dT}$$

where T is absolute temperature, T_H and T_C are the thermoelement hot and cold junction temperatures respectively and T_{eff} is the effective sublimation temperature of each thermoelement. The distribution function f(T) is the sublimation rate of the thermoelement material and for the 80 a/o Si - 20 a/o Ge alloy has been determined by interpolation from Figure 28 to be given by

$$f(T) = 5 \times 10^{11} e^{-\frac{51,000}{T}} .$$

It should be noted that because of the exponential character of the distribution function f(T), the effective sublimation temperature T_{eff} depends heavily on thermocouple hot junction temperature, T_H, and only very little on the cold junction temperature, T_C. In the present study the effective sublimation temperature, T_{eff} is calculated to be only some 20°C below thermocouple hot junction temperature T_H, at any given time.

Using the calculational model just discussed, the effects of sublimation on the performance of the MHW-RTG generator have been assessed. Figure 29 shows how the hot junction temperature of the generator varies with time and sublimation rate. The temperatures shown account for both the effects of silicon-germanium sublimation and isotope fuel decay with time. It is noted that at the beginning-of-life MHW-RTG design operating temperature of 1100°C, the hot junction temperature increases extremely rapidly and in a short time will lead to catastrophic generator failure. Although it takes longer for this to happen at beginning-of-life operating temperatures of 1050 and 1000°C it nevertheless happens in times relatively short compared to the required 12 year RTG operating time.

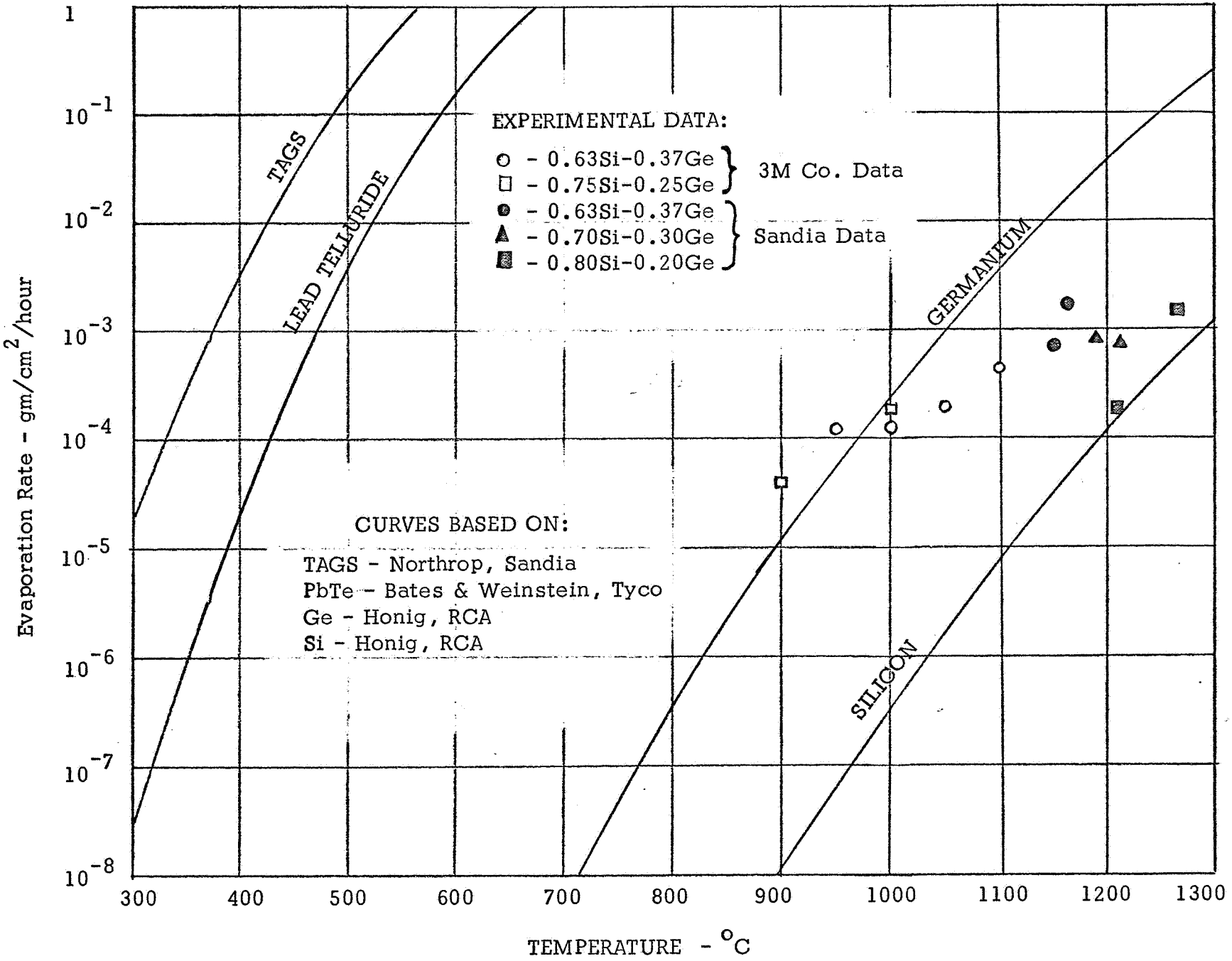
Evaporation Rate - gm/cm^2/hour
1
10^{-1}
10^{-2}
10^{-3}
10^{-4}
10^{-5}
10^{-6}
10^{-7}
10^{-8}
300
400
500
600
700
800
900
1000
1100
1200
1300
TEMPERATURE - °C
TAGS
LEAD TELLURIDE
GERMANIUM
SILICON
EXPERIMENTAL DATA:
○ - 0.63Si-0.37Ge
□ - 0.75Si-0.25Ge
3M Co. Data
● - 0.63Si-0.37Ge
▲ - 0.70Si-0.30Ge
■ - 0.80Si-0.20Ge
Sandia Data
CURVES BASED ON:
TAGS - Northrop, Sandia
PbTe - Bates & Weinstein, Tyco
Ge - Honig, RCA
Si - Honig, RCA

Figure 28

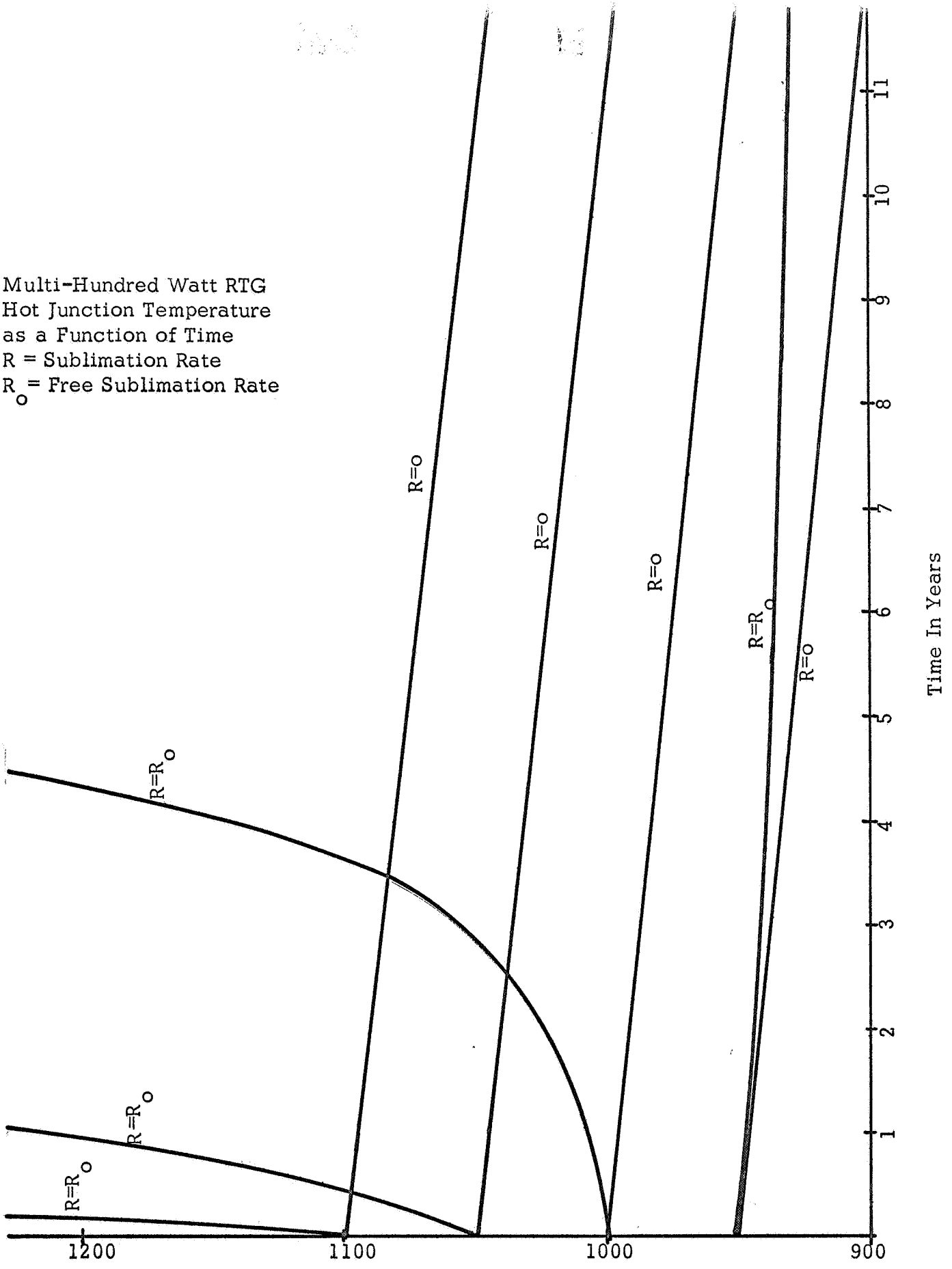
Multi-Hundred Watt RTG
Hot Junction Temperature
as a Function of Time
R = Sublimation Rate
R_o = Free Sublimation Rate
R=o
R=o
R=o
R=R_o
R=o
R=R_o
R=R_o
R=R_o
1200
1100
1000
900
1
2
3
4
5
6
7
8
9
10
11
Time In Years
Hot Junction Temperature - °C

Figure 29

The results shown in Figure 29 presuppose free sublimation of the silicon-germanium thermoelements. In an actual generator structure, however, the thermoelements are usually enclosed in insulation and the sublimed species in all liklihood is not removed as fast as it is formed. The effect of the resultant baffling is to reduce the sublimation rate of the material. Inasmuch as it is nearly impossible to analytically predict the reduction of effective sublimation rates of an actual generator structure, the calculations underlying Figure 29 have been repeated for assumed sublimation rates of one and two orders of magnitude below those shown in Figure 28 and used to calculate the MHW-RTG hot side operating temperatures shown in Figures 30 and 31. Figure 30 shows the results for a sublimation rate one order of magnitude lower than that used in Figure 29. It is to be noted that although the 1100 and 1050°C beginning-of-life operating temperatures still lead to catastrophic generator failure within the 12 year operating time, it is now possible to operate the RTG at a beginning of life temperature of 1000°C without the undue effects of sublimation. The corresponding results for silicon-germanium sublimation rates two orders of magnitude lower than the maximum rates shown in Figure 28 are given in Figure 31. It is noted that although noticeable sublimation effects still occur at most of the beginning of life operating temperatures shown, effects are relatively small, even at the 1100°C beginning-of-life operating temperature.

In view of the results obtained in this study it may be concluded:

1. Operation of silicon-germanium RTG's and specifically the MHW-RTG at beginning-of-life temperatures of 1100°C is advisable only if the effective sublimation rate of silicon-germanium alloys can be reliably reduced by some two orders of magnitude below the free sublimation rate. In view of stringent reliability requirements of most RTG applications it is questionable whether this can satisfactorily be accomplished.
2. Assuming the worst case of free sublimation of silicon-germanium, silicon-germanium RTG's should be designed for beginning-of-life operating temperatures at or below 1000°C.

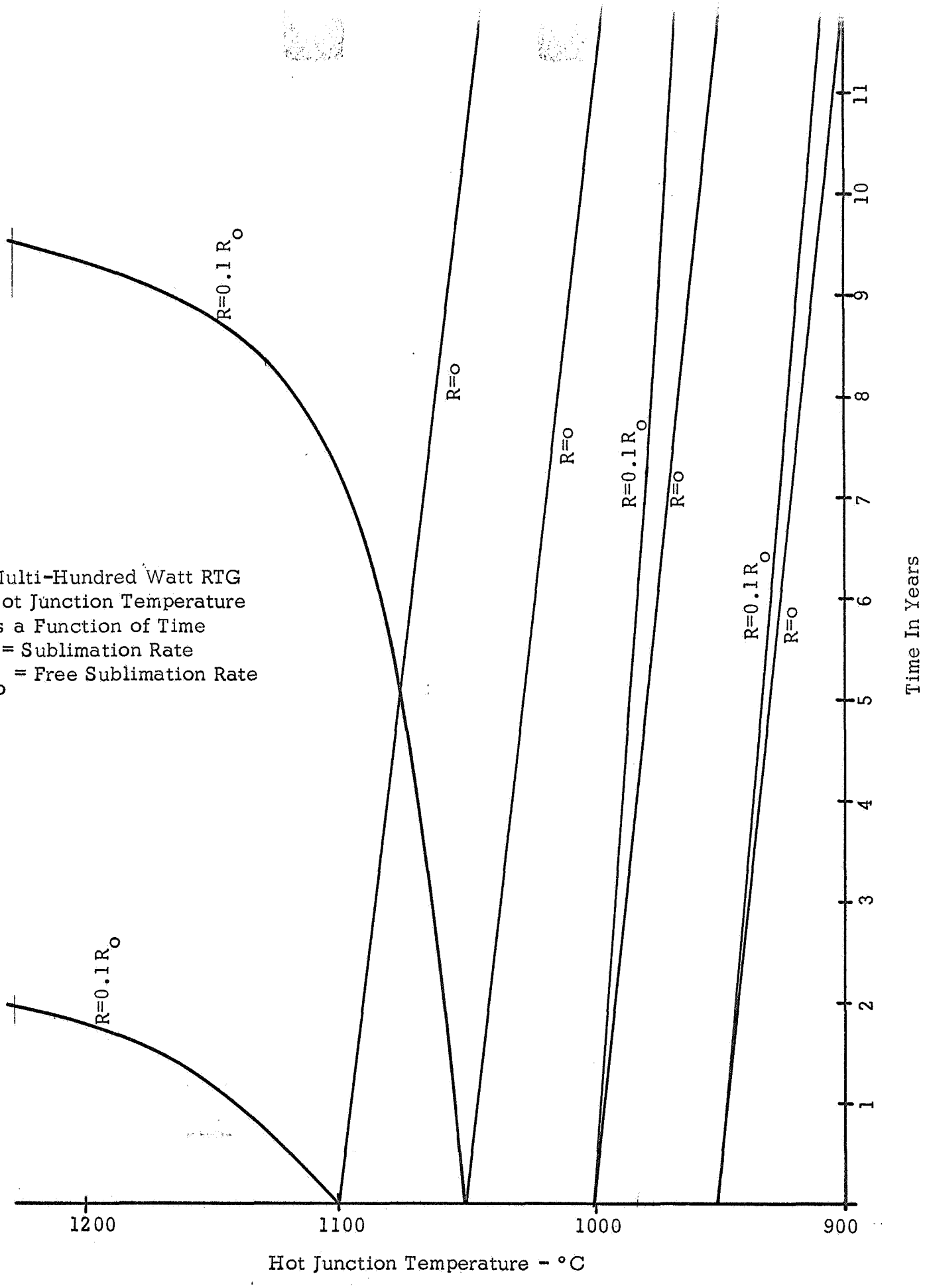
Multi-Hundred Watt RTG
Hot Junction Temperature
as a Function of Time
R = Sublimation Rate
R_o = Free Sublimation Rate
R=0.1 R_o
R=o
R=o
R=0.1 R_o
R=o
R=0.1 R_o
R=o
R=0.1 R_o
1200
1100
1000
900
Hot Junction Temperature - °C
Time In Years
1
2
3
4
5
6
7
8
9
10
11

Figure 30

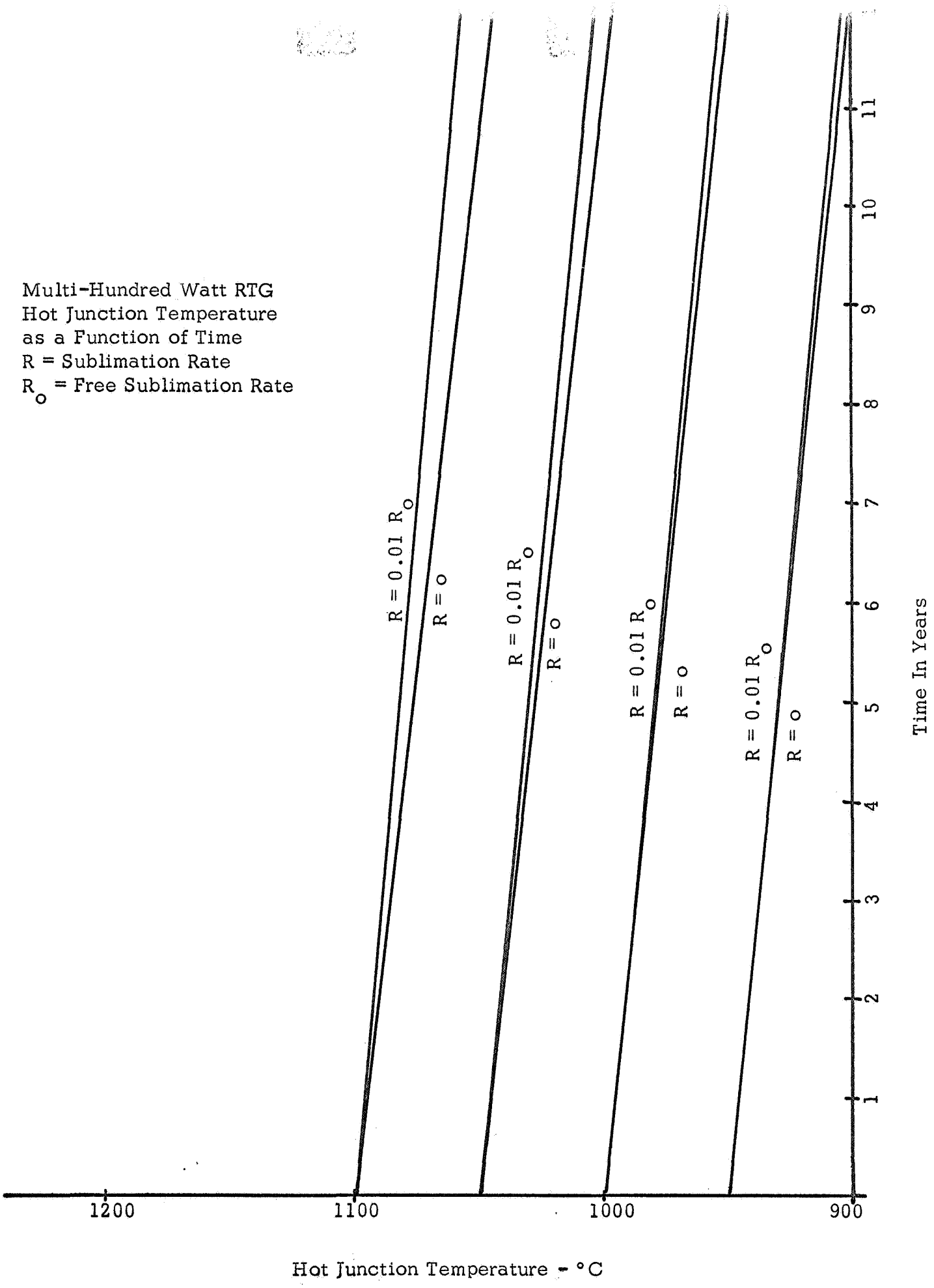
Multi-Hundred Watt RTG
Hot Junction Temperature
as a Function of Time
R = Sublimation Rate
R_o = Free Sublimation Rate
R = 0.01 R_o
R = o
R = 0.01 R_o
R = o
R = 0.01 R_o
R = o
R = 0.01 R_o
R = o
1200
1100
1000
900
1
2
3
4
5
6
7
8
9
10
11
Time In Years
Hot Junction Temperature - °C

Figure 31

3. Because silicon-germanium couples and generators are frequently tested under fixed temperature conditions, it is possible that the mechanisms leading to catastrophic thermocouple failure are not uncovered in such tests of even fairly long duration at temperatures in excess of 1000°C. The maintenance of fixed operating temperatures does not accurately depict the fixed heat input type operation that thermocouples experience in an actual RTG.

4. Relative sublimation effects can be reduced, but not eliminated, by the use of relatively large silicon-germanium thermocouples; therefore very small thermocouples should be avoided if possible. Because it is the thermocouple length to cross-sectional area ratio that has the first order bearing on the thermocouple performance, it may be suggested that the larger the thermocouple, for any given value of ℓ/A, the less are the effects of sublimation.

C. CHARACTERIZATION OF RTG PERFORMANCE IN VARIOUS ENVIRONMENTS

In this study the importance of Radioisotope Thermoelectric Generator (RTG) operation in air, vacuum, and inert gas environments was established. Since RTG's used on unmanned spacecraft are usually fueled prior to launch, the power system must operate in an environment different than the space environment for which it was designed. This study investigated and determined the effects of various environments on generator performance.

In determining RTG performance, a calculational model was developed and data therefrom applied to existing generators whose performance had already been established in the laboratory. After demonstrating the capability of the model to calculate generator performance in both air (nitrogen) and vacuum, the calculations were extended to include the Multi-Hundred Watt RTG operating in different inert gases, air and in vacuum. A brief summary of the calculational model as well as some of the more important results obtained in this study are presented below.

Of prime importance in the development of the calculational model was the heat transfer process which occurs at the heat rejection surface (radiator) and within the RTG. In air operation, the radiator surface temperature may be expected to decrease due to the addition of convective cooling; whereas, heat transfer within the generator could be modified according to the particular geometry selected. Both an "open" and "enclosed" configuration were considered. The possibility of including inert gases in the enclosed system was an added consideration. For both thermoelement lengths the effects of the gas were balanced by an appropriate adjustment of the insulation thermal conductivity.

The heat rejected from the radiator must be equal to the total heat input less that converted to electrical energy and mounting support losses. Assuming the rejection process is a combination of radiative as well as convective heat transfer, rejection can be expressed with the following equation:

$$Q_{Rej} = Q_{in}\,(1-\eta-\alpha) = A_R \sigma \epsilon_r \eta_f F\left(T_R^4 - T_{amb}^4\right) + KA_C \left(T_R - T_{amb}\right)^{\beta}$$

where η is the conversion efficiency, α is the fraction of conductive heat loss, A_R is the radiative area, σ is Stefan-Boltzman constant, ϵ_r is radiator emissivity, η_f is radiator fin efficiency, F is radiator view factor, T_R is radiator temperature, T_{amb} is ambient temperature, K is the convective heat transfer coefficient, A_c is convective area, and β is an exponent. The convective heat transfer coefficient, K, and the exponent, β, depend upon the particular mode of convective heat transfer applicable to a given situation. In the case of natural convection, the numerical values of K and β depend upon whether turbulent or laminar heat flow exist in the boundary layer between the radiator surface and the adjacent environment. In all the cases studied, both K and β were determined prior to using the equation in the calculational model. As it stands, the above equation contains two unknowns. First, the radiator temperature, T_R, and secondly, the generator efficiency, η. Additional equations required to affect a solution of the pertinent RTG temperatures are provided by the heat balance at the hot junction of the thermocouple:

$$\lambda Q_{in} = K_T \Delta T + \frac{\Gamma \Delta T}{(1+m)^2}\left[T_H(1+2m) + T_C\right]$$

and by the simple conductive identity:

$$T_C = T_R + \Delta T_C$$

λ is fraction of total heat input that traverses the generator in the radial direction, K_T is the total radial thermal conductance, Γ is a numerical quantity which depends upon the number and thermophysical properties of the individual thermocouples, T_H and T_C define the hot and cold junction temperatures respectively, ΔT_C is the conductive temperature drop across the cold stack, m is the load factor, and $\Delta T = T_H - T_C$.

An iterative solution of the above equations is obtained by employing the Newton-Raphson technique in combination with the RTG performance equations. Thus, with load voltage, power output, and load current additionally given, the performance characteristics of the generator are completely defined.

In order to test the validity of the mathematical model discussed above and in some instances, to calculate thermal conductivities of selected thermal insulations, the performance of RCA converters C-2, C-3 and C3Z[9,10] were calculated. The calculated performance values are compared to the experimental data reported in another part of this report. The thermoelectric material used by all of these converters is a silicon-germanium alloy of composition 63 a/o Si - 37 a/o Ge in the conventional "Air-Vac" configuration with silicon-molybdenum alloy hot shoes. Both the n- and p-type thermoelements have a 0.0889 cm^2 cross-sectional area with an active length of 2.155 cm in all three converters. All converters employ eighteen thermocouples arranged electrically in series and have an hexagonal overall geometry. The thermal insulation in each converter has an effective area of 171 cm^2.

The temperature drop between the cold junction of the thermoelements and the radiator base (ΔT_C) is calculated to be approximately equal to 0.5 times the heat input. This figure is based upon approximate thermal resistances of the various components of the cold stack and the connection to the radiator surface. The primary difference between the three converters in question is the type of thermal insulation and the exact radiator configuration of each.

Typical calculated results for converter C-3 are shown in Figures 32 and 33 for both vacuum and nitrogen environments. The agreement between calculated and experimental data was very close. For these calculations, the reported values of thermal conductivity for foil insulation (including penetration losses) were used. The effective conductivity curves for foil, Min-K and Zircar are shown in Figure 34 where the Min-K and ZrO_2 curves were obtained by adapting the described calculational model data to known generator performance. Since the generator performance is known from experimental data, the insulation thermal conductivity was adjusted until consistent calculated performance was obtained. In this manner we were able to "back calculate" the required conductivity values.

In evaluating the performance of the MHW-RTG, several distinct cases were considered. The calculations included performance evaluation of an RTG employing a

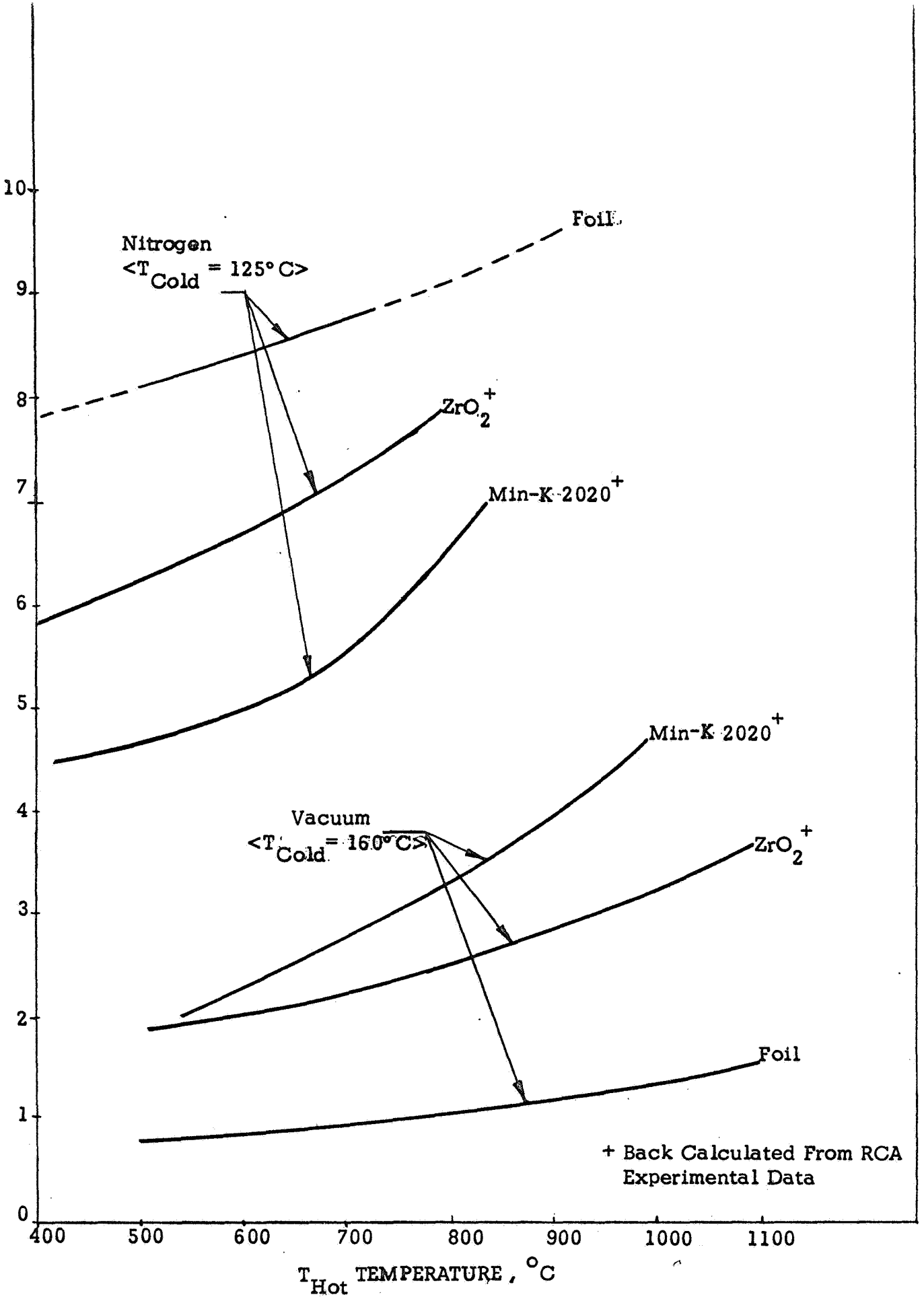

Fig. 34 Effective Thermal Conductivity in Vacuum and Nitrogen

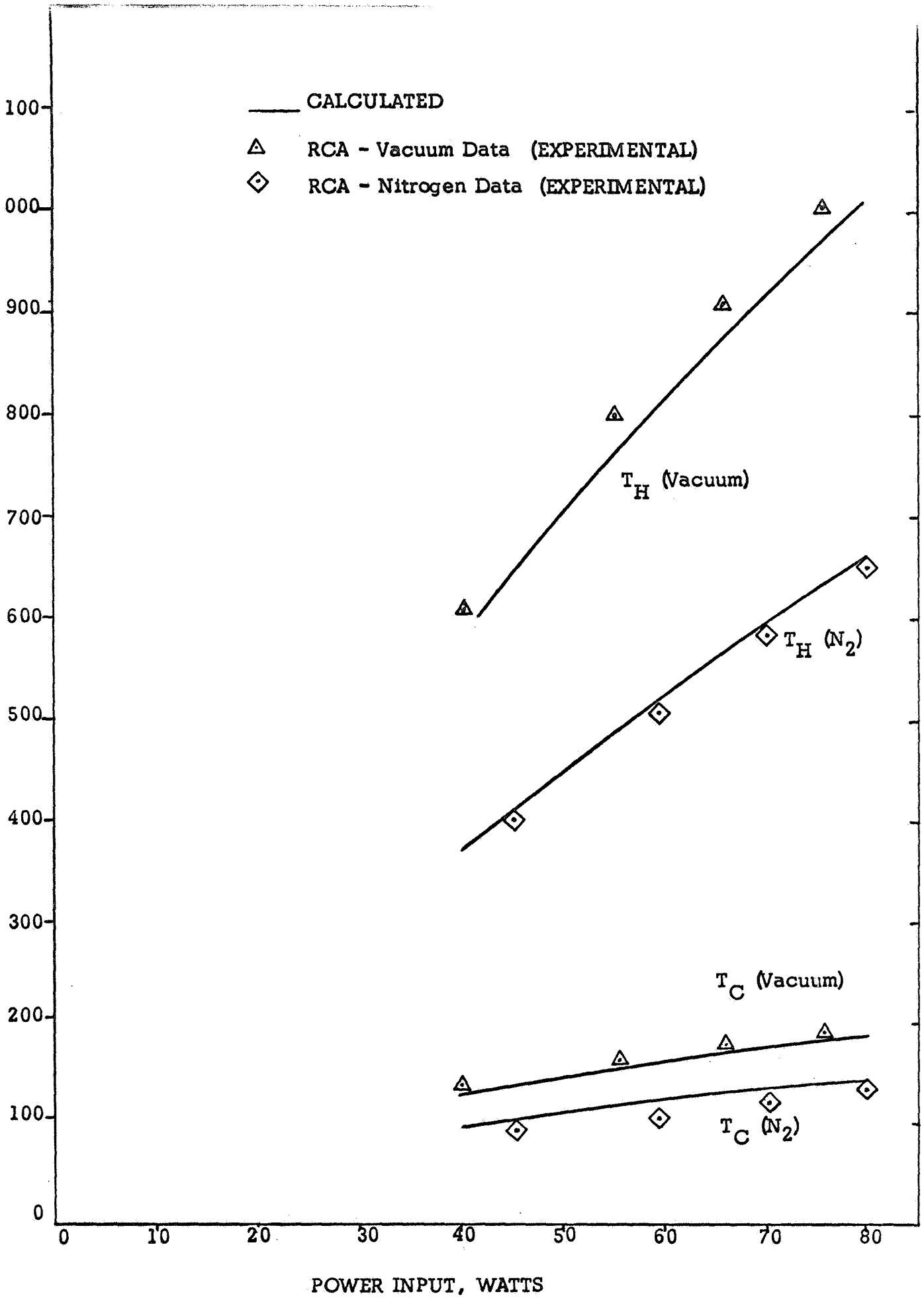

Fig. 32 C-3 Foil Insulated Converter Vacuum/Nitrogen Performance

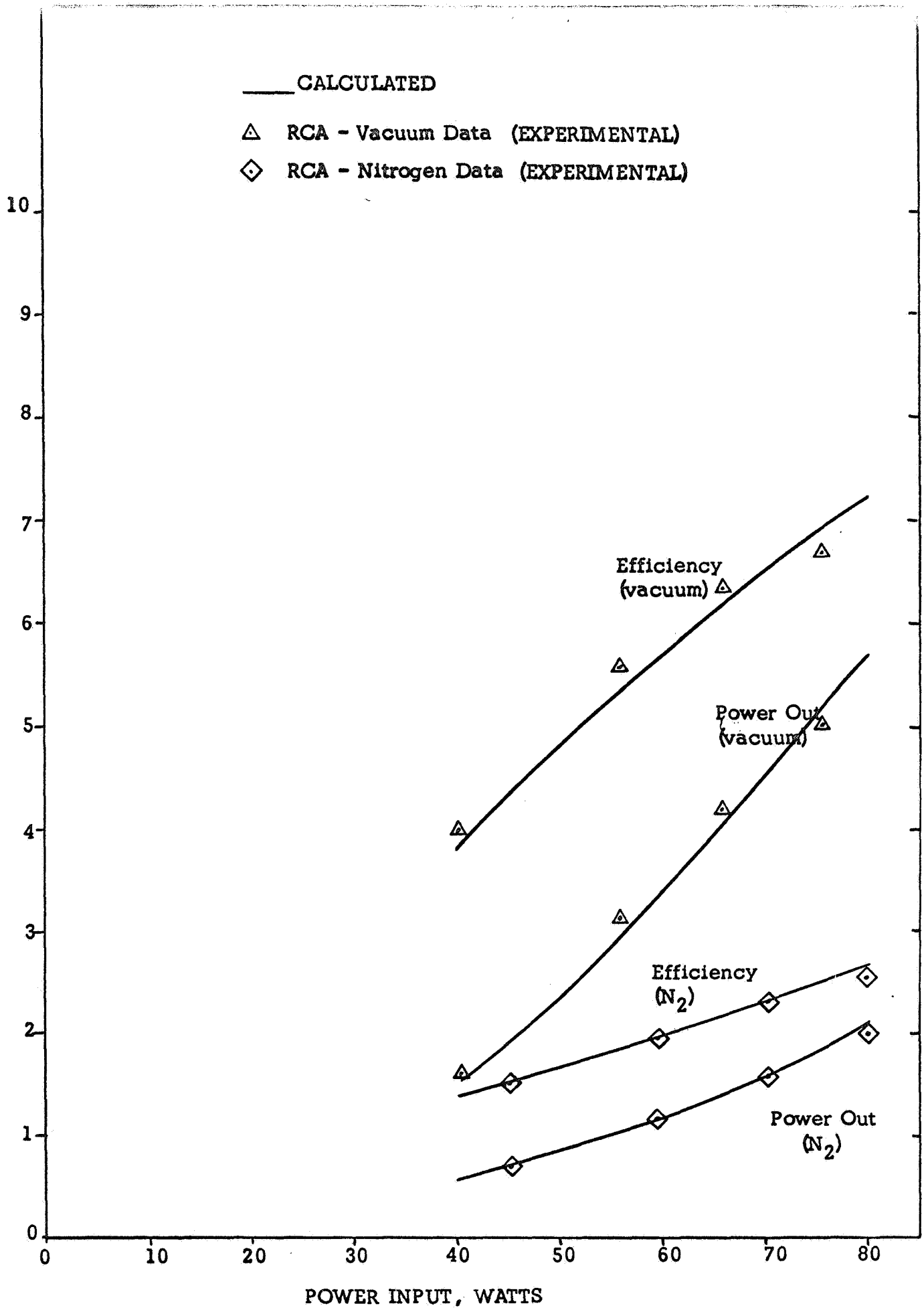

Fig. 33 C-3 Foil Insulated Converter Vacuum/Nitrogen Performance

multifoil, Zircar and Min-K 2020 thermal insulation. The first case (Case I) utilized generator geometry designed to optimize a RTG employing foil insulation which required a thermoelement length of 0.8 inch. The generator was initially considered "open", thus, allowing direct exposure of the internal components when operated in air. In the second case (Case II), the generator had an approximate 18% increase in the thermoelement ℓ/A ratio to permit RTG performance optimization with fibrous insulation. Again the generator was initially considered "open". The calculated performance was then established for both air and vacuum conditions.

For each of the above thermoelement lengths, the MHW-RTG was then considered hermetically sealed such that an inert gas could be contained within the generator during the air-operation phase. This was noted to eliminate many of the problems associated with generator operation in air. Although the generator exterior operated in air, the temperatures were found low enough to avoid most problems associated with chemical reaction, etc. By selecting a low thermal conductivity gas, such as Xenon, the generator could deliver a significant amount of power in the "pre-launch" condition. After reaching the eventual vacuum environment of space, the generator could be vented to allow its performance level to be re-established to that corresponding with vacuum operation.

The inert gases that were tested included argon, helium, krypton and xenon. The effects of these gases on the thermal conductivity of the insulation were established and the MHW-RTG performance was re-examined. To include gas conductance effects, the insulation thermal conductivity was described by:

$$K = k_v + Ak_g$$

where k_v was the effective vacuum conductivity, A an empirical constant and k_g, the conductivity of the particular gas being analyzed. The empirical constant A, as well as k_v, were determined from Figure 34 and the gas conductivity calculated from the Sutherland formula using the relationship $k/(\mu C)$ = Constant. Where k is the conductivity, C is the specific heat and μ is the viscosity of the gas.

The final results of the calculation of MHW-RTG performance in both of the gases mentioned are presented in Tables 1 and 2. In these tables, the maximum power output and the power output at 30 volts are shown for three different thermal insulations, foil, Zircar, and Min-K. The hot and cold-junction temperatures are also given at the maximum power output point.

In short, the object of the study was the development of a model to determine gas and vacuum performance of T/E generators. The validity of the model was verified by its applications to several existing generators which have been tested in both vacuum and air (actually nitrogen) environments. The model was also used to back-calculate the thermal conductivities of selected thermal insulations that are presently being considered for use in high temperature silicon-germanium RTG's. Finally the model was applied to the MHW generator, with two different thermoelement lengths, to determine its performance under various environmental conditions. The initial characterization was performed in vacuum and then the effects of various inert gases upon the insulation conductivity were included, the results of which established generator operability for air/vacuum pre-launch periods.

TABLE I

MHW-RTG Performance in Vacuum and Gas Environments
for Thermoelement Length of 0.8 in.

FOIL INSULATION						
GAS	VAC	HELIUM	AIR	ARGON	KRYPTON	XENON
$P_{Max,}$ Watt	138	17	69	84	106	118
$P_{30V,}$ Watt	137	-	56	80	105	117
$T_{H,}$ °C *	1065	543	810	872	939	972
$T_{C,}$ °C *	321	282	279	278	276	275
ZIRCAR INSULATION						
$P_{Max,}$ Watt	124	24	73	88	103	111
$P_{30V,}$ Watt	123	-	61	85	101	109
$T_{H,}$ °C *	1012	591	844	885	929	950
$T_{C,}$ °C *	323	282	279	278	277	276
MIN-K 2020 INSULATION						
$P_{Max,}$ Watt	116	35	84	94	103	108
$P_{30V,}$ Watt	115	-	77	91	101	106
$T_{H,}$ °C *	986	652	860	903	929	941
$T_{C,}$ °C *	323	281	279	278	277	277

* Temperatures are for maximum power points

TABLE 2

MHW-RTG Performance in Vacuum and Gas Environments
for Thermoelement Length of 1.2 in.

FOIL INSULATION						
GAS	VAC	HELIUM	AIR	ARGON	KRYPTON	XENON
$P_{Max,}$ Watt	161	28	92	114	135	145
$P_{30V,}$ Watt	155	-	91	114	132	140
$T_{H,}$ °C *	1195	641	934	1016	1070	1100
$T_{C,}$ °C *	320	282	277	276	274	273
ZIRCAR INSULATION						
$P_{Max,}$ Watt	135	37	101	110	123	130
$P_{30V,}$ Watt	134	8	101	110	122	128
$T_{H,}$ °C *	1125	700	970	1002	1039	1057
$T_{C,}$ °C *	321	281	277	276	275	275
MIN-K 2020 INSULATION						
$P_{Max,}$ Watt	123	51	110	105	112	115
$P_{30V,}$ Watt	122	32	110	105	112	114
$T_{H,}$ °C *	1102	774	1004	987	1006	1015
$T_{C,}$ °C *	322	280	276	276	276	276

* Temperatures are for maximum power points

D. PERFORMANCE OF MHW-RTG IN THE MARTIAN ENVIRONMENT

1. Introduction

The Multi-Hundred Watt (MHW) Radioisotope Thermoelectric Generator (RTG) is being designed for operation in the hard vacuum of deep space. However, for certain missions the RTG will be required to operate in environments other than that of deep space. Among these requirements are operation in an Earth environment (air at 1 atmosphere), operation on or near the planet Mars, and others. Of particular interest here is the operation on or near the planet Mars.

Obviously the environment in which the RTG operates will affect the external heat rejection characteristics of the RTG not only because heat rejection is a function of environmental temperatures but because it depends upon the presence or absence of surrounding gases, the type of gas and the thermal characteristics of the gas. In addition the external environment affects the internal operation of the RTG.

Nominally the RTG is designed as a sealed device and perhaps back-filled with an inert gas prior to launch in order to exclude air from internal parts sensitive to the damaging effects of oxygen. However, as will be shown later in this report, operation of the RTG in a gaseous environment impairs the performance and therefore it is desirable to vent any gases from the RTG once it becomes isolated from planetary influences. If the RTG then reenters a gaseous environment, the internal structure would be exposed to the gas as well as the external of the RTG. Thus to assess the influence of environment upon RTG operation the internal effect as well as the external effect must be considered and in the case at hand the internal effect is the more severe.

To assess the effect of the environment, the environment has to be established, the mechanisms by which that environment affects performance have to be identified and finally the effect upon performance has to be determined.

2. Martian Environment

The accuracy which can be achieved in predicting the performance of the RTG on Mars will depend directly upon the accuracy to which the Mars environment can be described. The uncertainty about an atmospheric model of Mars can only be

resolved by direct measurement. Lacking direct measurements, use is made of models of the Martian atmosphere which have been advanced.[11,12,13] The models are based upon evidence accumulated over the years from Earth observation, specifically data taken during the 1965 opposition, and from the Mariner IV occultation experiment in July, 1965 and Mariner probes of August, 1969.

Of primary concern to the performance of the RTG is the composition of the Martian atmosphere and the range of temperatures expected to be encountered.

The atmosphere of Mars is strongly indicated to be 80% CO_2. The balance is assumed to be optically undetectable gases such as nitrogen or argon. For purposes of this analysis, the composition is assumed to be 80% CO_2 - 20% N_2.

The mean surface temperature of Mars is estimated to be in the range of 225 to 300°K. The surface can be assumed to be an equivalent black body at 220°K[3] for purposes of heat transfer analysis.

In addition, the atmospheric pressure at the surface of Mars is estimated to be between 3.5 and 8.5 Torr. A mean value of 6 Torr has been used in this analysis.

3. Effect of Environment on RTG

There are two primary areas of concern relative to the effect of the environment upon RTG performance. The first of these is the effect of the environment upon the external heat rejection rate of the RTG. The second is the effect of the environment upon the heat transfer and temperature distribution within the RTG.

a. External Effects

As the MHW-RTG is designed for operation in a vacuum environment, the principal means of heat transfer from the exterior of the RTG is by radiation. If a gaseous environment surrounds the RTG then heat can be dissipated by conduction to the gas and if, in addition, a gravitational field exists, heat transfer by convection can occur. Thus, on Mars, heat rejection from the RTG could occur not only by radiation, but by conduction and convection as well.

b. Internal Effects

Though the MHW-RTG will be operated until shortly after launch with an internal inert gas atmosphere, it is assumed that for a Mars mission, as for outer planet

missions, this inert gas will be vented and the RTG will, in subsequent phases of operation, be exposed internally to its external environment.

To determine the effect of the Martian environment upon the effective conductivity of the RTG insulation, the pertinent properties (primarily the thermal conductivity) of the environment must be determined. There is a large amount of data[14,15,16] available for the thermal conductivity of CO_2 and N_2 at pressures ranging from about 50 Torr to about 5 atmospheres. The conductivity in this region is predicted fairly accurately by the kinetic theory of gases[17] and is essentially independent of pressure.

Figure 35 shows the conductivity of N_2 and CO_2 as a function of temperature for the pressure insensitive range. Also shown is the conductivity of the mixture 80% CO_2 - 20% N_2.

At pressures above and below the range of 50 Torr to 5 atmospheres the conductivity varies with pressure as well as temperature. In a dilute gas the conductivity varies with the viscosity and the specific heat in the following manner:

$$K = f\mu c_v$$

where f is nearly independent of temperature. Thus the conductivity can be computed from the viscosity and specific heat. A similar calculation for CO_2 and the mixture of CO_2 and N_2 was made and the results are plotted in Figure 36as a function of pressure for a temperature of 500°C. Note that the conductivity does not begin to decrease until the pressure has dropped to about 30 Torr. At 6 Torr the conductivity has decreased by about 15% from its 1 atmosphere value.

Three types of insulation are being considered for the MHW-RTG. These are multifoil, Zircar and Min-K. The latter two are fibrous and have an irregular internal geometry. The density of the fibrous types can vary considerably with the mechanical loading applied and the methods used during assembly and installation.

The conductivity of an insulation can be expressed[18] as

$$K = k_v + Mk_g$$

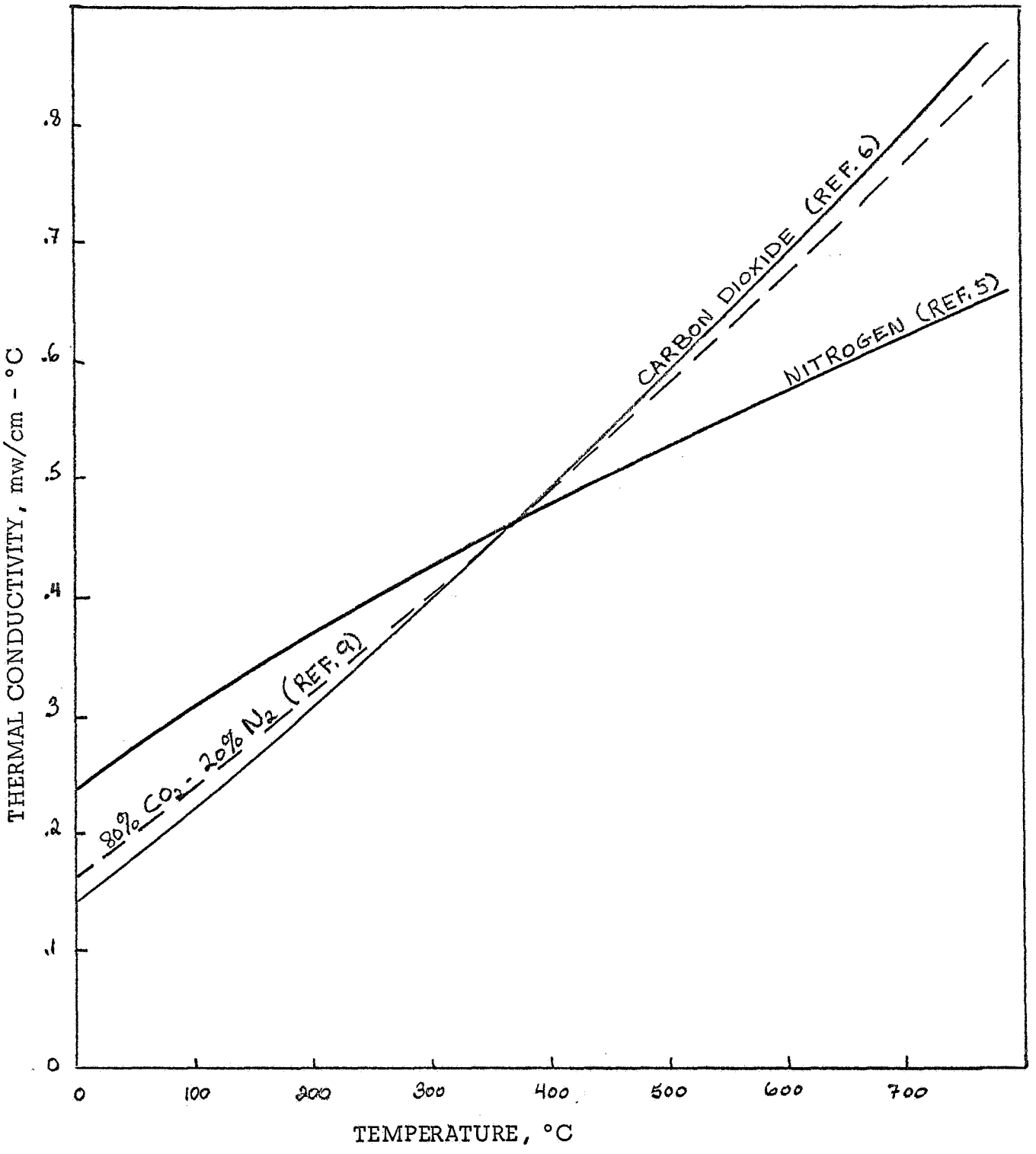

FIGURE 35 GAS THERMAL CONDUCTIVITY

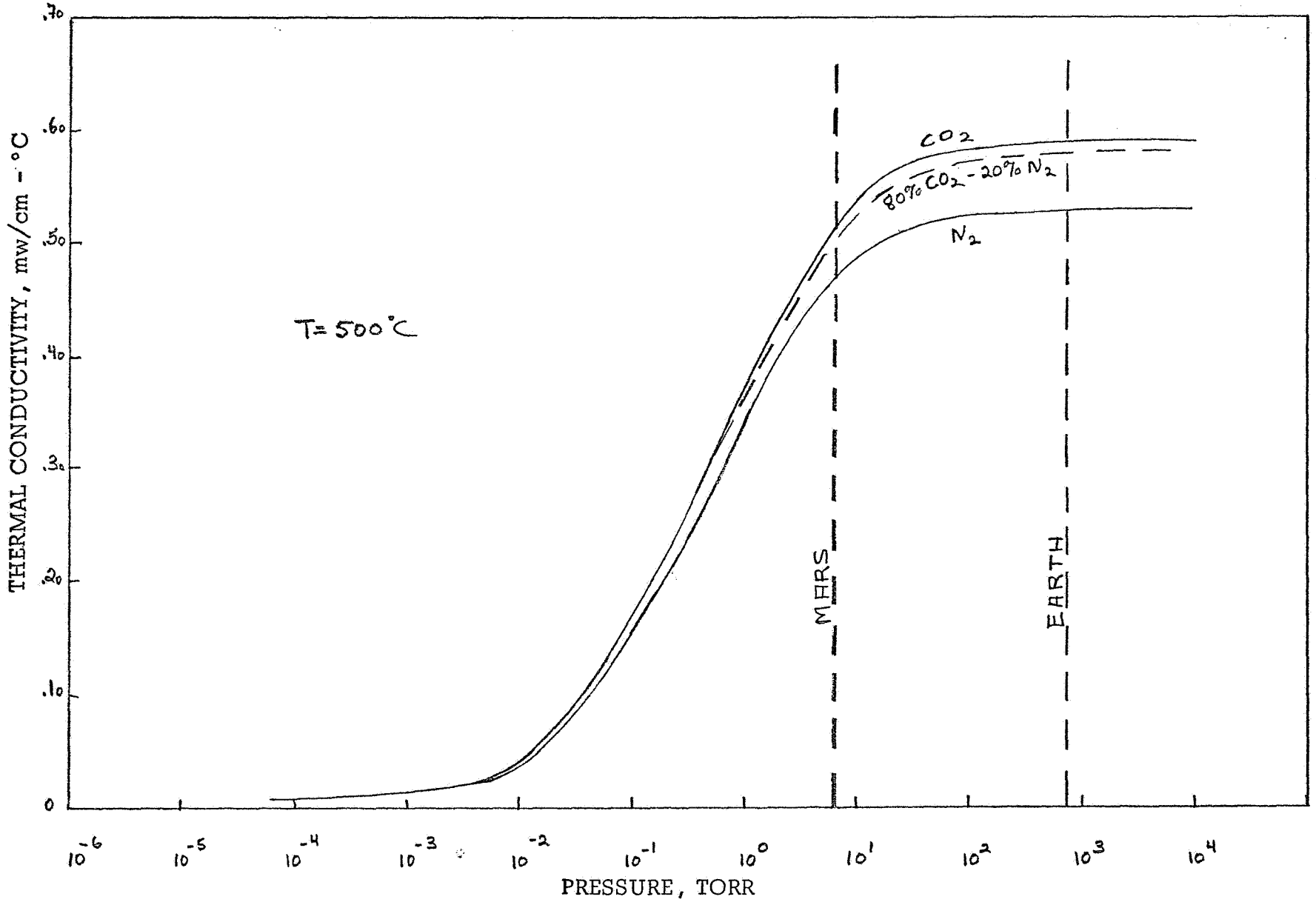

FIGURE 36 EFFECT OF PRESSURE ON GAS CONDUCTIVITY

where k_v = conductivity of insulation in a vacuum,

k_g = conductivity of gas, and

M = an empirical constant.

A study[19] was made to assess the effects of a nitrogen atmosphere versus a vacuum atmosphere on the conductivity of insulation. In that study it was found that the value of M for Min-K was about .65, for Zircar about 1.0 and for multifoil about 1.6. Thus this study indicates that the multifoils are very sensitive to gas conductivity while Min-K is not as sensitive.

Using the data of Reference 19 for vacuum thermal conductivity, the values of M discussed above, the CO_2 - N_2 gas mixture conductivity shown in Figure 35, and taking into account the pressure effect shown in Figure 36, the conductivity of the three types of insulation in a Mars environment was calculated and is shown in Figure 37 as a function of temperature.

Also shown in Figure 37 is the conductivity of Min-K corrected for pressure by using the Johns-Manville pressure relationship to nitrogen. Thus the difference between the Johns-Manville curve and the other Min-K curve is due to two effects: 1) a different gas pressure effect and 2) no allowance for penetration and edge effects being shown in the Johns-Manville curve.

4. RTG Performance

The performance of the cylindrical MHW-RTG was calculated as a function of insulation conductivity for mission times of 1500 hours, 5 years and 12 years. The beginning-of-mission heat input for all cases was 2200 watts. The load voltage was held at 30V. The results are plotted in Figure 38. Using this figure and Figure 37, the power output of the MHW-RTG in a Martian environment was calculated and the results are shown in Table 3 for the three types of insulation and for mission times up to 12 years. For Min-K a range of performance is shown to account for the possible range of effective conductivity for that material. The lower end of the range represents the power output using conductivity values calculated by neglecting the effect of mean

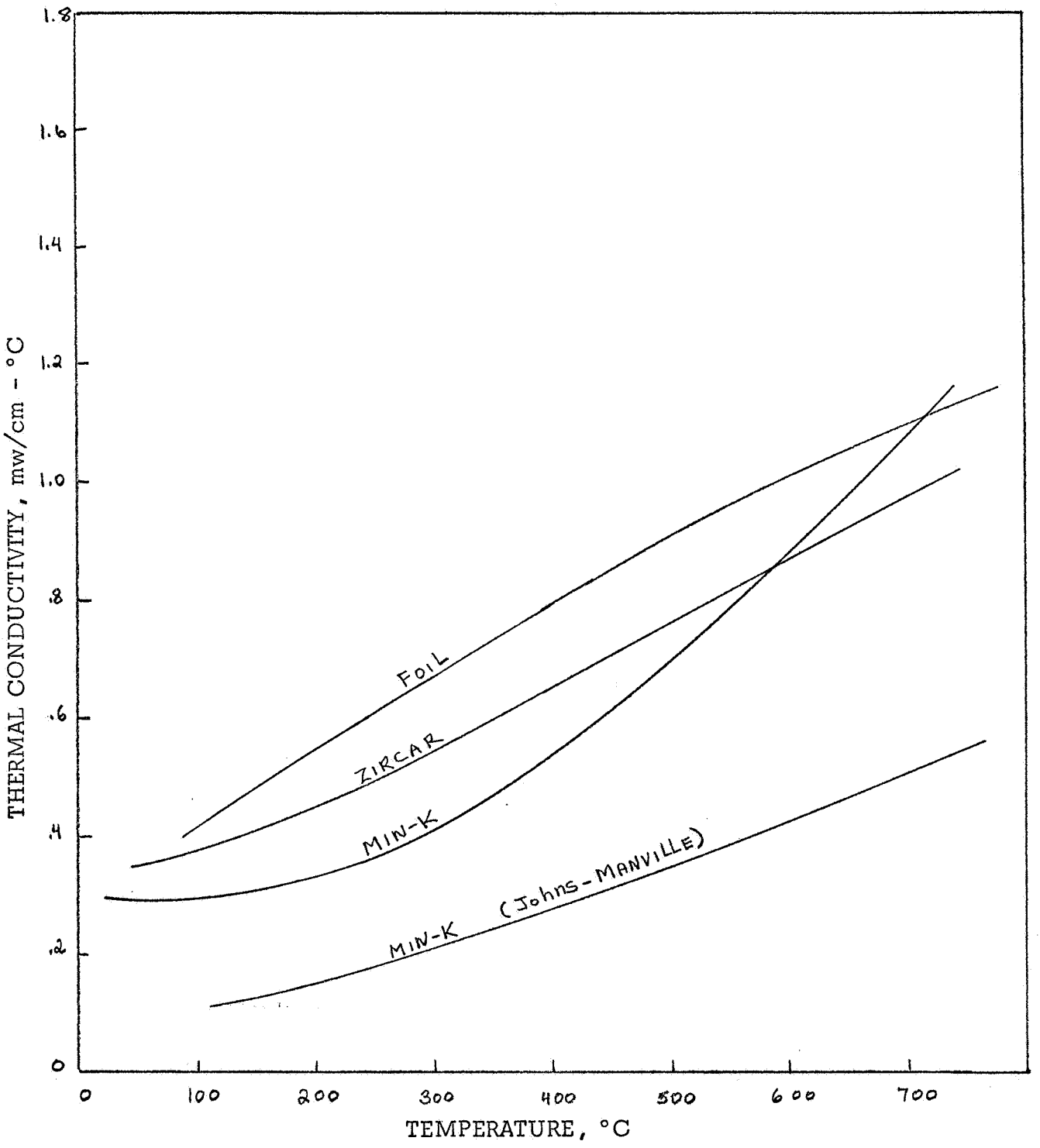

FIGURE 37 INSULATION CONDUCTIVITY IN
80% CO_2 - 20% N_2 MIXTURE AT 6 TORR

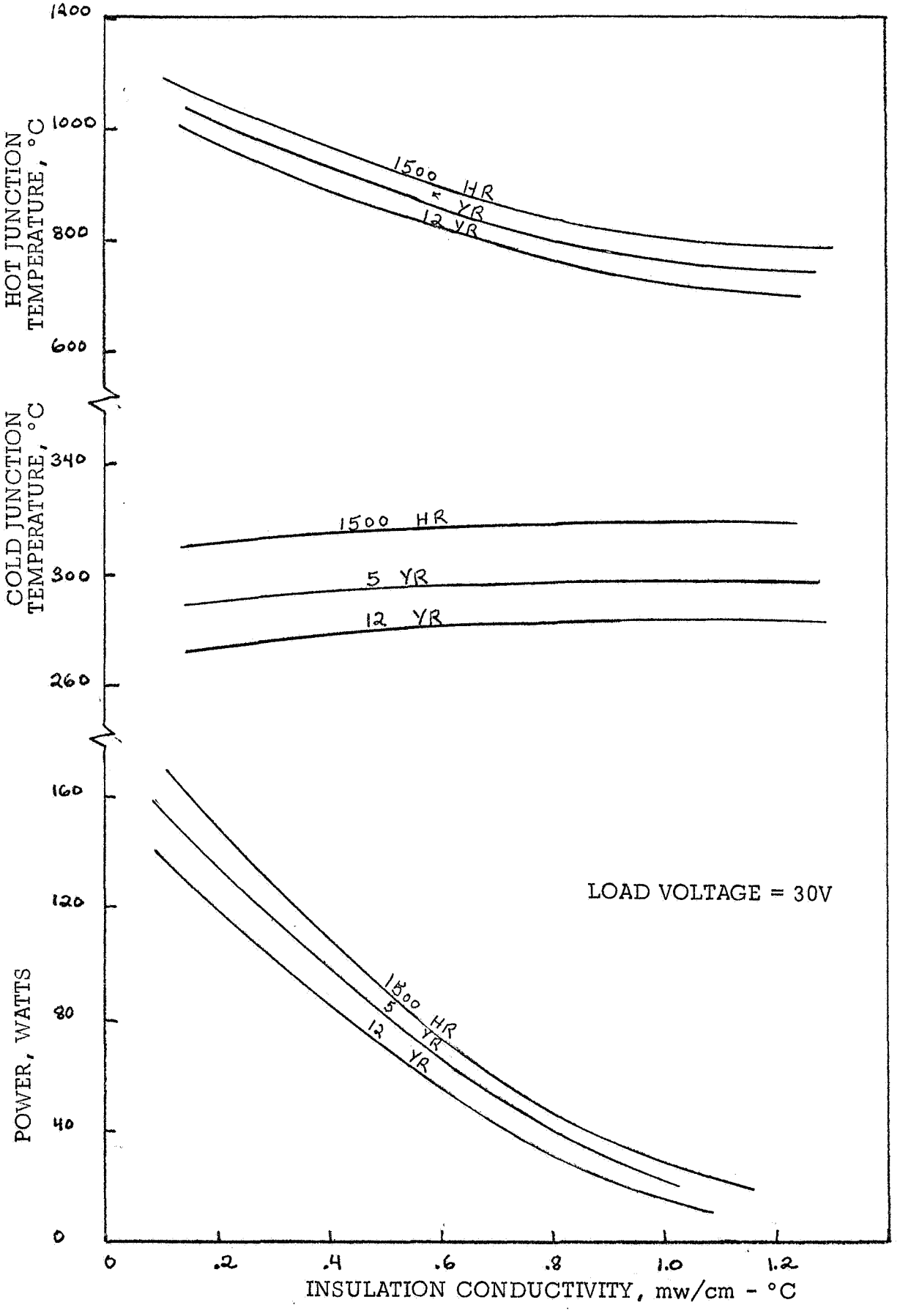

FIGURE 38 EFFECT OF INSULATION CONDUCTIVITY ON MHW-RTG PERFORMANCE

free path while the upper end of the range results from conductivity values based on the manufacturer's information.

TABLE 3

MHW-RTG POWER OUTPUT IN MARTIAN ENVIRONMENT

LOAD VOLTAGE = 30V

POWER IN WATTS

Mission Time	INSULATION		
	Min-K	Zircar	Foil
1500 hours	43-99	41	30
5 years	42-94	38	26
12 years	38-84	33	20

5. Summary

The performance of the MHW-RTG was found to be significantly poorer in a Mars environment than in a vacuum environment. In general, the power output of the RTG will only be 30-40% of the power output when operated in a vacuum environment. The primary reason for the reduced output is the fact that all of the insulation types proposed for the RTG suffer a significant increase in thermal conductivity when operated in a gaseous environment. Since less than 5% of the RTG area is occupied by thermoelements and the balance is filled with insulation, any changes in the conductivity of the insulation are very significant and drastically affect the temperature drop which can be maintained across the thermoelements.

The primary uncertainties in the calculation of the performance in a Martian environment are twofold. First is the uncertainty in the effect of reduced pressure upon the thermal conductivity of gases. While there is a significant body of data available for pressures from 1 to 50 atmospheres there are virtually no thermal conductivity data available for pressures in the range of that of Mars. In commenting on this point the authors of the Thermophysical Properties of Matter[20] state "We defer any detailed discussion of this point here with the comment that our knowledge and understanding in this rarified gas region is far from being adequate."

In a study[21] performed by S. H. Chue, et al, in which the problem of forced convection heat transfer in a Martian atmosphere was investigated, they chose to use thermal conductivity values which were essentially independent of pressure and were based upon those given by kinetic theory. Thus the procedure used here of calculating the low pressure conductivity from viscosity data is not overly conservative.

The other major area of uncertainty is the effect of pressure on the conductivity of insulations when immersed in a gaseous environment. In general when the distance between two surfaces is less than the mean free path of the gas that separates them, the classical gaseous conduction process as given by kinetic theory no longer applies. In this region gaseous conduction is seriously reduced below that predicted by kinetic theory. Thus the effect of gas conduction will be dependent upon the nominal pore size of the insulation relative to the mean free path of the gas.

For nitrogen and carbon dioxide at 1 atmosphere and 500°C, the mean free path is about 0.16 micron. At 6 Torr, the mean free path has increased to about 20 microns. For some types of insulation, notably Min-K, the nominal pore size probably is smaller than 20 microns depending upon the specific type of Min-K and its density. Data given in Reference 22 definitely indicate that the insulation density affects the response of insulation conductivity to changes in gas pressure.

In conclusion it can be said that:

1. The performance of the MHW-RTG in a Martian environment will definitely be poorer than in a vacuum; the power output will be some 50-70% lower depending upon the insulation type and density.

2. The conductivity of some types of insulation is more sensitive to the type of gas and its pressure than others; of the fibrous types, the more dense the insulation, the less sensitive it is.

3. A great deal of information is known about the conductivity of the insulation in gases at 1 atmosphere and at pressures less than 10^{-4} Torr. In between, very little is known.

4. At pressures below about 50 Torr very little is known about the conductivity of gases. In the low pressure region (less than 50 Torr) the conductivity becomes system dependent, i.e. in the case of insulations, the conductivity of the gas depends upon the pore size of the insulation.

5. Experimental work needs to be carried out to verify the conductivity of insulations in the gas pressure range of 10^{-2} to 50 Torr.

VI. REFERENCES

1. V. Raag, The Performance Characteristics of Silicon-Germanium Alloys in Thermoelectric Applications, Resalab Scientific Report.

2. V. Raag and H. Kowger, J. Appl. Phys. 36, 2045 (1965)

3. V. Raag, Research and Development of a Silicon-Germanium Alloy, Final Report, Contract No. NAS-5-3410, December 1963.

4. L. Ekstrom and J.P. Dismukes, Precipitation of Phosphorus from Solid Solution in Ge-Si Alloy, J. Phys. Chem. Solids 27, 857 (1966).

5. V. V. Slyozov and I. M. Lifshitz, The Kinetics of Precipitation from Supersaturated Solid Solutions, J. Phys. Chem. Solids 19, 35 (1961).

6. E. E. Steigmeier and I. Kudman, Phys. Rev. 132, 508 (1963).

7. D. Gerlich, B. Abeles and R. E. Miller, J. Appl. Phys. 36, 76 (1965).

8. R. C. Smith, High Temperature Specific Heat of Germanium, J. Appl. Phys. 37, 4860 (1966).

9. RCA, Twenty-Third Monthly Report on AEC Contract No. AT (29-2)-2510, Nov. 1969.

10. RCA, Twenty-Fourth Monthly Report on AEC Contract No. AT (29-2)-2510, Dec. 1969.

11. "Models of Mars Atmosphere (1967)", NASA SP-8010, May, 1968.

12. "Mars Surface Models (1968)", NASA SP-8020, May, 1969.

13. "Viking 75 Project Environmental Specification", Appendix B, RS-3703001, DRL Contract No. S1-0004, May 27, 1970.

14. J. R. Moszynski, Proceedings of the Fourth Symposium on Thermophysical Properties, ASME Publication, 1968.

15. Y. S. Touloukion, Thermodynamic and Transport Properties of Gases, Liquids and Solids, ASME Publication, McGraw Hill, New York, 1959.

16. S. Chapman and T. Cowling, The Mathematical Theory of Non-Uniform Gases, Cambridge, 1960.

17. J. O. Hirschfelder, C. F. Curtiss, and R. B. Bird, Molecular Theory of Gases and Liquids, John Wiley & Sons, Inc., New York, N.Y., 1954

18. "MHW-RTG Operation in Gas", JPL Memo #342-70-B-549, W. D. Leonard, April 28, 1970.

19. Dean Leonard, et al, "Characterization of RTG Performance in Both Air and Vacuum", Memorandum #7, Resalab Scientific, May 20, 1970.

20. Y. S. Touloukion, et al, Thermophysical Properties of Matter, Volume 3, Thermal Conductivity, IFL/PLENUM, New York, 1970.

21. S. H. Chue, N. Hanus, E.R. F. Winter, D. Ting, "Forced Convection Heat Transfer in a Simulated Martian Atmosphere", ASME paper 70-HT/SpT-29.

22. Volume VI, Lockheed Missiles & Space Company.